Oceanologia

Official Journal of the Polish Academy of Sciences: Institute of Oceanology and Committee on Maritime Research

EDITOR-IN-CHIEF
Janusz Pempkowiak
Institute of Oceanology Polish Academy of Sciences, Sopot, Poland

MANAGING EDITOR
Agata Bielecka - abielecka@iopan.gda.pl

Editorial Office Address
Institute of Oceanology Polish Academy of Sciences (IO PAN)
Powstańców Warszawy 55
81-712 Sopot, Poland
Mail:pempa@iopan.gda.pl

THEMATIC EDITORS
Alicja Kosakowska — Institute of Oceanology Polish Academy of Sciences, Sopot, Poland
Stanisław Massel — Institute of Oceanology Polish Academy of Sciences, Sopot, Poland
Jan Marcin Węsławski — Institute of Oceanology Polish Academy of Sciences, Sopot, Poland
Marek Zajączkowski — Institute of Oceanology Polish Academy of Sciences, Sopot, Poland
Tymon Zieliński — Institute of Oceanology Polish Academy of Sciences, Sopot, Poland

ADVISORY BOARD

Prof. Jerzy Dera
Institute of Oceanology Polish Academy of Sciences (IO PAN), Sopot, Poland

Prof. Howard Gordon
Dept. of Physics, University of Miami, USA

Prof. Genrik Sergey Karabashev
P.P. Shirshov Institute of Oceanology RAS, Moscow, Russia

Prof. Zygmunt Kowalik
Institute of Marine Science, School of Fisheries and Ocean Sciences, University of Alaska Fairbanks (UAF), USA

Prof. Matti Leppäranta
Department of Physics, University of Helsinki, Finland

Prof. Gennady Matishov
Murmansk Marine Biological Institute KSC, Russian Academy of Sciences (MMBI KSC RAS), Russia

Prof. Sergej Olenin
Coastal Research and Planning Institute, Klaipeda University CORPI, Lithuania

Prof. Anders Omstedt
University of Gothenburg, Dept. Earth Sciences: Oceanography, Gothenburg, Sweden

Prof. Janusz Pempkowiak
Institute of Oceanology Polish Academy of Sciences (IO PAN), Sopot, Poland

Prof. Marcin Pliński
Institute of Oceanography, University of Gdańsk, Gdynia, Poland

Prof. Xosé Antón Álvarez Salgado
Department of Oceanography, Marine Research Institute, Spanish Research Council (CSIC), Spain

Prof. Tarmo Soomere
Institute of Cibernetics, Tallinn University of Technology, Tallinn, Estonia

Prof. Hans von Storch
Institute for Coastal Research, Helmholtz Zentrum Geesthacht, Germany

Prof. Dariusz Stramski
Marine Physical Laboratory, Scripps Institution of Oceanography, University of California, San Diego, USA

Prof. Juergen Suendermann
Institut für Meereskunde, Universität Hamburg, Hamburg, Germany

Prof. Piotr Szefer
Department of Food Sciences, Medical University of Gdańsk, Gdańsk, Poland

Prof. Antoni Śliwiński
Insitute of Experimental Physics, University of Gdańsk, Gdańsk, Poland

Prof. David Turner
Department of Chemistry and Molecular Biology, University of Gothenburg, Sweden

Prof. Bogdan Woźniak
Institute of Oceanology Polish Academy of Sciences (IO PAN), Sopot, Poland

Prof. Ronald Zaneveld
Western Environmental Technology Laboratories, Philomath, USA

This journal is supported by the Ministry of Science and Higher Education, Warsaw, Poland

Indexed in: ISI Journal Master List, Science Citation Index Expanded, Scopus, Current Contents, Zoological Record, Thomson Scientific SSCI, Aquatic Sciences and Fisheries Abstracts, DOAJ

IMPACT FACTOR ANNOUNCED FOR 2014 IN THE 'JOURNAL CITATION REPORTS' IS 1,000; 5-year IF — 1.346

Publisher
Elsevier Sp. z o.o. 4/59,
02-796 Warsaw, Poland
Tel. +48 22 546 38 20, Fax. +48 22 546 38 21

Director of Journals Publishing
Ewa Kittel-Prejs

Publishing Editor
Joanna Lewczuk
j.lewczuk@elsevier.com
48 515 082 585, 48 22 546 38 24

Publishing Manager
Agnieszka Pawłowska
a.pawlowska@elsevier.com

Subscription and Distribution Manager
Jacek Sołtyk
prenumerata@elsevier.com
48 22 546 38 27, 48 510 134 282

Marketing & Promotion Manager
Anna Szkolut
a.szkolut@elsevier.com
48 22 546 38 40, 48 515 090 174

Advertising Pharma Solutions
Mariusz Radzio
m.radzio@elsevier.com
48 519 796 821

ISSN 0078-3234

Oceanologia (2016) 58, 1—12

Available online at www.sciencedirect.com

ScienceDirect

journal homepage: www.elsevier.com/locate/oceano

ORIGINAL RESEARCH ARTICLE

Significant increase of aerosol number concentrations in air masses crossing a densely trafficked sea area☆

Simonas Kecorius [a,b,*], Niku Kivekäs [c,d], Adam Kristensson [d], Thomas Tuch [b], David S. Covert [e], Wolfram Birmili [b], Heikki Lihavainen [c], Antti-Pekka Hyvärinen [c], Johan Martinsson [d], Moa K. Sporre [d], Erik Swietlicki [d], Alfred Wiedensohler [b], Vidmantas Ulevicius [a]

[a] *Center for Physical Sciences and Technology, Vilnius, Lithuania*
[b] *Leibniz-Institute for Tropospheric Research, Leipzig, Germany*
[c] *Finnish Meteorological Institute, Helsinki, Finland*
[d] *Division of Nuclear Physics, Lund University, Lund, Sweden*
[e] *Department of Atmospheric Sciences, University of Washington, Seattle, USA*

Received 4 March 2015; accepted 4 August 2015
Available online 22 August 2015

KEYWORDS
Ship emission;
Particle number size distribution;
Absorption Ångström exponent

Summary In this study, we evaluated 10 months data (September 2009 to June 2010) of atmospheric aerosol particle number size distribution at three atmospheric observation stations along the Baltic Sea coast: Vavihill (upwind, Sweden), Utö (upwind, Finland), and Preila (downwind, Lithuania). Differences in aerosol particle number size distributions between the upwind and downwind stations during situations of connected atmospheric flow, when the air passed each station, were used to assess the contribution of ship emissions to the aerosol number concentration (diameter interval 50—400 nm) in the Lithuanian background coastal environment.

☆ Simonas Kecorius acknowledges support by project "Promotion of Student Scientific Activities" (VP1-3.1-ŠMM-01-V-02-003) from the Research Council of Lithuania. This project is funded by the Republic of Lithuania and European Social Fund under the 2007—2013 Human Resources Development Operational Programme's priority 3. This research is also funded by NordForsk through the top-level initiative Cryosphere-atmosphere interactions in changing Arctic climate (CRAICC), the Swedish Research Council Formas (grant no. 2010—850), ACTRIS (Aerosols, Clouds, and Trace gases Research InfraStructure Network, No. 262254 in EU FP7-INFRASTRUCTURES-2010-1) and German Federal Environmental Agency FKZ 35101086 (WBA-WCCAP). The research leading to these results has received funding from the European Union Seventh Framework Programme (FP7/2007-2013) project No. 262254.

* Corresponding author at: Center for Physical Sciences and Technology, Savanoriu ave. 231, LT-02300, Vilnius, Lithuania.
Tel.: +370 643 94538.
E-mail address: kecorius@tropos.de (S. Kecorius).

Peer review under the responsibility of Institute of Oceanology of the Polish Academy of Sciences.

ELSEVIER Production and hosting by Elsevier

http://dx.doi.org/10.1016/j.oceano.2015.08.001

0078-3234/© 2015 Institute of Oceanology of the Polish Academy of Sciences. Production and hosting by Elsevier Sp. z o.o. This is an open access article under the CC BY-NC-ND license (http://creativecommons.org/licenses/by-nc-nd/4.0/).

A clear increase in particle number concentration could be noticed, by a factor of 1.9 from Utö to Preila (the average total number concentration at Utö was 791 cm^{-3}), and by a factor of 1.6 from Vavihill to Preila (the average total number concentration at Vavihill was 998 cm^{-3}). The simultaneous measurements of absorption Ångström exponents close to unity at Preila supported our conclusion that ship emissions in the Baltic Sea contributed to the increase in particle number concentration at Preila.

© 2015 Institute of Oceanology of the Polish Academy of Sciences. Production and hosting by Elsevier Sp. z o.o. This is an open access article under the CC BY-NC-ND license (http://creativecommons.org/licenses/by-nc-nd/4.0/).

1. Introduction

Aerosol particle emissions from global shipping might contribute to 60,000 premature deaths according to a health impact assessment (Corbett et al., 2007), and the emissions are thought to lead to a global temperature decrease due to an increased emission of sulfate particles (Bieltvedt Skeie et al., 2009). The contribution of particles is generally not extensively quantified, for instance how much the ships contribute to the number of particles and the soot concentrations. One study shows that when air is transported across one major shipping lane in the North Sea, it can increase the daily averaged particle number concentration by 11—19% at a coastal station 1 h downwind of the shipping lane (Kivekäs et al., 2014).

This study has a slightly different focus, and examines the influence that ships have on the particle number size distribution (PNSD) when the air travels along several shipping lanes and encounters multiple ship plumes. For this purpose, particle concentrations have been compared between two field stations upwind of the shipping lanes, and one station downwind of the shipping lanes several hundred kilometers from the upwind stations. In the Baltic Sea, two suitable upwind stations were found, Vavihill in southern Sweden, and Utö, an island in the Finnish archipelago. Preila in Lithuania was chosen as downwind station.

In Section 3, it will be quantified how much the particle number concentration in the size range 50—400 nm diameter increased during transport from the upwind stations to the downwind station. However, not only ship emissions affect the particles in this size range as the air is transported several hundred kilometers over the Baltic Sea. There could be in total 5 or more factors contributing to the increase: (1) Boundary layer evolution could affect PNSD; (2) Condensational growth of new or pre-existing particles can contribute to the particle concentration in the focused size ranges of the PNSD; (3) Land based emissions between the upwind stations and downwind station; (4) Emissions of sea spray aerosol particles; (5) Aerosol particle emissions from ships. In Section 4, the influence of each of the first 4 factors will be discarded as potentially significant for the observed increase in particle number concentration. It will instead be shown that the particle size distribution properties match well with those of aged ship emissions as indicated by the trajectory pathways. Measurements of the absorption Ångström exponent will further confirm the influence of ship emissions.

2. Material and methods

2.1. Measurement stations

Two background stations upwind of the shipping emissions were used, Utö in Finland and Vavihill in Sweden. The background station downwind of the shipping lanes was Preila in Lithuania (Fig. 1).

The Utö station (59°47′N, 21°23′E, 8 m above sea level, Hyvärinen et al., 2008) is located on a small island in the Baltic Sea about 60 km from the Finnish south-west coast and more than 10 km from the nearest inhabited islands. Turku, the closest town, is about 90 km to the north-east. The island is almost tree-free. Engler et al. (2007) has shown that at the Utö site, air masses with trajectories prevailing from northern sectors (320°—40°) are considered to be unaffected by anthropogenic land-based sources.

The Vavihill station (56°01′N, 13°09′E, 172 m above sea level) (Kristensson et al., 2008), is located in southern Sweden,

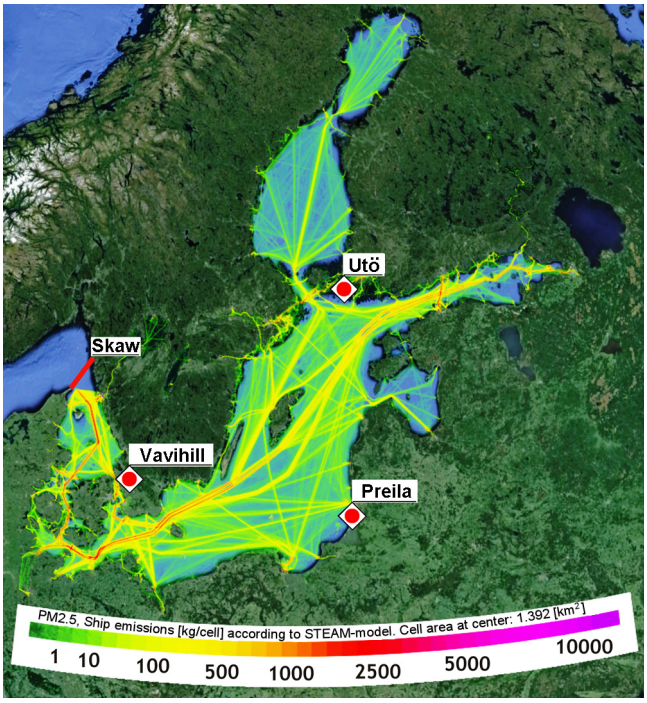

Figure 1 Shipping lanes and Skaw line in the Baltic Sea using Automatic Identification System (AIS, HELCOM, 2013), as well as location of the stations used in this study.

where the surroundings are dominated by deciduous forest. The densely populated areas of Helsingborg and Malmö town and the city of Copenhagen are located 25 km to the west, 50 km to the south, and 45 km to the south-east, respectively.

The Preila station (55°55′N, 21°00′E, 5 m above sea level, Ulevicius et al., 2010) is located in western Lithuania on the Curonian Spit, which is a narrow sandy strip that separates the Baltic Sea and the Curonian Bay. The dunes, up to 50 m height, as well as natural coniferous and dwarf pine trees in low-lying lands dominate in the region. The nearest towns are Klaipeda, 40 km to the north, and Kaliningrad, 90 km to the south.

All stations in this study can be considered to be representative for regional background aerosol measurements because the air is not affected by significant industrial or residential activities in the vicinity of the station. This means that measured aerosol particles are from long range transport, or produced by natural processes. At Preila only the air arriving from the Baltic Sea sector was studied excluding the nearby land based sources. At all stations, the few cases when local pollution sources were evident (high aerosol number concentration increase in certain size bins with short duration) were excluded from the data analysis. The particle number size distribution was measured both before crossing the Baltic Sea, at upwind stations and after the air had crossed the Baltic Sea, at the downwind station. This made it possible to separate the emissions taking place over the Baltic Sea from the pre-existing particle populations at the upwind sites.

Measurement data were collected between September 2009 and June 2010 on these three stations, since there was simultaneous overlap during longer periods in this date interval. PNSD and PM0.4 (particle mass concentrations for particles between 50 and 400 electrical mobility diameter) as well as the absorption Ångström exponent (only Preila and Utö) were measured and calculated using recorded light attenuation at the stations, respectively.

2.2. PNSD measurements and PM0.4 concentrations

Three mobility particle size spectrometers, operating on the same measurement principle (Wiedensohler, 1988), were used to obtain particle number size distributions at the three stations: a Differential Mobility Particle Sizer (DMPS) in Utö (Hyvärinen et al., 2008), a Twin Differential Mobility Particle Sizer (TDMPS) in Vavihill (Kristensson et al., 2008), and a TROPOS-type Scanning Mobility Particle Sizer (SMPS) in Preila. The inter-comparability of the data set is improved by the fact that the measurements were performed within the frame of the European research infrastructure projects EUSAAR (European Supersites for Atmospheric Aerosol Research) and ACTRIS (Aerosols, Clouds, and Trace gases Research InfraStructure Network) as well as the EMEP (European Monitoring and Evaluation Program). The stations were audited by the respective authorities and the instrument inter-comparison was performed annually to ensure high quality and comparable data as required by the individual projects. The stations are visited repeatedly for regular maintenance checks. The uncertainty in particle number concentration is estimated to be within the ranges reported by Asmi et al. (2011) and Wiedensohler et al. (2012). The Differential Mobility Analyzer (DMA) type and length, condensation particle counter (CPC) type, observable particle size range, number of size bin steps, time resolution, and flow rates are given in Table 1.

In Section 3, only PNSD and total number concentrations in the size range between 50 and 400 nm diameter are reported. The total number concentration in this range was integrated numerically from the measured size distributions. An enhanced number concentration of aged particles in the atmosphere from ship emissions is expected to be found partly in this size range (Kivekäs et al., 2014). Even though particles from ship emissions are found also in sizes below 50 nm, the size range below 50 nm diameter was not analyzed here because of influence of new particle formation and lower instrument inter-comparability due to diffusion losses (Wiedensohler et al., 2012). The counting statistic is poor for particles above 400 nm diameter due to the low ambient number concentration which causes relatively more noise in this size range (compare with Kivekäs et al., 2014), and is the reason the particle size range above 400 nm was not included in the analysis. The PNSD have been fitted into three log-normal modes using a least-squares fitting algorithm described by Birmili (2001).

PM0.4 concentrations have been calculated from the PNSD assuming spherical particles and a density of 1500 kg m^{-3}. The density is in reasonable agreement with ambient combustion particles measured in Copenhagen, Denmark (Rissler et al., 2014).

2.3. Light absorption measurements

At the Utö and Preila stations, two identical seven wavelength (370, 450, 520, 590, 660, 880, and 950 nm) aethalometers were used to determine the absorption Ångström exponent. The instrument uses the light transmission through a filter with collected aerosol particles to estimate the aerosol absorption coefficient, σ_{abs} at each given wavelength. To compensate for particle filter loading effects, the same empirical algorithm was used for both instruments (Müller et al., 2011; Virkkula

Table 1 Aerosol PNSD measurement instruments and their specifications at sampling sites.

Site	PNSD instrument	DMA type (length [cm]/type)	CPC type	Size range [nm]	Size steps	Time resolution [min]	Flow rates (aerosol/sheath [lpm])
Preila	SMPS	28/Hauke	UF-02proto[a]	8.7—839.6	71	5	1/10
Utö	DMPS	28/Hauke	TSI 3010	7.0—500.0	30	5	1/10
Vavihill	TDMPS	28 and 11/Hauke	TSI 3760 and 3025	3—900	37	10	1.5/19 and 0.91/5.9

[a] Custom build CPC (Mordas et al., 2005).

et al., 2007; Weingartner et al., 2003). However, because of possible high uncertainties due to applied corrections we will not report black carbon mass concentration in this study. On the other hand, Sandradewi et al. (2008), Ulevicius et al. (2010) and others have shown that the absorption Ångström exponent is a useful quantity to represent the origin of carbonaceous aerosol particles. As the light absorption coefficient decreases monotonically with wavelength, it can be approximated by a power-law expression, $\sigma_{abs} \sim \lambda^{-\alpha}$, where α is the absorption Ångström exponent. The absorption Ångström exponent was obtained by a power-law fit over all seven aethalometer wavelengths.

2.4. Selection of trajectory cases

The hourly trajectories (Fig. 2) at two different altitudes of 100 and 300 m above sea level, representing the Baltic Sea atmospheric boundary layer (Gryning and Batchvarova, 2002), were calculated using the Hybrid Single-Particle Lagrangian Integrated Trajectory (HYSPLIT4) model (Draxler and Rolph, 2003) with the Final Analyses (FNL, 2008–2009) and the Global Data Assimilation System (GDAS) meteorological databases at the NOAA Air Resources Laboratory's web server (Rolph, 2003).

To compare the particle properties between the downwind and upwind stations, only those trajectories passing the entire pathway between the stations over the Baltic Sea were selected. A few exceptions, however, were made to this criterion. In Utö to Preila case, some trajectories passed over the island of Gotland (around 40 km in width of rural land) between the upwind and downwind sites. It results in 7% of the integral of the trajectory pathway being over land. For the Vavihill to Preila trajectory cases there is 70–80 km of land directly downwind of Vavihill that constitutes around 16% of overall trajectory distance. The effects of the land based emissions are discussed later in Section 4. The differences of PNSD, PM0.4 and α between the stations were calculated for individual trajectory cases by comparing the values measured at Preila to the corresponding values at the upwind sites at the time when the air mass passed the upwind site according to the trajectory. This was done by

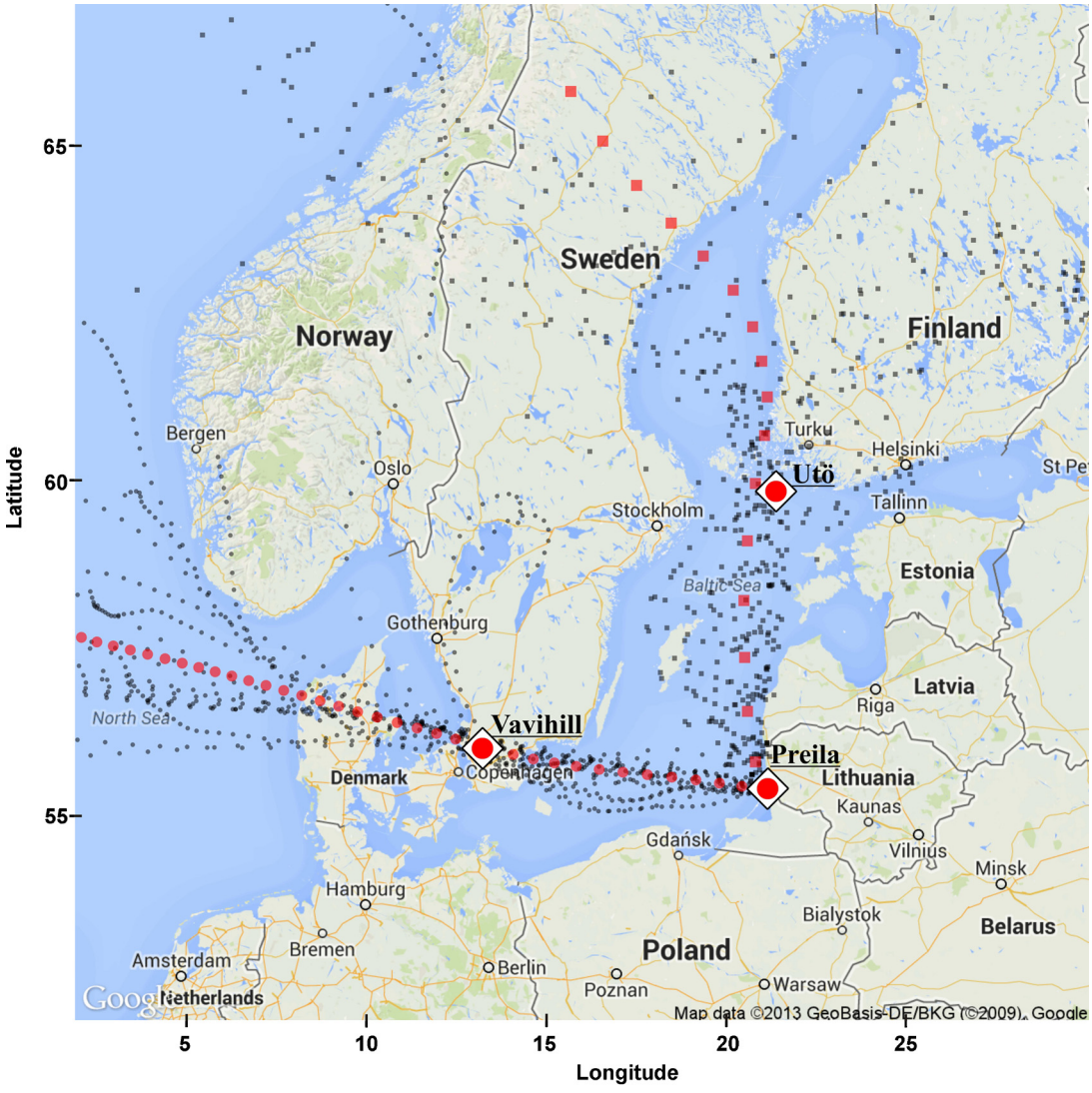

Figure 2 Air mass trajectories passing over the upwind stations and arriving at Preila: smaller dots represent individual hourly trajectories; larger — the mean of trajectories.

calculating the time the air mass needs to travel between the upwind and downwind sites and using this information as a time point at the upwind sites. Also seasonal averages and averages of all trajectory cases were calculated. As the trajectory selection criteria were strict and the simultaneous data coverage of different instruments was not 100%, finding more cases than those described in Section 3 was not possible. Lowering the criteria for the trajectories, for example allowing longer stretches over land, only resulted in a few more trajectories. These cases were more difficult to analyze, and hence did not improve the analysis and did not improve the statistical accuracy. Moreover, only Vavihill to Preila and Utö to Preila, but not vice versa, air mass transports were analyzed. This is because continental air arriving

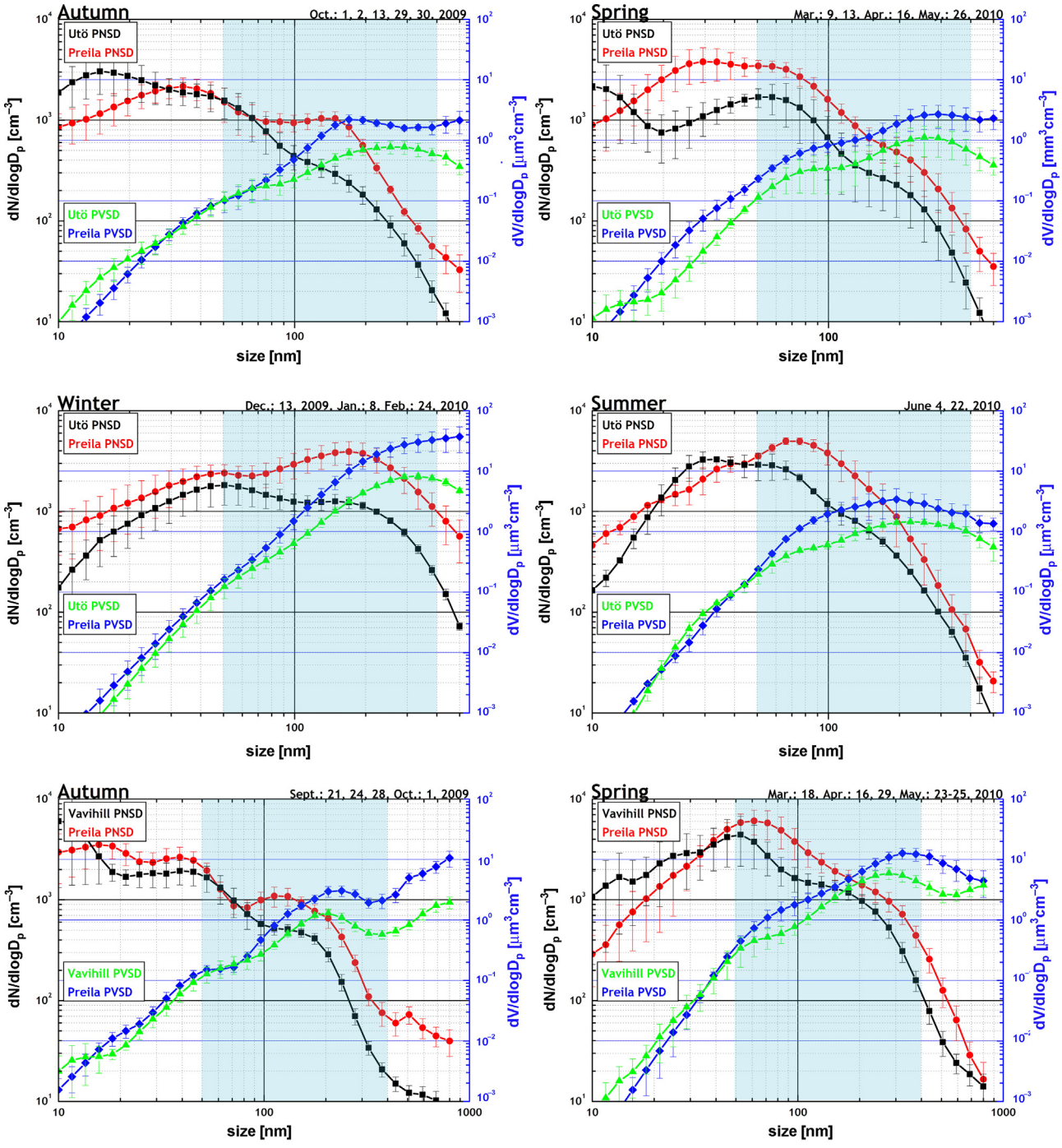

Figure 3 Comparison of average aerosol PNSD and PVSD at Utö, Vavihill, and Preila stations divided by season for our 14 trajectory cases for transport between Utö and Preila and for our 17 trajectory cases for transport between Vavihill and Preila. The 50—400 nm particle diameter range is highlighted with blue color. Here $dN/dlogD_p$ and $dV/dlogD_p$ represent normalized particle number and volume concentrations, respectively. Bars represent a time variability (standard deviation) over the hours sampled. (For interpretation of the references to color in this figure legend, the reader is referred to the web version of this article.)

Table 2 Average aerosol properties at the three stations by season for the 14 trajectory cases between Utö and Preila and for 17 trajectory cases between Vavihill and Preila.

Parameter	Autumn		Winter		Spring		Summer	
	Utö	Preila	Utö	Preila	Utö	Preila	Utö	Preila
$^{50-400}N$ [cm^{-3}] [a]	437 ± 260	697 ± 304	1135 ± 446	2219 ± 1350	587 ± 528	1256 ± 411	1006 ± 197	2131 ± 849
$^{50-400}(N_{Preila}/N_{Utö})$	1.6 ± 1.2		1.9 ± 1.4		2.1 ± 2.0		2.1 ± 0.9	
PM0.4 [$\mu g\ m^{-3}$] [b]	0.7 ± 0.2	1.6 ± 0.3	4.5 ± 0.2	12.7 ± 8.6	0.8 ± 0.8	2.0 ± 1.2	1.3 ± 0.03	2.9 ± 2.2
α [c]	1.2	1.0	1.0	0.9	0.8	1.0	1.0	1.3
Average distance/average time of trajectory [km h^{-1}]	546/18		556/17		575/22		484/15	

Parameter	Autumn		Winter		Spring		Summer	
	Vavihill	Preila	Preila	Vavihill	Vavihill	Preila	Preila	Vavihill
$^{50-400}N$ [cm^{-3}]	508 ± 231	743 ± 238			1489 ± 770	2627 ± 1171		
$^{50-400}(N_{Preila}/N_{Vavihill})$	1.5 ± 0.8				1.8 ± 1.2			
PM0.4 [$\mu g\ m^{-3}$]	0.9 ± 0.3	2.0 ± 0.7	No data		3.7 ± 1.1	6.9 ± 2.4	No data	
Average distance/average time of trajectory [km h^{-1}]	486/10				502/14			

[a] The total aerosol particle number concentration in a range from 50 to 400 nm derived from the PNSD.
[b] Integrated total mass concentration (assuming 1500 kg m^{-3} density).
[c] Absorption Ångström exponent.

at Preila from inland is highly affected by the continental pollution thus lowering the ratio of Baltic Sea emissions to the total PNSD and thereby making the shipping influence harder to quantify. Also the number of cases when air is transported from Preila to the upwind sites is lower due to the prevailing westerly winds in the region.

Lateral position uncertainties of air mass trajectories are known to vary between 10 and 30% of the trajectory length (Stohl, 1998). The distances from Preila to Vavihill and Preila to Utö are about 490 and 530 km respectively, which results in ±50–150 km lateral uncertainty at the distance of the upwind station in trajectories ending at Preila. Within that distance from Vavihill there are several significant centers of population, most notably Copenhagen with a population of almost 2 million people. An aerosol PNSD measured at Preila might carry a significant signal from Copenhagen or other population centers even though the center of the trajectory does not pass through these areas. In such case the same signal would not be present in the Vavihill PNSD. This can cause a difference between the aerosol properties measured at Preila and Vavihill in individual cases. It cannot, however, be assumed that every trajectory calculated to pass over Vavihill passes over Copenhagen in reality. This means that the influence of Copenhagen can be present in some cases but cannot explain systematic changes on the Vavihill to Preila transport route. The trajectories arriving to Preila from Utö do not have such a problem with trajectory uncertainty and large scale anthropogenic sources, as the anthropogenic sources within 150 km from Utö are minor.

3. Results

After analyzing air mass trajectories and measurement data, 14 and 17 cases were chosen when air was transported directly from Utö to Preila or from Vavihill to Preila, respectively, as shown in Fig. 2. Vavihill to Preila air mass transport cases took place mainly in spring (1 case in March, 2 cases in April, 6 cases in May) and autumn (6 cases in September, 2 cases in October). Utö to Preila cases covered all four seasons: Summer (2 cases in June), Spring (2 cases in March, 1 case in April and 1 case in May), Winter (1 case in December, 1 case in January, 1 case in February) and autumn (5 cases in October). The average PNSD and PVSD (Particle Volume Size Distribution) as well as absorption Ångström exponent for the different seasons at the three sites are shown in Fig. 3 and

Table 3 Aerosol PNSD log-normal fit modal parameters.

Mode parameters	Autumn		Winter		Spring		Summer	
	Utö	Preila	Utö	Preila	Utö	Preila	Utö	Preila
Mode 1								
N_1 [cm^{-3}][a]	1327 ± 961	695 ± 249	16	311 ± 288	1432 ± 1872	852 ± 864	230 ± 215	–
$\sigma_{g,1}$ [b]	1.6 ± 0.1	1.9 ± 0.2	2.0	1.9 ± 0.1	1.7 ± 0.2	2.0 ± 0.1	2.0	–
$d_{g,1}$ [nm][c]	12 ± 2	12 ± 1	4	9 ± 2	9 ± 3	9 ± 2	11 ± 2	–
Mode 2								
N_2 [cm^{-3}]	1113 ± 644	1340 ± 682	802 ± 496	1431 ± 791	845 ± 342	2151 ± 1520	1284 ± 253	1588 ± 267
$\sigma_{g,2}$	1.7 ± 0.1	1.7 ± 0.1	1.7 ± 0.1	1.7 ± 0.1	1.7 ± 0.1	1.6 ± 0.1	1.6 ± 0.2	1.6 ± 0.1
$d_{g,2}$ [nm]	36 ± 8	33 ± 7	45 ± 19	43 ± 14	46 ± 17	46 ± 12	49 ± 13	52 ± 2
Mode 3								
N_3 [cm^{-3}]	83 ± 62	366 ± 42	546 ± 43	1854 ± 984	85 ± 114	283 ± 255	113 ± 11	129 ± 47
$\sigma_{g,3}$	1.5 ± 0.3	1.4 ± 0.1	1.6 ± 0.1	1.6 ± 0.1	1.5 ± 0.2	1.5 ± 0.1	1.4	1.4 ± 0.1
$d_{g,3}$ [nm]	179 ± 53	134 ± 12	179 ± 16	169 ± 10	209 ± 35	191 ± 55	186 ± 12	184 ± 4

Mode parameters	Autumn		Winter		Spring		Summer	
	Vavihill	Preila	Vavihill	Preila	Vavihill	Preila	Vavihill	Preila
Mode 1								
N_1 [cm^{-3}]	5665 ± 7547	2922 ± 1359			1053 ± 1569	183 ± 157		
$\sigma_{g,1}$	1.7 ± 0.1	1.5 ± 0.1			1.8 ± 0.2	1.9		
$d_{g,1}$ [nm]	8 ± 1	11 ± 2			10 ± 3	8 ± 2		
Mode 2								
N_2 [cm^{-3}]	875 ± 439	1689 ± 1273			1763 ± 1009	2661 ± 1603		
$\sigma_{g,2}$	1.7 ± 0.1	1.8 ± 0.1	No data		1.6 ± 0.1	1.6 ± 0.1	No data	
$d_{g,2}$ [nm]	42 ± 9	33 ± 5			48 ± 8	50 ± 17		
Mode 3								
N_3 [cm^{-3}]	136 ± 69	334 ± 113			526 ± 193	611 ± 265		
$\sigma_{g,3}$	1.4 ± 0.1	1.4 ± 0.1			1.9 ± 0.1	1.5 ± 0.1		
$d_{g,3}$ [nm]	156 ± 22	152 ± 16			170 ± 18	199 ± 36		

[a] Mode number concentration.
[b] Geometric mode standard deviation.
[c] Geometric mode mean diameter.

Table 2. In Table 2 and Table 3 "±" is used for standard deviation and in the ratios $N_{Preila}/N_{Utö}$ and $N_{Preila}/N_{Vavihill}$ "±" is used as an error from the error propagation formula. The concentrations for each of the 31 cases were calculated from several hour values, which were then used for seasonal averages (in total 69 data points were averaged).

In all seasons and on both transport routes the measured aerosol particle number concentration, in the range from 50 to 400 nm ($^{50-400}N$) was higher by a factor of 1.5–2.1 at Preila than at the upwind station (Table 2). When looking at individual cases, only 7% of Utö to Preila cases and 10% of Vavihill to Preila cases, respectively, showed a slight decrease in $^{50-400}N$ during the transport. In 67% of Utö to Preila cases and 58% of Vavihill to Preila cases the observed increase in $^{50-400}N$ was more than 50% of the value measured at the upwind site. In absolute terms the (seasonally averaged) increase of $^{50-400}N$ in Utö to Preila air mass transport was 260–1125 cm^{-3}, and in the Vavihill to Preila air mass transport 235–1138 cm^{-3}. On Utö to Preila transport path PM0.4 increased by a factor of 2.5, 2.8, 2.4, and 2.2 for autumn, winter, spring, and summer, respectively. On Vavihill to Preila transport path PM0.4 increased by a factor of 2.2 and 1.9 for autumn and spring seasons, respectively. All aerosol PNSDs were also described as a sum of 2 or 3 log-normal modes using an automatic mode fitting algorithm. The modes were defined as: nucleation (particle mean diameter 8–15 nm), Aitken (15–100 nm) and accumulation (100–500 nm) mode. The seasonally averaged modal parameters are presented in Table 3. The increase in N of the accumulation mode is clear in these values.

The Ångström exponent remained around unity (seasonal averages 0.8–1.3) in all cases at both the Utö and Preila sites.

The mobility particle size spectrometers comparability study by Wiedensohler et al. (2012) has shown 5–10% uncertainty in total integrated particle number concentration between the instruments. It can be assumed that a similar range of instrumental uncertainty should be present in this study. However observed increase in $^{50-400}N$ is larger than what the instrumental uncertainty can explain.

The observed changes in $^{50-400}N$ were similar on both transport routes (Utö to Preila and Vavihill to Preila). This was expected because both atmospheric conditions and ship traffic intensity are similar on both routes crossing the main basin of the Baltic Sea.

4. Discussion

4.1. Potential sources of particles. Meteorology: is the change real?

The observed increase in $^{50-400}N$ concentration was significant across both transport routes over the Baltic Sea. A change in observed particle number concentration can, in general, be a result of changed boundary layer (PBL) height (e.g. Ma et al., 2011). Increased PBL height during daytime mixes the particles near the surface with air above. If the air above the PBL has lower particle concentration, this can result in dilution with time and a decrease in N at surface level and the downwind site. The opposite has also been observed when the air aloft is more polluted (Clarke et al., 1998). At night the turbulence weakens leaving the particles equally distributed in the air layer. This does not change N at the surface. New emissions from surface, however, are trapped in the low boundary layer leading to higher increase in N at surface per emission unit compared to the daytime situation. Gryning and Batchvarova (2002) have studied variables which influence boundary layer height over the Baltic Sea. They showed that boundary layer height varies over different time scales, but shows no clear diurnal variation, as seen typically over land cases. This can be explained by the high heat capacity of water making the diurnal variation of sea surface temperature very small and leading to very weak and relatively constant thermal turbulence. Therefore this phenomenon is expected to have an effect only at Vavihill site, which is located inland. In this study the boundary layer height was not examined, but no systematic effects were found when comparing cases in which air had passed the upwind site at daytime and arrived at Preila at night, or vice versa. Also the trajectories at 3000 m altitude showed very similar behavior to those at 100 and 300 m levels, excluding the possibility of significant pollution from the air above. Based on these findings we can assume that the observed systematic changes in $^{50-400}N$ cannot be explained by changes in PBL height only.

The accumulation mode particle number concentrations at both Utö and Preila stations were highest during winter. This might be a result of low boundary layer depths along with stronger inversion conditions and regional scale anthropogenic sources. These sources can be domestic heating in the entire northern Europe. Smaller vertical mixing leads to higher aerosol particle transport efficiency over a longer distance compared to other seasons. This could explain the high values, but not any change during transport between the stations.

4.2. Potential sources of particles. Growth of pre-existing particles and regional new particle formation

Generalized qualitative evidence in particle number concentration changes during transport over the Baltic Sea can be characterized using the relation between the number concentration N of each mode (from Table 3) in the size distributions and the corresponding modal geometric mean diameter. If each mode is assumed to change as a whole, the particle growth rates required to explain the changes between the upwind stations and Preila can be calculated. This was done for both transport routes.

This study is focused on the particle diameter range from 50 to 400 nm. Therefore, the dynamics of new particle formation and growth to Aitken mode are not examined, even though Hyvärinen et al. (2008) and Kristensson et al. (2014) have shown that there is relatively frequent new particle formation over the Baltic Sea. In case of Utö to Preila transport the nucleation and Aitken modes at Utö, as well as new particle formation along the transport path, could have contributed to the measured accumulation mode at Preila only if particle growth rates of at least 7.4 nm h^{-1} (for growing the nucleation mode into an accumulation mode) and 5.7 nm h^{-1} (for Aitken mode to accumulation mode) were assumed (using lowest averaged trajectory speeds). For Vavihill to Preila air mass transport these numbers would have to be as high as 11.9 and 9.3 nm h^{-1} for

nucleation mode to accumulation mode and Aitken mode to accumulation mode, respectively. Recent studies have shown that mean growth rate (GR) of particles with marine origin is 3 ± 0.5 nm h^{-1} (Ehn et al., 2010). This is clearly much less than the growth rates required to explain the changes observed in this study, and therefore the growth of nucleation or Aitken mode particles as the main factor causing the increase in accumulation mode and in $^{50-400}N$ can be ruled out. For new particles formed during the air mass transport the required growth rates would have to be even higher. This rules out the emissions of organics or di-methyl-sulfide from the sea water as an explanation, as well as from new particle formation in ship plumes. The observed changes in the upper Aitken mode and accumulation mode can only be explained by a source of primary emitted particles between the sites.

4.3. Potential sources of particles. Land based emissions between the sites

The air masses advecting over Vavihill pass over a 70–80 km stretch of land between Vavihill and Preila. This can result in significant emissions of primary aerosol particles from land areas east of Vavihill. Even though southern Sweden is densely populated (compared to other parts of Scandinavia), most of the population is located towards west and south of Vavihill. The stretch of land east of Vavihill is mostly used for agriculture and forestry. From this area one can expect emissions from domestic wood combustion and traffic in winter, and from biogenic and traffic sources in summer. These emissions can have an effect on the particle population arriving to Preila from the Vavihill direction. On the transport route from Utö to Preila there is practically no land between the sites, except for the few trajectories passing over Gotland island in the middle of the Baltic Sea. If the land-based emissions were a significant contributor to the observed changes, much smaller changes would be observed on the Utö to Preila transport route. The observed change on Utö to Preila transport path was, however, greater than at Vavihill to Preila transport path in both absolute and relative numbers. Therefore it can be assumed that land based emissions between the sites are not a major or systematic contributor to the observed changes.

4.4. Potential sources of particles. Sea spray

One potential explanation for increased particle number concentration during transport over the Baltic Sea is sea spray; sea salt particles created by breaking waves (Lewis and Schwartz, 2004). Different laboratory methods used to generate surrogate marine aerosols within enclosed tanks confirm the production of accumulation mode particles with geometric mean diameter of 200 nm in marine environment (Stokes et al., 2013).

In this study the contribution of sea salt could not be estimated from chemical composition of the particles, because the only chemical data available was black carbon concentration estimated from absorption measurements. Pettersson et al. (2012) have reported a series of environment fact sheets including monthly wave height variation over a Baltic Sea since 2004. It was shown that the minimum wave height (0.6 m) is mostly common during the late spring to early fall months. After the height minimum, waves start to grow in height and reach maximum (2.0 m) during winter. Taking into account the relatively low wave heights and low salinity of the Baltic Sea the sea salt emissions are expected to be low.

The influence of sea spray emissions on the number concentration was calculated with a parameterization by Sofiev et al. (2011) using the following assumptions: (a) wind speed at 10 m height is the same as trajectory speed at 100 m altitude; (b) salinity of 9.2‰ (southern Baltic sea); (c) temperature of +5°C in winter, +15°C during other seasons; (d) no deposition or coagulation of sea salt particles; (e) well mixed 300 m boundary layer. Using the average seasonal trajectory speeds (Table 2) the sea salt emissions in a size range between 50 and 400 nm were about 1–2 particles per cm^3. Using the highest trajectory speed observed in this study, the emissions were slightly above 10 cm^{-3}. To produce the observed increases in aerosol particle number concentration average wind speeds of 50 m s^{-1} would be required. With this in mind, sea salt aerosol particles can explain only a minor fraction of the observed increase in particle number concentration.

4.5. Potential sources of particles. Shipping

The most plausible explanation for the increased $^{50-400}N$ is emissions from ship traffic. The Baltic Sea Skaw line (Fig. 1) was crossed 62,743 times during 2009, so the presence of intensive ship activity is clear. The main shipping lanes on the Baltic Sea can be seen in Fig. 1. Most of the lanes are located at least 100 km from Preila (except the one leading to Klaipeda harbor), so the plumes have had enough time to disperse, and individual peaks (such as in Kivekäs et al., 2014) can no longer be identified. In a recent study of individual ship exhaust plumes measured at a distance of 1 km (Diesch et al., 2013), either uni- or bi-modal aerosol PNSD were found to be common. These modes included an ultra-fine particle mode at around 10 nm consisting mostly of sulfuric acid (González et al., 2011) and an Aitken mode at 40 nm. A notable increase in particle number concentrations at diameter about 150 nm was also found to be common. This carbon-containing mode is made up of mainly soot and absorbed organic materials. This study is focused mostly on the 50–400 nm particle diameter range where the Aitken mode and the carbon-containing mode is the most prominent one. The size of the increased particle number concentrations, as well as the absorption Ångström exponent near unity can be explained by emissions from shipping. The added particles from shipping would probably not be from the ultra-fine mode or new particle formation in the emission plume, as those would require very high growth rates to make it to the observed size range. The observed Ångström exponents at Utö and Preila are consistent with values measured in engine combustion studies, but lower than values associated with wood burning soot (Sandradewi et al., 2008; Ulevicius et al., 2010).

5. General remarks on this study

Most prior particle measurements of ship emissions have focused on laboratory engine studies (e.g. Kasper et al., 2007), single ship plumes (e.g. Petzold et al., 2008), harbor

or single shipping lane influences on coastal areas (e.g. Kivekäs et al., 2014). In a review study by Kumar et al. (2013) there were no studies of measured total ship emissions over a longer stretch of sea. Ship emissions have been modeled on large scales (e.g. Jalkanen et al., 2009) and even globally (e.g. Corbett and Koehler, 2003). When such models are extended past the exhaust pipe of the ship the dispersion, transport, and deposition of the emissions need to be included (e.g. Stipa et al., 2007). For such models long term measurement data of ambient air is needed for comparison.

The main problem with long term measurements of particles downwind of one or several shipping lanes is how to separate the ship emissions from background particle properties. There are two approaches to this. One is to identify the ship plumes in the data at a downwind station and estimate the background particle properties from the non-plume periods (Kivekäs et al., 2014). This approach can only be used close to the shipping lane, where the individual plumes can be separated (Kivekäs et al., 2014; Petzold et al., 2008). The other approach is the one used in this study. If particle properties in the same air mass are measured prior to and after the air trajectory crossing with a ship lane, all changes can be attributed to phenomena taking place between the measurement sites. As discussed above, there are other factors than just ship emissions affecting the particle properties and that need to be taken into account. The longer the air mass travel distance and travel time between the measurement stations, the more uncertainty there is in the results. Also a longer distance between the stations usually leads to fewer cases when air is advected over both stations. This approach is not suitable for detailed process studies, but can reveal the total influence of shipping to a coastal area. This kind of data is needed for validation of model results.

The observed increase in particle number concentration between the upwind stations and Preila was large. In air masses arriving from Utö 37—53% (seasonal averages) of $^{50-400}N$ measured at Preila came from sources and processes during transport between the sites. For air masses arriving from Vavihill to Preila the corresponding range was 30—45%. This increase is the sum of several factors, but as stated above, emissions from ship traffic are likely the dominant contributor. The measured PNSDs at Utö and Vavihill can also be affected by ship emissions outside the main basin of the Baltic Sea, increasing the total contribution from ship emissions even more. The values obtained in this study are larger than the 11—19% contribution observed by Kivekäs et al. (2014) at North Sea. When comparing these studies one should keep in mind that the observed particle diameter range is different, and this study estimates the combined effect of several shipping lanes, whereas Kivekäs et al. (2014) focused on effects from a single shipping lane.

6. Conclusions

This study focuses on the changes in particle properties during transport over the Baltic Sea. All cases with air passing over the Utö measurement station in Finland or the Vavihill measurement station in Sweden, and then later arriving at the Preila measurement station in Lithuania were analyzed. In this way, the same air was measured before and after crossing the main basin of the Baltic Sea. Aerosol particle size distribution with focus on the 50—400 nm diameter range and absorption Ångström exponent at Preila were compared to those at the upwind sites in the same air mass. The analyzed time period was 10 months (September 2009 to June 2010), allowing qualitative estimation of seasonal variation in the changes. In the authors knowledge no similar study with same air masses measured before and after a long fetch over a heavily trafficked sea area have been published before.

The increase in the number concentration of 50—400 nm particles $^{50-400}N$ was substantial. 26—53% of particles arriving at Preila were generated by processes and emissions taking place between the upwind stations and Preila. The number of analyzed cases was 14 for the Utö to Preila transport path and 17 for the Vavihill to Preila transport path. A clear increase in $^{50-400}N$ was, however, present in almost all studied cases.

The observed increase was the sum of all emissions and processes taking place during the air transport between the sites. These include differences in boundary layer height, growth of pre-existing particles or new particles formed between the sites, land-based emissions between the sites, sea salt emissions, and emissions from ship traffic. The potential contribution of each source was discussed, and shipping was found to be the only source that could explain most of the change. Furthermore, the observed changes were in line with other published ship emission studies.

To reduce the particle emissions from shipping, the International Maritime Organization (IMO) has restricted the sulfur content in ship fuels globally, and especially in defined Sulfur Emission Control Areas (SECAs), which include the Baltic Sea (IMO, 2008). For measuring the total effect of ship emissions on particle properties, and further on health and climate, more long term measurements of ship emissions are needed. The effect of the sulfur regulations on particle properties in large scale also needs to be quantified.

Acknowledgments

The authors would also like to thank State Research Institute Center for Physical Sciences and Technology, Institute of Physics, Finnish Meteorological Institute and Lund University for the measurement data at Preila, Utö, and Vavihill, respectively. Jukka-Pekka Jalkanen at Finnish meteorological Institute is acknowledged for providing the PM2.5 emission map in Fig. 1. Finnish Center of Excellence 272041 (Centre of Excellence in Atmospheric Science — From Molecular and Biological processes to The Global Climate). The study is a contribution to the Lund University Strategic Research Areas: Modeling the Regional and Global Earth System (MERGE).

References

Asmi, A., Wiedensohler, A., Laj, P., Fjaeraa, A.-M., Sellegri, K., Birmili, W., Weingartner, E., Baltensperger, U., Zdimal, V., Zikova, N., Putaud, J.-P., Marinoni, A., Tunved, P., Hansson, H.-C., Fiebig, M., Kivekäs, N., Lihavainen, H., Asmi, E., Ulevicius, V., Aalto, P.P., Swietlicki, E., Kristensson, A., Mihalopoulos, N., Kalivitis, N., Kalapov, I., Kiss, G., de Leeuw, G., Henzing, B., Harrison, R.M., Beddows, D., O'Dowd, C., Jennings, S.G., Flentje, H., Weinhold, K., Meinhardt, F., Ries, L., Kulmala, M., 2011. Number size distributions and seasonality of submicron particles in Europe 2008—2009. Atmos. Chem. Phys. 11, 5505—5538.

Bieltvedt Skeie, R., Fuglestvedt, J., Berntsen, T., Tronstad Lund, M., Myhre, G., Rypdal, K., 2009. Global temperature change from the transport sectors: historical development and future scenarios. Atmos. Environ. 43, 6260–6270.

Birmili, W., 2001. A moment-preserving parameterization of wide particle size distributions. J. Aerosol Sci. 32, S191–S192.

Clarke, A.D., Varner, J.L., Eisele, F., Mauldin, R.L., Tanner, D., Litchy, M., 1998. Particle production in the remote marine atmosphere: cloud outflow and subsidence during ACE 1. J. Geophys. Res. 103 (D13), 16397–16409, http://dx.doi.org/10.1029/97JD02987.

Corbett, J.J., Koehler, H.W., 2003. Updated emissions from ocean shipping. J. Geophys. Res. 108 (D20), 4650, http://dx.doi.org/10.1029/2003JD003751.

Corbett, J.J., Winebrake, J.J., Green, E.H., Kasibhatla, P., Eyring, V., Lauer, A., 2007. Mortality from ship emissions: a global assessment. Environ. Sci. Technol. 41, 8512–8518.

Diesch, J.M., Drewnick, F., Klimach, T., Borrmann, S., 2013. Investigation of gaseous and particulate emissions from various marine vessel types measured on the banks of the Elbe in Northern Germany. Atmos. Chem. Phys. 13, 3603–3618.

Draxler, R.R., Rolph, G.D., 2003. HYSPLIT (HYbrid Single-Particle Lagrangian Integrated Trajectory). NOAA Air Resources Laboratory, Silver Spring, MD Model access via NOAA ARL READY Website, http://www.arl.noaa.gov/ready/hysplit4.html.

Ehn, M., Vuollekoski, H., Petaja, T., Kerminen, V.M., Vana, M., Alto, P., de Leeuw, G., Ceburnis, D., Dupy, R., O'Dowd, C.D., Kulmala, M., 2010. Growth rates during coastal and marine new particle formation in western Ireland. J. Geophys. Res. 115, http://dx.doi.org/10.1029/2010JD014292.

Engler, C., Lihavainen, H., Komppula, M., Kerminen, V.M., Kulmala, M., Viisanen, Y., 2007. Continuous measurements of aerosol properties at Baltic Sea. Tellus B 59, 728–741.

González, Y., Rodríguez, S., García, J.C.G., Trujillo, J.L., García, R., 2011. Ultrafine particles pollution in urban coastal air due to ship emissions. Atmos. Environ. 45, 4907–4914.

Gryning, S-E., Batchvarova, E., 2002. Marine boundary layer and turbulent fluxes over the Baltic Sea: measurements and modelling. Bound.-Lay. Meteorol. 103, 29–47.

Hyvärinen, A.-P., Komppula, M., Engler, C., Kivekäs, N., Kerminen, V. M., Dal Maso, M., Viisanen, Y., Lihavainen, H., 2008. Atmospheric new particle formation at Utö, Baltic Sea 2003–2005. Tellus B 60, 345–352.

IMO (International Maritime Organization), 2008. Amendments to the annex of the protocol of 1997 to amend the international convention for the prevention of pollution from ships, 1973, as modified by the protocol of 1978 relating thereto. Available at: http://www.imo.org/ (March 6th, 2014).

Jalkanen, J.-P., Brink, A., Kalli, J., Pettersson, H., Kukkonen, J., Stipa, T., 2009. A modelling system for the exhaust emissions of marine traffic and its application to the Baltic Sea area. Atmos. Chem. Phys. 9, 9209–9223.

Kasper, A., Aufdenblatten, S., Forss, A., Mohr, M., Burtscher, H., 2007. Particulate emissions from a low-speed marine diesel engine. Aerosol Sci. Technol. 41, 24–32.

Kivekäs, N., Rusnak, V., Carreno Correa, S., Massling, A., Skov, H., Lange, R., Kristensson, A., 2014. Contribution of ship traffic to aerosol particle concentrations downwind of a major shipping route. Atmos. Chem. Phys. 14, 8419–8454.

Kristensson, A., Dal Maso, M., Swietlicki, E., Hussein, T., Zhou, J., Kerminen, V.-M., Kulmala, M., 2008. Characterization of new particle formation events at a background site in Southern Sweden: relation to air mass history. Tellus B 60, 330–344.

Kristensson, A., Johansson, M., Swietlicki, E., Kivekäs, N., Hussein, T., Nieminen, T., Kulmala, M., Dal Maso, M., 2014. NanoMap: Geographical mapping of atmospheric new particle formation through analysis of particle number size distribution data. Boreal Environ. Res. 19 (Suppl. B), 329–342.

Kumar, P., Pirjola, L., Ketzel, M., Harrison, R.M., 2013. Nanoparticle emissions from 11 non-vehicle exhaust sources – a review. Atmos. Environ. 67, 252–277.

Lewis, E.R., Schwartz, S.E., 2004. Sea salt Aerosol Production: Mechanisms, Methods, measurements, and models – A Critical review. Geophys. Monogr. Series, vol. 152. American Geophysical Union, Washington, DC, 413 pp.

Ma, N., Zhao, C.S., Nowak, A., Müller, T., Pfeifer, S., Cheng, Y.F., Deng, Z.Z., Liu, P.F., Xu, W.Y., Ran, L., Yan, P., Göbel, T., Hallbauer, E., Mildenberger, K., Henning, S., Yu, J., Chen, L.L., Zhou, X.J., Stratmann, F., Wiedensohler, A., 2011. Aerosol optical properties in the North China Plain during HaChi campaign: an in-situ optical closure study. Atmos. Chem. Phys. 11, 5959–5973.

Mordas, G., Kulmala, M., Petäjä, T., Aalto, P.P., Matulevicius, V., Grigoraitis, V., Ulevicius, V., Grauslys, V., Ukkonen, A., Hämeri, K., 2005. Design and performance characteristics of a condensation particle counter UF-02proto. Boreal Environ. Res. 10, 543–552.

Müller, T., Henzing, J.S., de Leeuw, G., Wiedensohler, A., Alastuey, A., Angelov, H., Bizjak, M., Collaud Coen, M., Engström, J.E., Gruening, C., Hillamo, R., Hoffer, A., Imre, K., Ivanow, P., Jennings, G., Sun, J.Y., Kalivitis, N., Karlsson, H., Komppula, M., Laj, P., Li, S.-M., Lunder, C., Marinoni, A., Martins dos Santos, S., Moerman, M., Nowak, A., Ogren, J.A., Petzold, A., Pichon, J.M., Rodriquez, S., Sharma, S., Sheridan, P.J., Teinilä, K., Tuch, T., Viana, M., Virkkula, A., Weingartner, E., Wilhelm, R., Wang, Y.Q., 2011. Characterization and intercomparison of aerosol absorption photometers: result of two intercomparison workshops. Atmos. Meas. Tech. 4, 245–268, http://dx.doi.org/10.5194/amt-4-245-2011.

Pettersson, H., Lindow, H., Brüning, T., 2012. Wave climate in the Baltic Sea in 2012. HELCOM Baltic Sea Environment Fact Sheets. Online. 2014. http://www.helcom.fi/baltic-sea-trends/environment-fact-sheets/.

Petzold, A., Hasselbach, J., Lauer, P., Baumann, R., Franke, K., Gurk, C., Schlager, H., Weingartner, E., 2008. Experimental studies on particle emissions from cruising ship, their characteristic properties, transformation and atmospheric lifetime in the marine boundary layer. Atmos. Chem. Phys. 8, 2387–2403, http://dx.doi.org/10.5194/acp-8-2387-2008.

Rissler, J., Nordin, E.Z., Eriksson, A.C., Nilsson, P.T., Frosch, M., Sporre, M.K., Wierzbicka, A., Svenningsson, B., Londahl, J., Messing, M.E., Sjogren, S., Hemmingsen, J.G., Loft, S., Pagels, J.H., Swietlicki, E., 2014. Effective density and mixing state of aerosol particles in a near-traffic urban environment. Environ. Sci. Technol. 48, 6300–6308, http://dx.doi.org/10.1021/es5000353.

Rolph, G.D., 2003. Real-time Environmental Applications and Display sYstem (READY). NOAA Air Resources Laboratory, Silver Spring, MD Website (http://www.arl.noaa.gov/ready/hysplit4.html).

Sandradewi, J., Prevot, A.S.H., Weingartner, E., Schmidhauser, R., Gysel, M., Baltensperger, U., 2008. A study of wood burning and traffic aerosols in an Alpine valley using a multi-wavelength Aethalometer. Atmos. Environ. 42, 101–112.

Sofiev, M., Soares, J., Prank, M., de Leeuw, G., Kukkonen, J., 2011. A regional-to-global model of emission and transport of sea salt particles in the atmosphere. J. Geophys. Res. 116 (D21), http://dx.doi.org/10.1029/2010JD014713.

Stipa, T., Jalkanen, J.-P., Hongisto, M., Kalli, J., Brink, A., 2007. Emissions of NOx from Baltic Shipping and First Estimates of their Effects on Air Quality and Eutrophication of the Baltic Sea. Univ. Turku, ISBN: 978-951-53-3028-4, 33 pp.

Stohl, A., 1998. Computation, accuracy and applications of trajectories – a review and bibliography. Atmos. Environ. 32, 947–966.

Stokes, M.D., Deane, G.B., Prather, K., Bertram, T.H., Ruppel, M.J., Ryder, O.S., Brady, J.M., Zhao, D., 2013. A Marine Aerosol Reference Tank system as a breaking wave analogue for the production of foam and sea-spray aerosols. Atmos. Meas. Tech. 6, 1085–1094.

Ulevicius, V., Bycenkiene, S., Remeikis, V., Garbaras, A., Kecorius, S., Andriejauskiene, J., Jasineviciene, D., Mocnik, G., 2010.

Characterization of pollution events in the East Baltic region affected by regional biomass fire emissions. Atmos. Res. 2, 190—200.

Virkkula, A., Makela, T., Hillamo, R., Yli-Tuomi, T., Hirsikko, A., Hameri, K., Koponen, I.K., 2007. A simple procedure for correcting loading effects of Aethalometer data. J. Air Waste Manage. 57, 1214—1222.

Weingartner, E., Saathoff, H., Schnaiter, M., Streit, N., Bitnar, B., Baltensperger, U., 2003. Absorption of light by soot particles: determination of the absorption coefficient by means of aethalometers. J. Aerosol Sci. 34, 1445—1463.

Wiedensohler, A., 1988. An approximation of the bipolar charge distribution for particles in the submicron size range. J. Aerosol Sci. 19, 387—389.

Wiedensohler, A., Birmili, W., Nowak, A., Sonntag, A., Weinhold, K., Merkel, M., Wehner, B., Tuch, T., Pfeifer, S., Fiebig, M., Fjäraa, A. M., Asmi, E., Sellegri, K., Depuy, R., Venzac, H., Villani, P., Laj, P., Aalto, P., Ogren, J.A., Swietlicki, E., Williams, P., Roldin, P., Quincey, P., Hüglin, C., Fierz-Schmidhauser, R., Gysel, M., Weingartner, E., Riccobono, F., Santos, S., Grüning, C., Faloon, K., Beddows, D., Harrison, R., Monahan, C., Jennings, S.G., O'Dowd, C.D., Marinoni, A., Horn, H.-G., Keck, L., Jiang, J., Scheckman, J., McMurry, P.H., Deng, Z., Zhao, C.S., Moerman, M., Henzing, B., de Leeuw, G., Löschau, G., Bastian, S., 2012. Mobility particle size spectrometers: harmonization of technical standards and data structure to facilitate high quality long-term observations of atmospheric particle number size distributions. Atmos. Meas. Tech. 5, 657—685.

Oceanologia (2016) 58, 13—24

Available online at www.sciencedirect.com

ScienceDirect

journal homepage: www.elsevier.com/locate/oceano

ORIGINAL RESEARCH ARTICLE

Impact of wild forest fires in Eastern Europe on aerosol composition and particle optical properties☆

Tymon Zielinski*, Tomasz Petelski, Agata Strzalkowska, Paulina Pakszys, Przemyslaw Makuch

Institute of Oceanology, Polish Academy of Sciences, Sopot, Poland

Received 13 May 2015; accepted 23 July 2015
Available online 23 August 2015

KEYWORDS
Biomass burning aerosols;
Optical properties;
AOD;
Regional aerosol modifications;
AERONET

Summary In this paper the authors discuss the changes of aerosol optical depth (AOD) in the region of eastern Europe and the Baltic Sea due to wild fire episodes which occurred in the area of Belarus and Ukraine in 2002. The authors discuss how the biomass burning aerosols were advected over the Baltic area and changed the composition of aerosol ensemble for a period of several summer weeks. The air pressure situation and slow wind speeds also facilitated the development of such conditions. As a consequence very high AOD levels were recorded, by an order of 3—4 higher versus normal conditions and they significantly increased the annual averages. On particular days of August 2002 the AOD values reached a level of over 0.7. On these days fine particles fully dominated the entire ensemble of aerosol particles. They were either sulfates or smoke particles. Such situation was unique over a period of many years and it had its serious consequences for the region and especially for the Baltic Sea.
© 2015 Institute of Oceanology of the Polish Academy of Sciences. Production and hosting by Elsevier Sp. z o.o. This is an open access article under the CC BY-NC-ND license (http://creativecommons.org/licenses/by-nc-nd/4.0/).

☆ The support for this study was partly provided by the project Satellite Monitoring of the Baltic Sea Environment — SatBałtyk founded by European Union through European Regional Development Fund contract No. POIG 01.01.02-22-011/09. It has also been made within the framework of the NASA/AERONET Program and POLAND-AOD network.
* Corresponding author at: Institute of Oceanology, Polish Academy of Sciences, Powstańców Warszawy 55, 81-712 Sopot, Poland. Tel.: +48 507300208.
E-mail address: tymon@iopan.gda.pl (T. Zielinski).
Peer review under the responsibility of Institute of Oceanology of the Polish Academy of Sciences.

ELSEVIER Production and hosting by Elsevier

http://dx.doi.org/10.1016/j.oceano.2015.07.005
0078-3234/© 2015 Institute of Oceanology of the Polish Academy of Sciences. Production and hosting by Elsevier Sp. z o.o. This is an open access article under the CC BY-NC-ND license (http://creativecommons.org/licenses/by-nc-nd/4.0/).

1. Introduction

Climate change results from both natural and human-induced modifications of the Earth's energy balance. These climate-related factors include variations in the amounts of greenhouse gases, aerosols, changes in land use, and the amount of energy Earth receives from the Sun (IPCC, 2007, 2013).

Atmospheric aerosols are responsible for radiative forcing on the surface, and they affect from local and regional weather patterns to global climate. Atmospheric aerosols are considered among the factors which play a significant role in the Earth's energy budget and thus affect global climate. However, as the IPCC reports show uncertainties are still significant regarding their radiative and climate effects (IPCC, 2007, 2013). Aerosol particles with their scattering and absorptive properties (so-called direct effect), are responsible for a number of environmental effects, i.e. they play a major role in the visibility problem, and they can also have a significant impact on UV radiation (Torres et al., 1998, 2007), and photochemistry in the boundary layer (Graber and Rudich, 2006; Kirchstetter et al., 2004).

Regional scale variations in radiative forcing have significant regional and global climatic implications, which cannot be addressed through the idea of global mean radiative forcing (Markowicz et al., 2011). Until now only a small number of studies has been dedicated to regional radiative forcing and response. It is still very difficult to describe a regional forcing and response in the observational record. Regional forcings may induce global climate responses, while global forcings can be connected with regional scale climate responses (Shindell et al., 2010; Tosca et al., 2013).

Aerosols' direct radiative effects are manifested in scattering and absorbing of radiation in both shortwave and longwave. The state of our knowledge of direct radiative forcing of aerosol particles is limited mainly due to difficulties of the proper quantification of global distributions and mixing states of aerosols. The state of mixing of aerosol particles affects particle optical properties, which thus are not well understood and are difficult to parameterize in climate models. Additionally, small-scale variability of such meteorological parameters as humidity and temperature, which also influences aerosol optical properties, is also difficult to represent in models (Byčenkiene et al., 2013; Petelski et al., 2014; Smirnov et al., 2011; Zielinski and Zielinski, 2002).

Wild fires have been modifying atmospheric composition for centuries. They have significant impact on the physical environment including modifications of land cover, land use, biodiversity or inducing climate changes and this impact is on both regional and global scales (Chubarova et al., 2012; Pio et al., 2008). Differences in aerosol composition on a regional scale as a result of advection of particulates from the regions of wild fires have been described before (Pio et al., 2008).

Additionally such disasters also have impact on human health and even on the socio-economic situations in the affected regions (Beringer et al., 2003). In order to describe and quantify the role of biomass burning as a source of atmospheric gases and aerosol particles to the atmosphere, information is required on the global magnitude of biomass burning (Chubarova et al., 2012; Zawadzka et al., 2013). Biomass burning aerosols include two important chemical components: black carbon and organic carbon. The first component primarily absorbs solar radiation, and the second scatters solar radiation (Cooke and Wilson, 1996; Haywood and Ramaswamy, 1998; Liousse et al., 1996). Takemura et al. (2002) made 3-D model simulations of radiative forcing of various aerosol species. In their model they divided all the main tropospheric aerosols into the following groups — carbonaceous (organic and black carbons), sulfate, soil dust, and sea salt aerosols. They compared their model simulations of total aerosol optical thickness, Ångström exponent, and single-scattering albedo for mixtures of four aerosol species with the observed data from both optical ground-based measurements and satellite remote sensing retrievals at a great number of stations. They reported the mean difference between the simulation and observations to be less than 30% for the optical depth and less than 0.05 for the single-scattering albedo in most regions (Takemura et al., 2002).

According to Bond et al. (2013) the estimate for the period 1750—2005, i.e. the industrial-era, direct radiative forcing of atmospheric black carbon is +0.71 W m^{-2} with 90% uncertainty bounds of (+0.08, +1.27) W m^{-2}. However, total direct forcing of black carbon from all known sources, with the pre-industrial background included, estimates to +0.88 (+0.17, +1.48) W m^{-2}. Bond et al. (2013) also report that: "the best estimate of industrial-era climate forcing of black carbon through all forcing mechanisms, including clouds and cryosphere forcing, is +1.1 W m^{-2} with 90% uncertainty bounds of +0.17 to +2.1 W m^{-2}".

The Baltic Sea is a unique basin of the World Ocean. It is a small and shallow sea located in the north-eastern part of Europe, and is surrounded by nine highly industrialized countries — Denmark, Estonia, Finland, Germany, Lithuania, Latvia, Poland, Russia and Sweden with some 85 million people living in the catchment area. Additionally, largely forest covered areas in Poland, Lithuania, Belarus and Ukraine are in the close vicinity of the Baltic.

According to Zdun et al. (2011) summer wind patterns for station in Gotland, located in the middle part of the Baltic Sea over a period between 1999 and 2003 show that around 50% come from easterly and southerly directions, thus crossing areas of Belarus and Ukraine. Zielinski (2004) reported that majority of winds in summer come to Sopot area, in the southern part of the Baltic Sea, from NE and SE directions, which is in accordance with Zdun's observations. Therefore, aerosol particles over the Baltic Sea, especially in summer, usually originate from a number of continental sources and it is difficult to observe one type of aerosols, e.g. marine over the Baltic. A number of aerosol studies have been conducted in the region, however, regular sunphotometric aerosol measurements have not been made in the Baltic area until 1999, when such studies had been originated within the NASA/AERONET program (http://aeronet.gsfc.nasa.gov/).

Year 2002 was unique in terms of air temperatures which were recorded in the region of central Europe and the Baltic area. Seven consecutive months were warm or very warm, and between February and September the multiannual average air temperature was higher than the normal temperature by over 1°C. May and August 2002 were extraordinarily warm. Such conditions were very conducive to wild fire outbreaks in the areas of Eastern Europe, which are widely covered by forests and meadows.

Years 2007 and 2008 were also very hot in the discussed region, however, warm periods were shorter than in 2002 and

lasted mostly 4 weeks. Then temperatures returned to the multiannual average for some time and warm periods returned. These years and 2010 were also fire abundant in the discussed region but the air mass trajectories were such that the smoke plume did not reach the area of the Baltic Sea. Thus these years have not been analyzed in this paper.

This paper presents information on the impact of wild fires in the Eastern Europe on aerosol optical properties in that region with a special emphasis on the Baltic Sea area. The authors discuss how the biomass burning aerosols were advected over the Baltic area and changed the composition of aerosol ensemble for a period of several weeks. Further the authors provide justification that those aerosols were fine particles and they increased the aerosol optical depth by an order of 3—4 versus normal conditions.

2. Description of the study area and research methodology

Location of the selected AERONET stations around the Baltic Sea is shown in Fig. 1. All three stations have used CIMEL sunphotometers with 7 wavelengths (http://aeronet.gsfc.nasa.gov/).

The authors decided to analyze the data from these three stations since all three of them operated in summer 2002 and are representative for this study. The AERONET stations selected for analyses in this paper include: Sopot station, on the Baltic Sea coast, operating between 1999 and 2002 and the Gotland station, located in the northern part of the island of Gotland, 50 m inshore. Owing to the location of the island in the central Baltic Sea this station is sometimes regarded as representative for the Baltic Sea conditions (Zdun et al., 2011). The data were collected at the station from 1999 to 2004. The third station analyzed is the Minsk station which has been operated since 2002. The station coordinates and the CIMEL wavelengths at each of the three stations are presented in Table 1.

For the analyses the authors have used only level 2.0 quality assured and with pre- and post-field calibration applied, cloud-screened data (http://aeronet.gsfc.nasa.gov/).

The type of aerosol particles can be deduced using two optical parameters: aerosol optical depth (AOD) and the Ångström parameter (Bokoye et al., 1997; Zielinski and Zielinski, 2002). Both of these parameters strongly depend on the sources of particle generation and the type of air masses (Smirnov et al., 2011). On a regional scale or in cases of such regional seas like the Baltic Sea, aerosols are often difficult to define since both marine and continental types of particles mix in the air, depending on wind direction. Such mixture comprises particles of different optical properties. The Ångström parameter is used to estimate particle size. Large values of this parameter indicate fine particles while small values indicate coarse aerosols (Zawadzka et al., 2013).

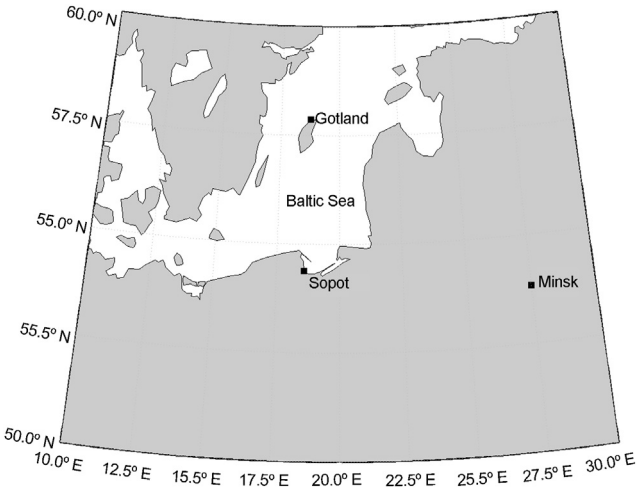

Figure 1 Selected AERONET stations located in the vicinity of the Baltic Sea.

The wavelength dependence of aerosol optical depth can be expressed as follows (Carlund et al., 2005; Eck et al., 1999; Smirnov et al., 1994):

$$\tau(\lambda) = \beta(\lambda)^{-\alpha}, \tag{1}$$

where α is the Ångström parameter, $\tau_\alpha(\lambda)$ is AOD at a wavelength λ, and β is Ångström coefficient of turbidity.

The spectral dependence of the AOD as well as the Ångström exponent are sensitive to the calibration coefficients. In this study we used the Ångström exponent α defined at two wavelengths as follows:

$$\alpha = -\frac{\ln(\tau_1/\tau_2)}{\ln(\lambda_1/\lambda_2)}. \tag{2}$$

The air mass back trajectories have been calculated at 500, 1500 and 3000 m using the NOAA-HYSPLIT model (Draxler and Rolph, 2010). In order to obtain additional information about transport of air pollution a long-range pollution transport model was applied. For this purpose the authors used the Navy Aerosol Analysis and Prediction System (NAAPS) (Christensen, 1997; Witek et al., 2007). The NAAPS simulations are presented in Fig. 11. Additionally, the AOD results have been supported by the analyses of satellite aerosol optical depth data from the Moderate Resolution Imaging Spectroradiometer (MODIS), mounted onboard the Aqua and Terra satellites.

3. Results and discussion

In summer 2002 vast areas in Belarus and Ukraine were subject to serious and long-lasting wild fires, which were a source for significant production of biomass burning

Table 1 Three selected AERONET stations; coordinates and CIMEL wavelengths at each site.

AERONET station	Coordinates	CIMEL wavelengths [nm]
Sopot, Poland	54°27′03″N, 18°33′54″E	340, 380, 440, 500, 675, 870, 1020
Gotland, Sweden	57°55′N, 18°57′E	340, 380, 440, 500, 675, 870, 1020
Minsk, Belarus	53.92°N, 27.60°E	340, 380, 440, 500, 675, 870, 1020

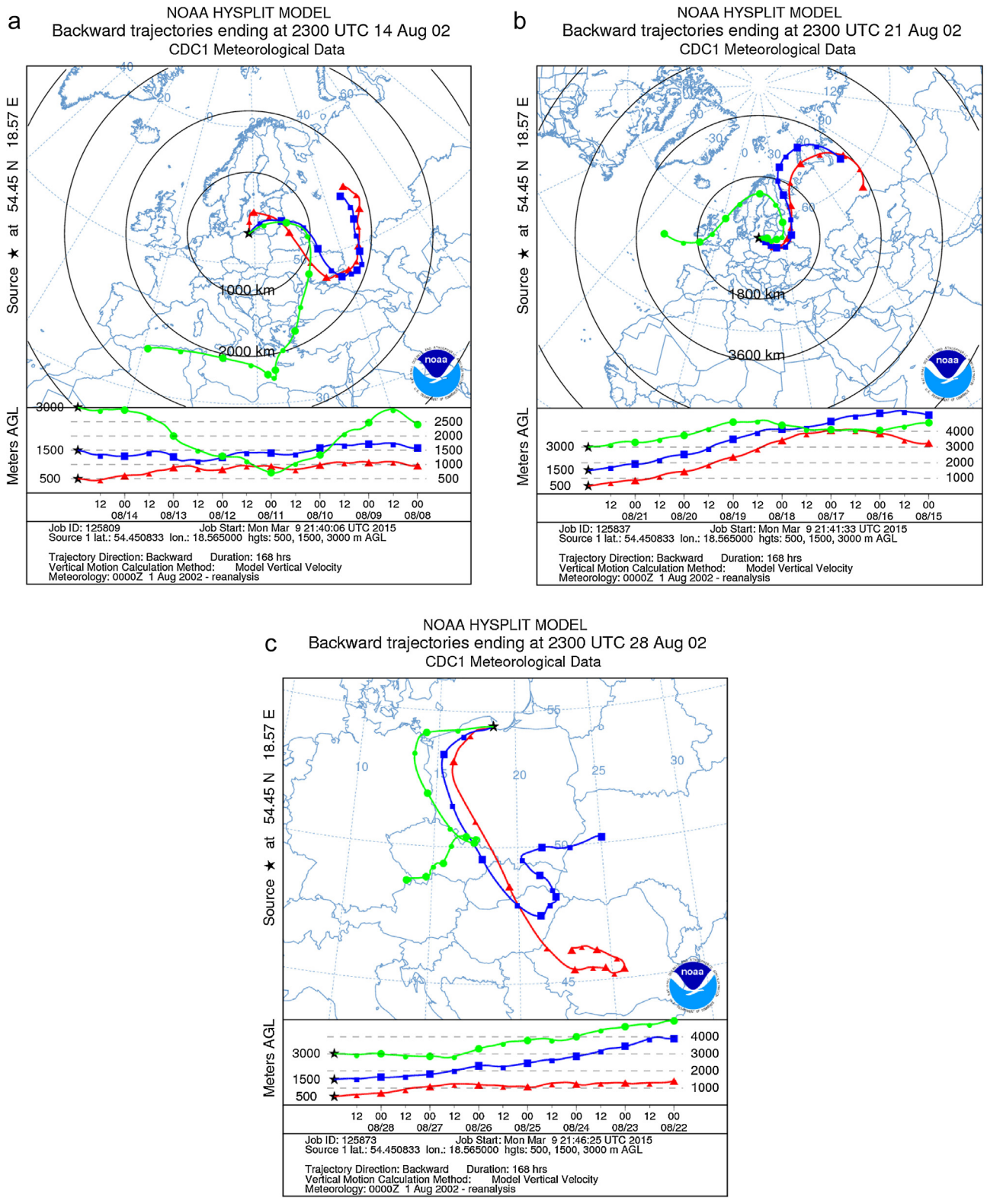

Figure 2 The 168 h NOAA HYSPLIT air-mass back trajectories for August 2002 at 500, 1500 and 3000 m above sea level (a.s.l.) ending in Sopot (on 14 August (a), 21 August (b) and 28 August (c)). (For interpretation of the references to color in this figure legend, the reader is referred to the web version of this article.)

particulates injected to the atmosphere, which reached atmospheric layers beyond the boundary layer (Evangeliou et al., 2015). The fire breakouts started in July and their peak was observed in late July and all over August 2002. In August 2002 wind patterns were such that the locally produced aerosols in the region of Belarus and Ukraine were transported over the area of the Baltic Sea (Figs. 2 and 3).

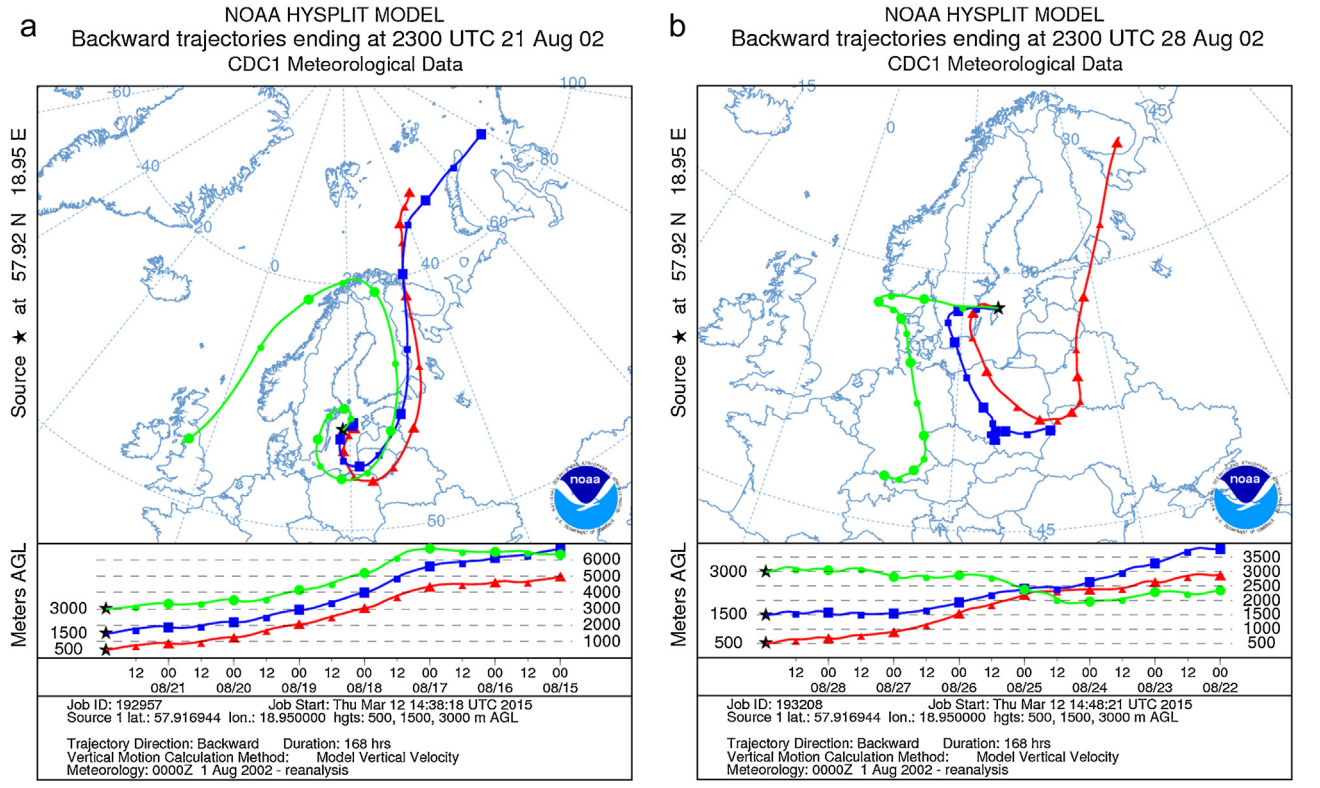

Figure 3 The 168 h NOAA HYSPLIT air-mass back trajectories for August 2002 at 500, 1500 and 3000 m above sea level (a.s.l) ending in Gotland (on 21 August (a) and 28 August (b)). (For interpretation of the references to color in this figure legend, the reader is referred to the web version of this article.)

Figs. 2 and 3 show that between 8 and 28 August 2002 air masses moved over the area of wild fire regions towards the Baltic Sea. For the station in Sopot this is especially true for the first 2 decades of August and less for the last 10 days. The trajectories for Sopot crossed the wild fire areas at all three chosen altitudes, i.e. 500, 1500 and 3000 m a.s.l. In case of the Gotland station basically entire month is characterized by the air masses which crossed the region of wild fires at all three altitudes. In majority of cases all air masses passed over the station in Minsk.

Figs. 4 and 5 show level 2.0 AOD values at all three stations for entire 2002 and August 2002, respectively.

These 2 figures provide a general overview of the AOD changes over a period of an entire year. They reveal that AOD values in summer, especially in August are significantly increased in comparison to other months in 2002. The average annual AODs at all stations are unusually high and they differ from those in 1999 and 2003 (Table 2). These two years have been chosen for comparison since there are level 2.0 data available from the 3 stations to compare with year 2002 and especially August 2002.

The differences presented in Table 2 clearly show that the AOD values were dramatically increased in 2002, especially in August 2002 in comparison with 1999 and 2003, when no wild fires of the same intensity as in 2002 were observed in the region. The differences at stations in Sopot and Gotland reach a level of 2.85 and 4.88 in August 1999 and 2002, respectively. The difference for the Minsk station between August 2002 and 2003 is of an order of 3.42. This tendency is true for all other years at all three stations, whenever data are available. Table 3 shows the level 2.0 Ångström values calculated in the same manner as in case of the AODs presented in Table 2.

Clearly the values of the Ångström exponent are high, which is normal for summer conditions since prevailing winds reach the Baltic stations from the continental areas, thus transporting large amounts of dust and generally small particles. Therefore, the annual exponent differences are far less pronounced than in case of the AODs, still the August values are the ones which differ from other years the most. The situation during particular days in August was such that on certain days the AOD values were almost unrealistically

Table 2 Average annual and August level 2.0 AOD values at 500 nm (Sopot and Gotland) and at 440 nm (Minsk) for selected years (1999, 2002 and 2003).

Station	1999	August 1999	2002	August 2002	2003	August 2003
Sopot, Poland	0.113	0.145	0.239	0.413	N/A	N/A
Gotland, Sweden	0.089	0.065	0.170	0.317	0.142	0.204
Minsk, Belarus	N/A	N/A	0.431	0.557	0.224	0.163

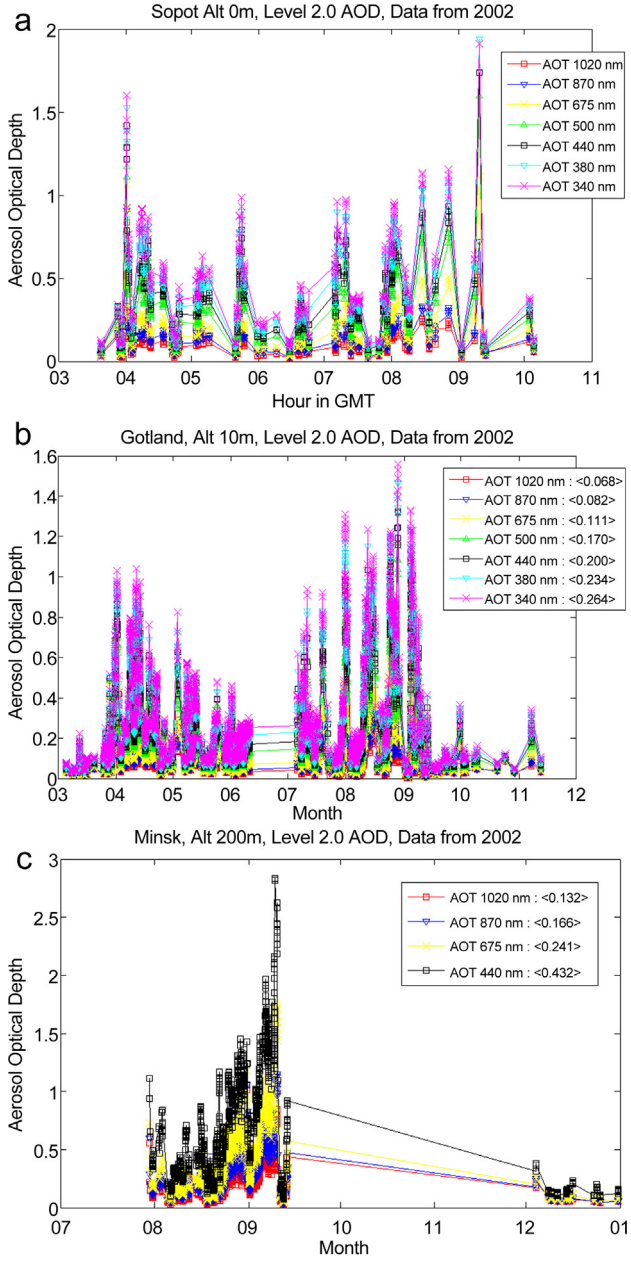

Figure 4 Aerosol optical depth measured in 2002 at three AERONET stations: Sopot (a), Gotland (b) and Minsk (c). (For interpretation of the references to color in this figure legend, the reader is referred to the web version of this article.)

high for regular aerosol conditions in the region. Table 4 shows the daily averaged level 2.0 AOD values at stations in Sopot and Gotland for all available measurement days at both stations in August 2002.

Table 4 The daily averaged level 2.0 AOD values (500 nm) at stations in Sopot and Gotland for all available measurement days at both stations in August 2002.

Day in August 2002	Sopot	Gotland
1	0.400	0.471
4	0.547	0.079
7	0.319	0.087
8	0.234	0.093
9	0.186	0.118
15	0.731	0.661
18	0.206	0.074
21	0.374	0.093
27	0.755	0.545

The data presented in Table 4 clearly indicate high AOD values at the station in Sopot during all measurement days. However, between 7 and 9 August 2002 these values are only slightly higher than on "clean" years of 1999 and 2003 (Table 2). The AOD values on 15 and 27 August 2002 are so high that they exceed the regular values (Table 2) by an order of almost 4 or 5. There is a similar situation at the station in Gotland, however the 7–9 August 2002 values are practically indicating very clean atmosphere in the station area. Again 15 and 27 August 2002 show outrageously high AODs. Therefore, in the reminder of the paper the authors concentrate on these two days. Fig. 6a–d shows level 2.0 AOD values (at seven wavelengths) on 15 and 27 August 2002 at the stations in Sopot and Gotland.

On both days and at both stations the AOD values are very high at all seven wavelengths. With exception to 27 August 2002 at the station in Gotland the AODs are rather uniform during the measurement period. The average daily level 2.0 Ångström parameters calculated from 440 and 870 nm wavelengths for 15 and 27 August 2002 for stations in Sopot and Gotland were 1.475, 1.595 and 1.492, 1.662, respectively. All these values indicate presence of fine particles in the atmosphere, which were absolutely dominating on these two days (Fig. 7a–d).

On both days fine particles were dominating the atmosphere measured at both stations and on 27 August 2002 they were basically the only fraction present in the air over the both stations. This indicates that the particles could have been advected to the measurement area from other regions and thus the NOAA HYSPLIT model was applied to calculate the air mass back trajectories. The 96 h air mass back trajectories calculated for 15 and 27 August 2002 for the stations in Sopot and Gotland are presented in Fig. 8a–d.

On 15 August 2002 air masses were advected to both stations from the area of Belarus and Ukraine at all three

Table 3 Average annual and August level 2.0 Ångström values (440/870 nm) at stations in Sopot, Gotland and Minsk for selected years (1999, 2002 and 2003).

Station	1999	August 1999	2002	August 2002	2003	August 2003
Sopot, Poland	1.232	1.693	1.188	1.561	N/A	N/A
Gotland, Sweden	1.120	1.510	1.258	1.650	1.003	1.290
Minsk, Belarus	N/A	N/A	1.369	1.505	1.312	1.586

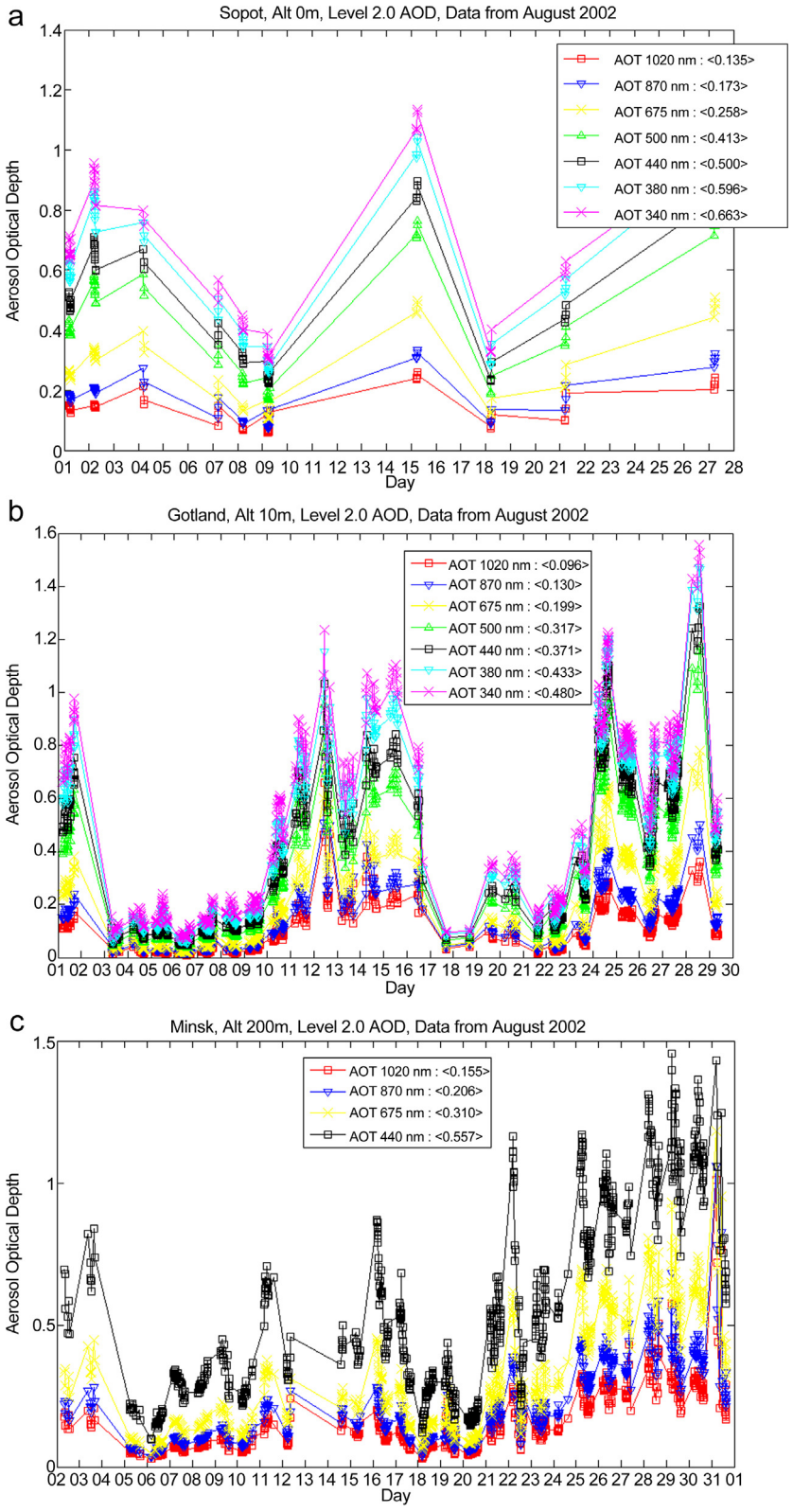

Figure 5 Aerosol optical depth measured in August 2002 at three AERONET stations: Sopot (a), Gotland (b) and Minsk (c). (For interpretation of the references to color in this figure legend, the reader is referred to the web version of this article.)

chosen levels, 500, 1500 and 3000 m a.s.l. Considering that majority of particles represented the fine mode the indication is that these particles must have travelled, and probably stayed in the measurement areas for some time, at higher altitudes, above the boundary layer (the 3000 m a.s.l. trajectory is the one which crossed over the fire areas). On 27 August 2002 the situation is slightly different since the Sopot trajectories again crossed the fire areas, especially the

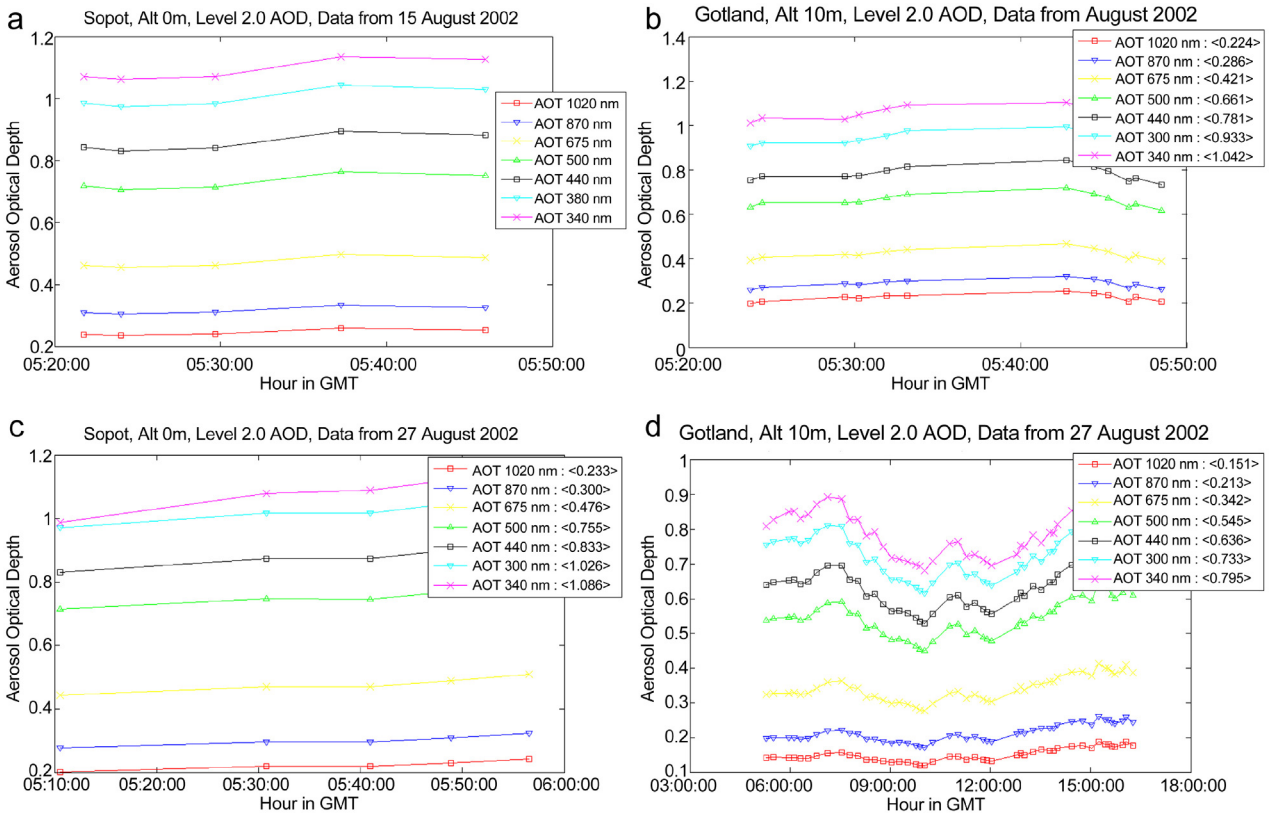

Figure 6 Level 2.0 AOD values (at seven wavelengths) on 15 and 27 August 2002 at the stations in Sopot and Gotland. (For interpretation of the references to color in this figure legend, the reader is referred to the web version of this article.)

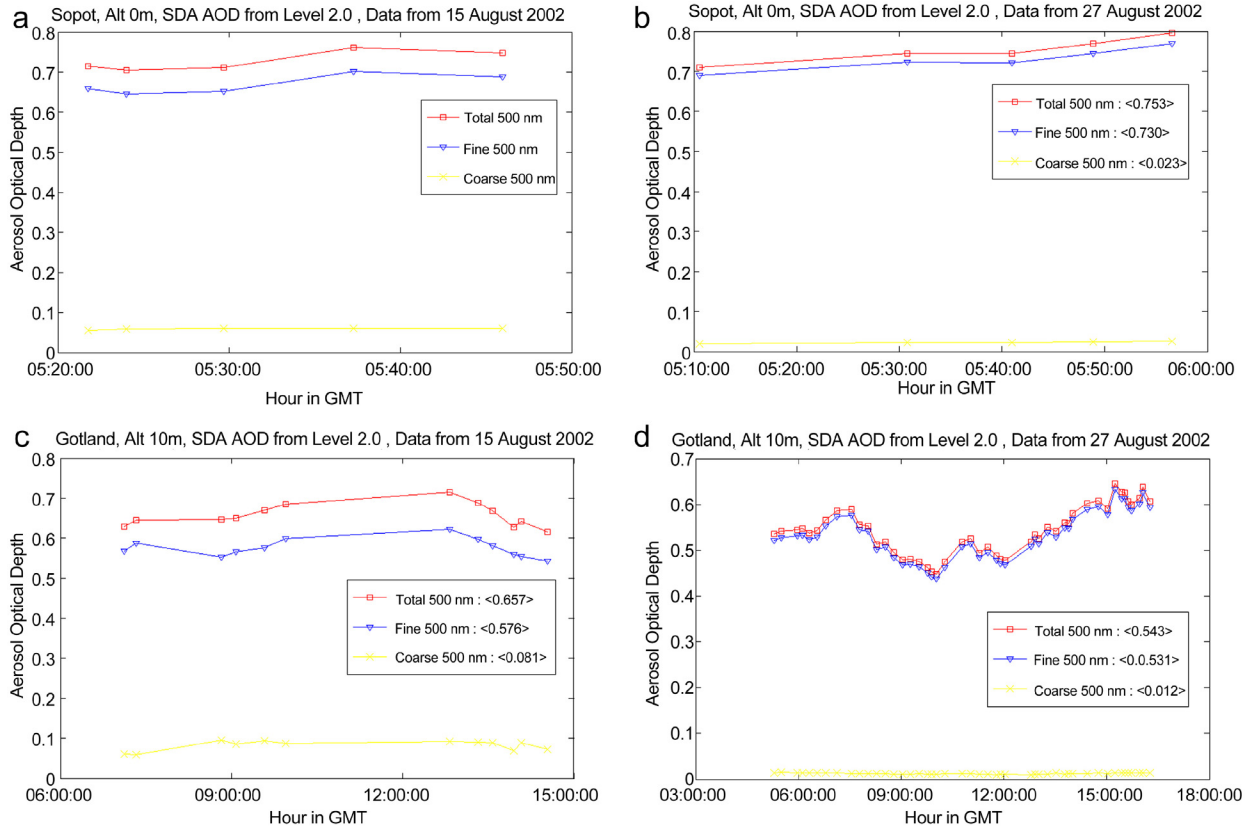

Figure 7 The level 2.0 SDA fine/coarse AOD values on 15 and 27 August 2002 for stations in Sopot and Gotland. (For interpretation of the references to color in this figure legend, the reader is referred to the web version of this article.)

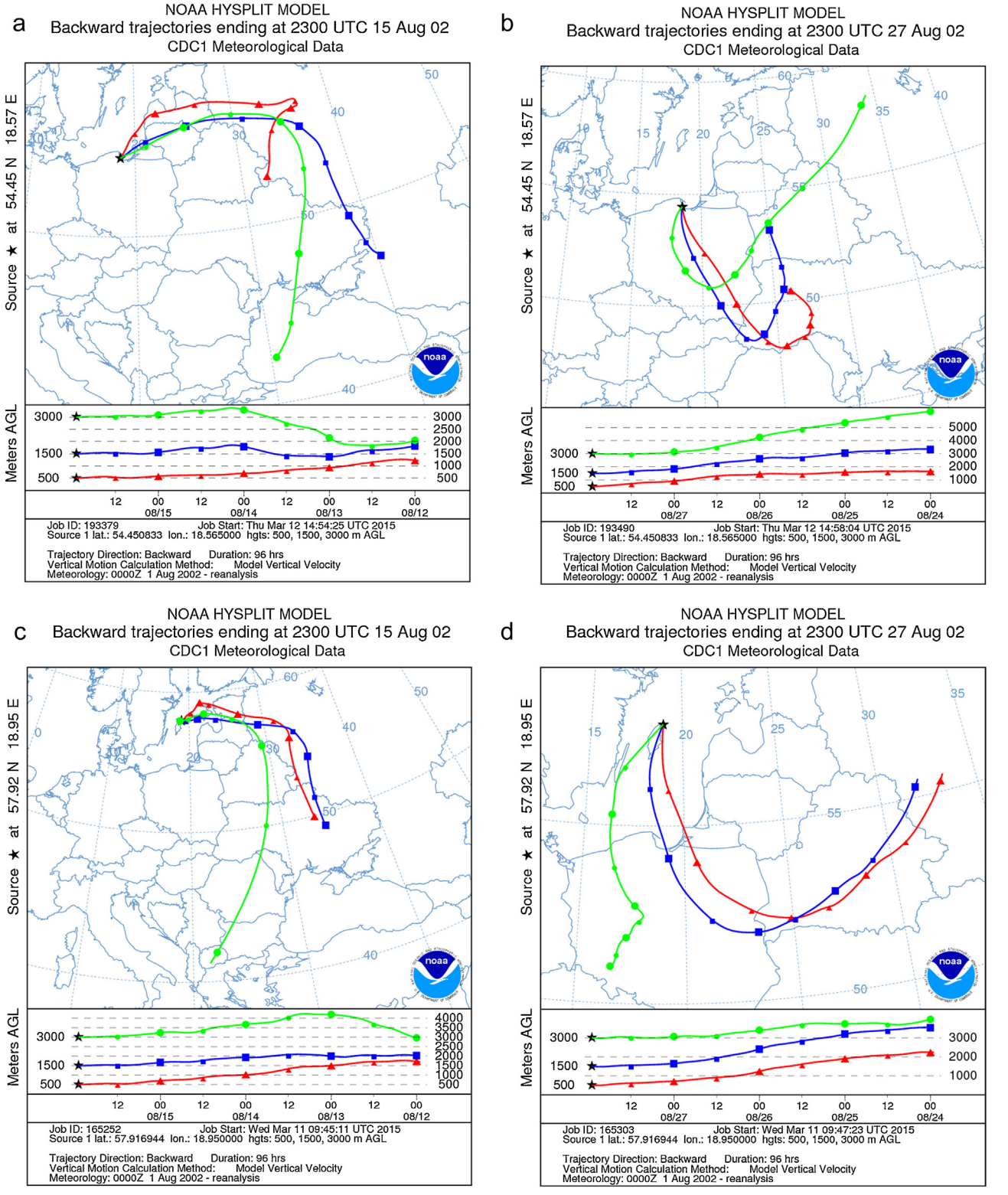

Figure 8 The 96 h air mass back trajectories at three altitudes calculated for 15 and 27 August 2002 for the stations in Sopot and Gotland. (For interpretation of the references to color in this figure legend, the reader is referred to the web version of this article.)

3000 m one, but in case of the Gotland station they also travelled over the Baltic Sea, earlier crossing Sopot. In this case it seems like the air masses might have transported fine particles over the Gotland station at altitudes lower than 3000 m but higher than 1500 m a.s.l.

The entire region on both days showed much higher AOD values than expected. Fig. 9 shows the MODIS obtained AODs at 550 nm for the Baltic and Poland, Lithuania, Belarus and Ukraine regions for 15 and 27 August 2002.

The increased AODs for the Belarus, Ukraine and the Baltic region (0.6—0.7) are evident on both days and in comparison to the rest of Europe. These pictures together with the air mass back trajectories show that the fine particles were advected to the Baltic region with south westerly winds which moved the air masses from the areas of wild fires.

Between June and mid-September 2002 the Baltic region was within the low pressure system from the area of the Mediterranean with very low speed winds from the south and south-east. On 15 August 2002 the Baltic region and especially both stations were in between the high pressure system over Scandinavia and Finland and low pressure system over Ukraine. On 27 August 2002 the situation was different since

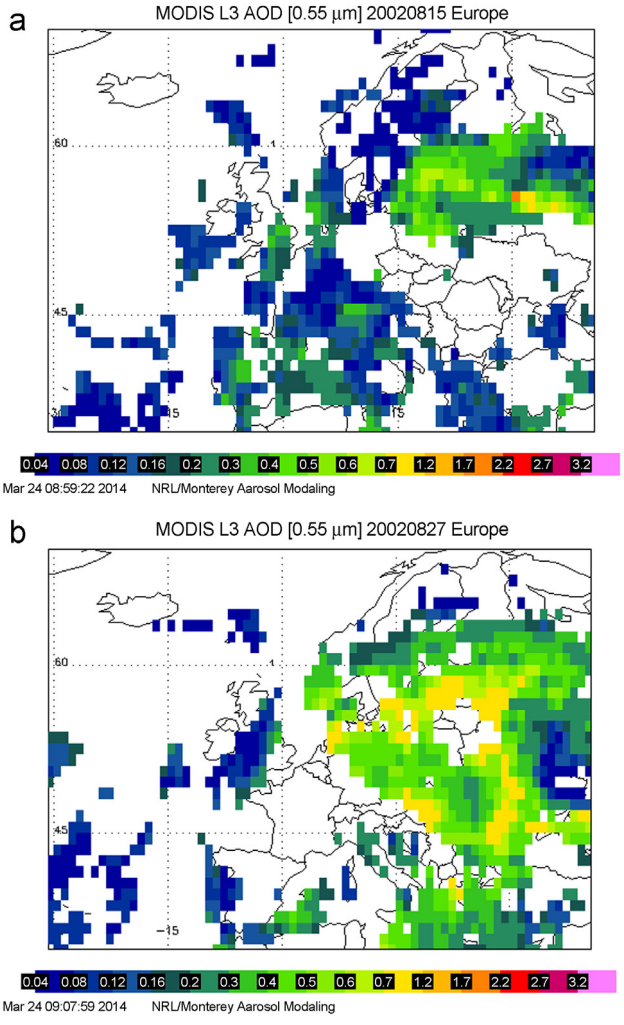

Figure 9 MODIS derived AODs at 550 nm for the Baltic and Belarus and Ukraine regions for 15 and 27 August 2002. (For interpretation of the references to color in this figure legend, the reader is referred to the web version of this article.)

both western part of the Baltic and Scandinavia were under the low pressure system and the eastern part of Europe, including Ukraine, under the high pressures system. As a result in both cases Sopot and Gotland stations were affected by the slow descent of air masses (Fig. 10a and b).

Additional information about potential transport of air pollution from the simulations of optical depths can be obtained from a long-range pollution transport model. For this purpose the authors used the Navy Aerosol Analysis and Prediction System (NAAPS) (Christensen, 1997; Witek et al., 2007). The NAAPS simulations of optical depth for 15 and 27 August 2002 for the discussed region are presented in Fig. 11.

Fig. 11 reveals that the pollution plumes on 15 and 27 August 2002 might have differed in both composition and dynamics. On 15 August 2002 the optical depth values were high in the entire region and they increased between midnight and noon. The optical depth values indicate presence of sulfate particulates in the air, while their surface concentrations are relatively low. They are produced by chemical reactions in the atmosphere from gaseous precursors. The two main sulfuric acid precursors are sulfur dioxide (SO_2) from anthropogenic sources, biomass burning and volcanoes, and dimethyl sulfide (DMS) from biogenic sources, especially marine plankton. Clearly their increased presence in the air may be connected with wild fires in the region. On 27 August 2007 situation is different since majority of optical depth values are related to a smoke plume, presumably black

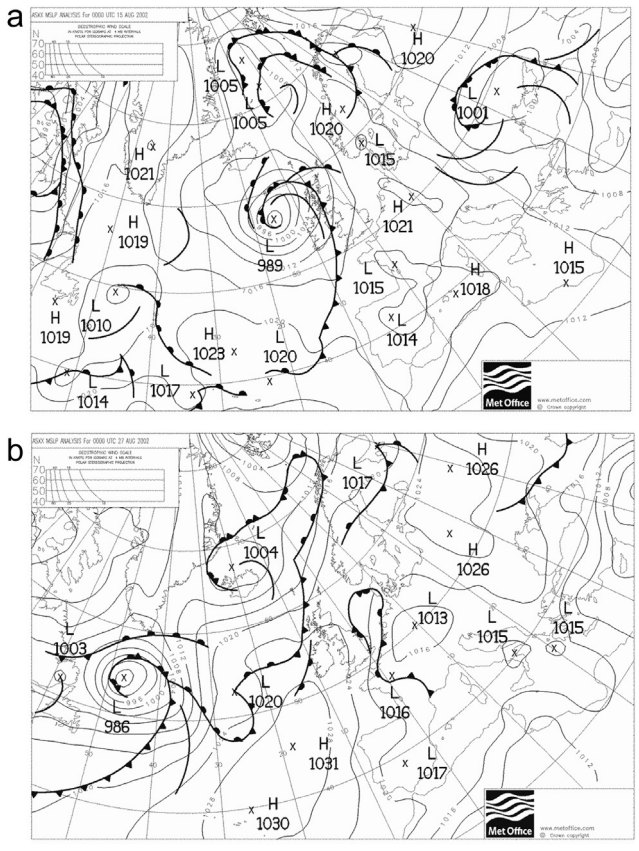

Figure 10 Air pressure systems on 15 and 27 August 2002 in the study area. (For interpretation of the references to color in this figure legend, the reader is referred to the web version of this article.)

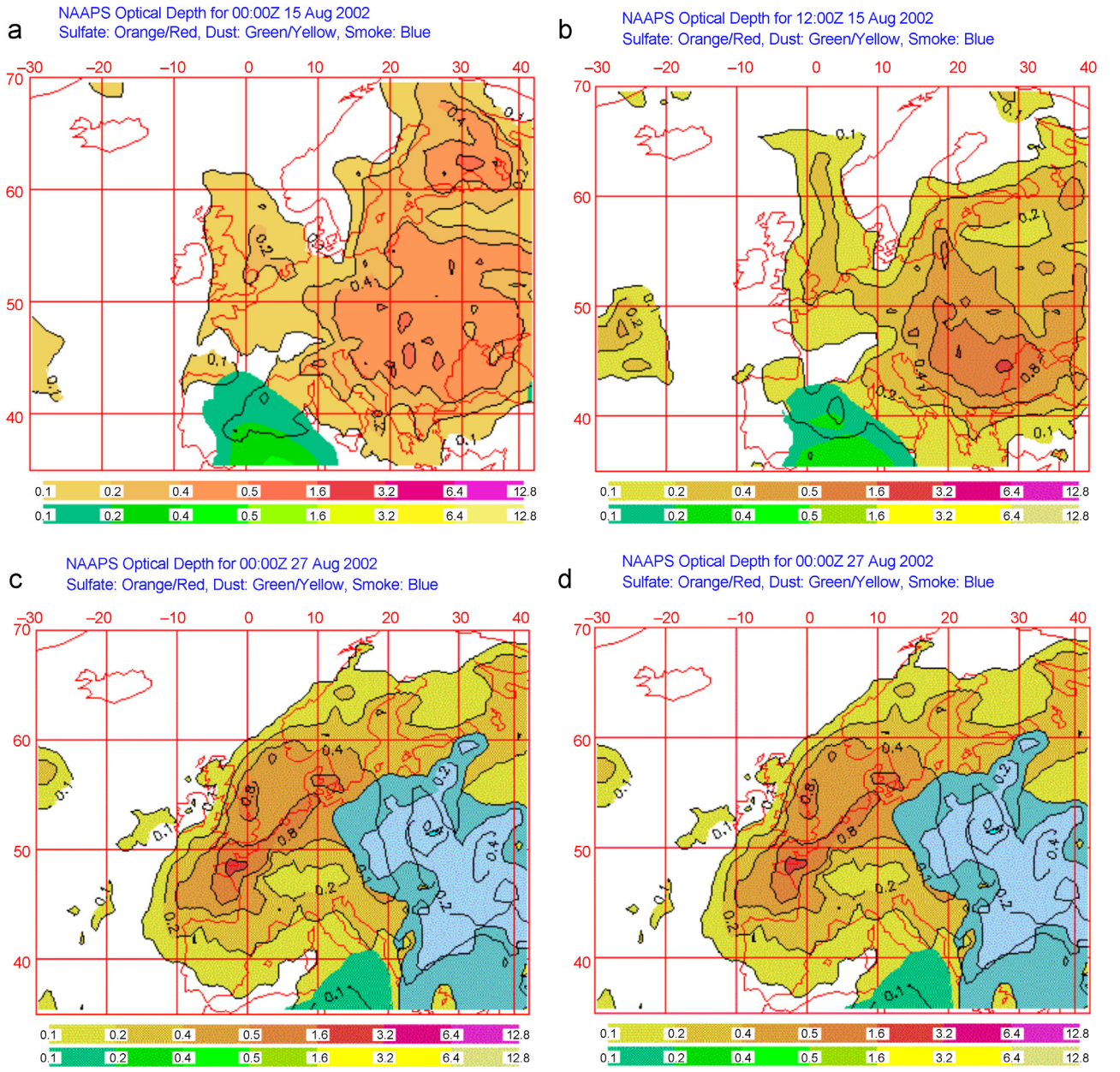

Figure 11 The NAAPS simulations of optical depths for 15 and 27 August 2002 at 00:00 and 12:00 for the discussed region. (For interpretation of the references to color in this figure legend, the reader is referred to the web version of this article.)

carbon, which did not really change much with time. The aerosol concentrations are slightly increased and also did not change significantly during the day.

4. Conclusions

The authors discussed the changes of aerosol optical depth in the region of eastern Europe and the Baltic Sea due to wild fire episodes which occurred in the area of Belarus and Ukraine in 2002. It is evident that during August 2002 the entire region was under the influence of polluted air masses from over the wild fire areas. The air pressure situation and slow wind speeds also facilitated the development of such conditions. This resulted in very high AOD levels, which significantly increased the annual averages. On particular days of August 2002 the AOD values reached a level of over 0.7. In all cases fine particles had been responsible for such situation and they fully dominated the entire ensemble of aerosol particles. They were either sulfates or smoke particles. Such situation was unique over a period of many years and it had its serious consequences for the region and especially for the Baltic Sea.

References

Beringer, J., Hutley, L.B., Tapper, N.J., Coutts, A., Kerley, A., O'Grady, A.P., 2003. Fire impacts on surface heat, moisture and carbon fluxes from a tropical savanna in northern Australia. Int. J. Wildland Fire 12, 333–340.

Bokoye, A.I., de la Cosiniere, A., Cabot, T., 1997. Angstrom turbidity parameters and aerosol optical thickness: a study over 500 solar

beam spectra. J. Geophys. Res. 102 (D18), 21905–21914, http://dx.doi.org/10.1029/97JD01393.

Bond, T.C., Doherty, S., Fahey, D., Forster, P.M., Berntsen, T., DeAngelo, B.J., Flanner, M.G., Ghan, S., Kärcher, B., Koch, D., Kinne, S., Kondo, Y., Quinn, P.K., Sarofim, M.C., Schultz, M.G., Schulz, M., Venkataraman, C., Zhang, H., Zhang, S., Bellouin, N., Guttikunda, S.K., Hopke, P.K., Jacobson, M.Z., Kaiser, J.W., Klimont, Z., Lohmann, U., Schwarz, J.P., Shindell, D., Storelvmo, T., Warren, S.G., Zender, C.S., 2013. Bounding the role of black carbon in the climate system: a scientific assessment. J. Geophys. Res. Atmos. 118, 5380–5552, http://dx.doi.org/10.1002/jgrd.50171.

Byčenkiene, S., Ulevicius, V., Prokopčiuk, N., Jasinevičiene, D., 2013. Observations of the aerosol particle number concentration in the marine boundary layer over the south-eastern Baltic Sea. Oceanologia 55 (3), 573–598, http://dx.doi.org/10.5697/oc.55-3.573.

Carlund, T., Hakansson, B., Land, P., 2005. Aerosol optical depth over the Baltic Sea derived from AERONET and SeaWiFS measurement. Int. J. Remote Sens. 26 (2), 233–245.

Christensen, J.H., 1997. The Danish Eulerian hemispheric model – a three-dimensional air pollution model used for the Arctic. Atmos. Environ. 31 (24), 4169–4191, http://dx.doi.org/10.1016/S1352-2310(97)00264-1.

Chubarova, N., Nezval, Ye., Sviridenkov, I., Smirnov, A., Slutsker, I., 2012. Smoke aerosol and its radiative effects during extreme fire event over Central Russia in summer 2010. Atmos. Meas. Tech. 5, 557–568, http://dx.doi.org/10.5194/amt-5-557-2012.

Cooke, W.F., Wilson, J.J.N., 1996. A global black carbon aerosol model. J. Geophys. Res. 101, http://dx.doi.org/10.1029/96JD00671.

Draxler, R.R., Rolph, G.D., 2010. HYSPLIT (HYbrid Single-Particle Lagrangian Integrated Trajectory). NOAA Air Resources Laboratory, Silver Spring, MD, USA Model access via NOAA ARL READY Web-site (http://ready.arl.noaa.gov/HYSPLIT.php).

Eck, T.F., Holben, B.N., Reid, J.S., Dubovik, O., Smirnov, A., O'Neill, N. T., Slutsker, I., Kinne, S., 1999. Wavelength dependence of the optical depth of biomass burning, urban, and desert dust aerosols. J. Geophys. Res. 104, http://dx.doi.org/10.1029/1999JD900923.

Evangeliou, N., Balkanski, Y., Cozic, A., Hao, W.M., Mouillot, F., Thonicke, K., Paugam, R., Zibtsev, S., Mousseau, T.A., Wang, R., Poulter, B., Petkov, A., Yue, C., Cadule, P., Koffi, B., Kaiser, J.W., Møller, A.P., 2015. Fire evolution in the radioactive forests of Ukraine and Belarus: future risks for the population and the environment. Ecol. Monogr. 85 (1), 49–72.

Graber, E., Rudich, Y., 2006. Atmospheric HULIS: how humic-like are they? A comprehensive and critical review. Atmos. Chem. Phys. 6, 729–753, http://dx.doi.org/10.5194/acp-6-729-2006.

Haywood, J.M., Ramaswamy, V., 1998. Global sensitivity studies of the direct radiative forcing due to anthropogenic sulfate and black carbon aerosols. J. Geophys. Res. 103, http://dx.doi.org/10.1029/97JD03426.

Kirchstetter, T.W., Novakov, T., Hobbs, P.V., 2004. Evidence that the spectral dependence of light absorption by aerosols is affected by organic carbon. J. Geophys. Res. 109, http://dx.doi.org/10.1029/2004JD004999.

Liousse, C., Penner, J.E., Chuang, C., Walton, J.J., Eddleman, H., Cachier, H., 1996. A global three-dimensional model study of carbonaceous aerosols. J. Geophys. Res. 101, http://dx.doi.org/10.1029/95JD03426.

Markowicz, K., Zielinski, T., Pietruczuk, A., Posyniak, M., Zawadzka, O., Makuch, P., Stachlewska, I., Jagodnicka, A., Petelski, T., Kumala, W., Sobolewski, P., Stacewicz, T., 2011. Remote sensing measurements of the volcanic ash plume over Poland in April 2010. Atmos. Environ. 48, 66–75, http://dx.doi.org/10.1016/j.atmosenv.2011.07.015.

Petelski, T., Markuszewski, P., Makuch, P., Jankowski, A., Rozwadowska, A., 2014. Studies of vertical coarse aerosol fluxes in the boundary layer over the Baltic Sea. Oceanologia 56 (4), 697–710, http://dx.doi.org/10.5697/oc.56-4.697.

Pio, C., Legrand, M., Alves, C., Oliveira, T., Afonso, J., Caseiro, A., Puxbaum, H., Sanchez-Ochoa, A., Gelencsér, A., 2008. Chemical composition of atmospheric aerosols during the 2003 summer intense forest fire period. Atmos. Environ. 42, 7530–7543.

Shindell, D., Schulz, M., Ming, Y., Takemura, T., Faluvegi, G., Ramaswamy, V., 2010. Spatial scales of climate response to inhomogeneous radiative forcing. J. Geophys. Res. Atmos. 115, D19110, http://dx.doi.org/10.1029/2010JD014108.

Smirnov, A., Holben, B., Giles, D., Slutsker, I., O'Neill, N., Eck, T., Macke, A., Croot, P., Courcoux, Y., Sakerin, S., Smyth, T., Zielinski, T., Zibordi, G., Goes, J., Harvey, J., Quinn, P., Nelson, N., Radionov, V., Duarte, C., Losno, R., Sciare, J., Voss, K., Kinne, S., Nalli, N., Joseph, E., Moorthy, D., Covert, S., Gulev, S., Milinevsky, G., Larouche, P., Belanger, S., Horne, E., Chin, M., Remer, L., Kahn, R., Reid, J., Schulz, M., Heald, C., Zhang, J., Lapina, K., Kleidman, R., Griesfeller, J., Gaitley, B., Tan, Q., Diehl, T., 2011. Maritime aerosol network as a component of AERONET – first results and comparison with global aerosol models and satellite retrievals. Atmos. Meas. Tech. 4, http://dx.doi.org/10.5194/amt-4-583-2011.

Smirnov, A., Royer, A., O'Neill, N., Tarussov, A., 1994. A study of the link between synoptic air mass type and atmospheric optical parameters. J. Geophys. Res. 99 (D10), 20967–20982.

Takemura, T., Nakajima, T., Dubovik, O., Holben, B., Kinne, S., 2002. Single-scattering albedo and radiative forcing of various aerosol species with a global three-dimensional model. J. Climate 15 (4), 333–352, http://dx.doi.org/10.1175/1520-0442(2002)015<0333:SSAARF>2.0.CO;2.

IPCC – Intergovernmental Panel on Climate Change, 2007, https://www.ipcc.ch/publications_and_data/publications_and_data_reports.shtml.

IPCC – Intergovernmental Panel on Climate Change, 2013, https://www.ipcc.ch/publications_and_data/publications_and_data_reports.shtml.

Torres, O., Bhartia, P., Herman, J., Ahmad, Z., 1998. Derivation of aerosol properties from satellite measurements of backscattered ultraviolet radiation: theoretical basis. J. Geophys. Res. 103, 17099–17110.

Torres, O., Tanskanen, A., Veihelmann, B., Ahn, C., Braak, R., Bhartia, P., Veefkind, P., Levelt, P., 2007. Aerosols and surface UV products from Ozone Monitoring Instrument observations: an overview. J. Geophys. Res. 112, D24S47, http://dx.doi.org/10.1029/2007JD008809.

Tosca, M., Randerson, J., Zender, C., 2013. Global impact of smoke aerosols from landscape fires on climate and the Hadley circulation. Atmos. Chem. Phys. 13, 5227–5241, http://dx.doi.org/10.5194/acp-13-5227-2013.

Witek, M.L., Flatau, P., Quinn, P., Westphal, D., 2007. Global sea-salt modeling: results and validation against multicampaign shipboard measurements. J. Geophys. Res. 112, D08215, http://dx.doi.org/10.1029/2006JD007779.

Zawadzka, O., Markowicz, K.M., Pietruczuk, A., Zielinski, T., Jaroslawski, J., 2013. Impact of urban pollution emitted in Warsaw on aerosol properties. Atmos. Environ. 69, 15–28.

Zdun, A., Rozwadowska, A., Kratzer, S., 2011. Seasonal variability in the optical properties of Baltic aerosols. Oceanologia 53 (1), 7–34, http://dx.doi.org/10.5697/oc.53-1.007.

Zielinski, T., 2004. Studies of aerosol physical properties in coastal areas. Aerosol Sci. Tech. 38 (5), 513–524.

Zielinski, T., Zielinski, A., 2002. Aerosol extinction and optical thickness in the atmosphere over the Baltic Sea determined with lidar. J. Aerosol Sci. 33 (6), 47–61.

Oceanologia (2016) 58, 25—38

Available online at www.sciencedirect.com

ScienceDirect

journal homepage: www.elsevier.com/locate/oceano

ORIGINAL RESEARCH ARTICLE

Thermoelastic surface properties of seawater in coastal areas of the Baltic Sea

Katarzyna Boniewicz-Szmyt [a,*], **Stanisław J. Pogorzelski** [b]

[a] *Department of Physics, Gdynia Maritime University, Gdynia, Poland*
[b] *Institute of Experimental Physics, University of Gdańsk, Gdańsk, Poland*

Received 13 August 2015; accepted 17 August 2015
Available online 3 September 2015

KEYWORDS
Baltic Sea;
Surface tension;
Crude oil-seawater interface;
Thermodynamic parameters;
Surface viscoelasticity

Summary Correlations and data for the thermoelastic surface properties of seawater were determined by means of surface tension-temperature and surface pressure-area isotherm measurements performed in Baltic Sea coastal waters (Gulf of Gdańsk, Poland). Thermodynamic surface parameters examined include: surface free energy-γ, entropy, enthalpy, surface specific heat of air-seawater (AW), air-crude oil (AO) and crude oil-seawater (OW) interfaces, and the surface elasticity was quantified in terms of complex viscoelasticity modules with relaxation times of the transition processes. The spatial and temporal evolution of the parameters differed significantly from the literature data for seawater since the effect of surface active substances of natural and municipal origin was likely to be present in these coastal waters. The seawater surface turned out to have the viscoelastic 2D character as well as other interfacial systems AO and OW where three crude oils in contact with the seawater were studied for comparison. The dilational elasticity modules were found to follow the sequence $E_{AW} > E_{OW} > E_{AO}$. Composite oil lens-covered seawater exhibited a significant drop of E from E_{AW} (crude oil free surface) even for low oil coverage fraction F_0.

The obtained surface and interfacial tension-temperature dependences allowed to correct the spreading coefficient ($S = \gamma_{AW} - \gamma_{AO} - \gamma_{OW}$) to the desired temperature range, for example. The latter parameter with the sea surface elasticity data allows one to test the modified model of crude oil spreading proposed by the authors (Boniewicz-Szmyt and Pogorzelski, 2008), for spreading kinetics phenomenon at the surface-tension regime.

© 2015 Institute of Oceanology of the Polish Academy of Sciences. Production and hosting by Elsevier Sp. z o.o. This is an open access article under the CC BY-NC-ND license (http://creativecommons.org/licenses/by-nc-nd/4.0/).

* Corresponding author at: Department of Physics, Gdynia Maritime University, Morska 81-87, 81-225 Gdynia, Poland. Tel.: +48 585232250.
E-mail addresses: kbon@am.gdynia.pl (K. Boniewicz-Szmyt), fizsp@ug.edu.pl (S.J. Pogorzelski).

Peer review under the responsibility of Institute of Oceanology of the Polish Academy of Sciences.

Production and hosting by Elsevier

http://dx.doi.org/10.1016/j.oceano.2015.08.003

0078-3234/© 2015 Institute of Oceanology of the Polish Academy of Sciences. Production and hosting by Elsevier Sp. z o.o. This is an open access article under the CC BY-NC-ND license (http://creativecommons.org/licenses/by-nc-nd/4.0/).

1. Introduction

The knowledge of seawater surface thermal and elastic properties is important in several surface tension-mediated processes like: wind waves generation and damping, gas bubbles formation, sea foam and oil emulsion stability, spreading and kinetics of contamination expansion, for instance. Literatures contain many data for the properties of seawater, but only a few sources provide full coverage for all of these properties. The data are mainly based on experimental measurements carried out in and before the 1970s, and usually span a limited temperature and salinity range. Most of the data require interpolation and extrapolation to conditions of interest, and not all desirable properties are given, particularly transport and surface elastic properties affecting to a great extent physical and dynamical oceanographical processes mediated by interfaces. The International Association for the Properties of Steam (IAPS) has approved an international table of values for the surface tension (ST) of water in equilibrium with its vapor over the entire liquid range (Vargaftik et al., 1983). However, seawater is a particular water phase which SF can significantly differ from the recent reference dependences (Sharqawy et al., 2010), particularly in coastal waters enriched in surface-active contaminants (Pogorzelski and Kogut, 2003). As a first approximation, most physical properties of seawater are similar to those of pure water, which can be described by functions of temperature. The general trend for liquid surface tension is that it decreases with an increase of temperature. Solutes can have different effects on surface tension depending on their structure. Inorganic salts, which are the type of salts in seawater, increase the surface tension of the solution. Organic contamination in seawater may also have a considerable effect on the surface tension, particularly when surfactants, capable of forming surface layers of surface elasticity E, are involved. Any relative area change $\Delta A/A$ of the interfacial system of dilational elasticity modulus E leads to the surface tension drop from the initial value γ_{AW} to $\gamma_{AW}-E(\Delta A/A)$, as demonstrated in Boniewicz-Szmyt and Pogorzelski (2008), where kinetics model of crude oil spreading at sea was corrected. Since the spreading phenomenon depends on the spreading coefficient $S = \gamma_{AW} - \gamma_{AO} - \gamma_{OW}$, the remaining interfacial tensions A/O, O/W and their temperature dependences, for the exemplary crude oils in contact with seawater, were evaluated during the course of this study. Moreover, the commonly met at sea composite surface consisting of lens-shaped crude oil areas covering a fraction F_0 was also considered.

A certain fraction of dissolved organic matter (DOM) in the sea has surface-active (SA) properties and makes up a very reactive part of the organic matter (Druffel and Bauer, 2000). According to their SA properties, these substances accumulate at marine interfaces thereby influencing gas, mass, momentum and energy transfer between the thus modified interfaces. The composition of sea surface films is largely undefined, although significant enrichments of many specific classes of compounds in the surface microlayer have been demonstrated (for review, see Hunter and Liss, 1981). Natural sea films most resemble layers composed of proteins, polysaccharides, humic-type materials and long chain alkanoic acid esters (Van Vleet and Williams, 1983). In particular, the Polish coastal zone of the southern Baltic Sea is a recipient of riverine waters and remains under severe anthropogenic pressure that leads to formation films of undefined composition with a complex interfacial architecture. The exhibited natural film parameters variability with the environmental factors (film temperature, ionic strength, pH of the aqueous subphase, wind speed, time scale of relaxation processes taking place in a mulicomponent natural film) have been already discussed in detail elsewhere (Mazurek et al., 2008).

The aim of the paper was twofold: (1) to determine the apparent sea surface thermodynamic functions (entropy, enthalpy, surface tension, surface specific heat), and their temperature variability also in the contact with model crude oils; (2) to quantify the surface-active substances effect on the dilational viscoelasticity of the seawater surface in shallow coastal areas of the Baltic Sea and on the interfacial systems: crude oil/seawater and air/crude oil affecting composite air/crude oil/seawater surface elasticity. The collected data will be further used in the corrected model of crude oil spreading at sea proposed by the authors (Boniewicz-Szmyt and Pogorzelski, 2008), for model evaluations.

2. Surface thermodynamics and viscoelasticity — theory

2.1. Thermodynamic functions

In the studies of ST of liquids, one needs data for calibration of instruments at different temperatures. The variation of γ for water with temperature t [°C] is given as follows by various investigators, as reviewed in Vargaftik et al. (1983).

By Harkins (1952):

$$\gamma_{water} = 75.680 - 0.138t - 0.05356t^2 + 0.0647t^3. \quad (1)$$

The high accuracy is important in such data, since we use these for calibration purposes. More recent and reliable data by Cini et al. (1972) indicate that

$$\gamma_{water} = 75.668 - 0.139t - 0.2885 \times 10^{-3}t^2. \quad (2)$$

The International Association for the Properties of Steam (IAPS) has approved an international table of values for the surface tension of water in equilibrium with its vapor over the entire liquid range (Vargaftik et al., 1983). However, seawater is a particular water phase which SF can differ significantly from the recent reference dependences (Sharqawy et al., 2010), particularly in coastal waters enriched in surface-active contaminants and solid dust particles (Pogorzelski and Kogut, 2003). The surface entropy and total enthalpy (per unit area) can be derived from ST versus T dependence (Adamson and Gast, 1997).

The surface entropy, S_s, corresponding to the above relation is

$$S_s = \frac{-d\gamma}{dT} \quad (3)$$

and the corresponding expression for surface enthalpy, H_s, is

$$H_s = \gamma - T\left(\frac{d\gamma}{dT}\right). \quad (4)$$

Since ST is a type of Helmholtz free energy, the expression for surface entropy is $S_s = -d\gamma/dT$. Hence, an amount of heat (H_s)

must be generated and absorbed by the liquid when the surface is extended.

The surface specific heat C_s is given as:

$$C_s = \frac{dH_s}{dT}. \tag{5}$$

Since $d\gamma/dT$ is negative equal to -0.16 mN m^{-1} K^{-1} (for pure water), H_s is greater than γ. The entropic term in Eq. (4) takes into account the energy losses related to the new surface creation. H_s is frequently the more informative of the two quantities, or at least it is more easily related to molecular arrangements at the interface.

2.2. Viscoelasticity modules — effect of surfactants and solid particles

Elastic surfactant film parameters may be derived from the surface pressure-film area (π-A)$_T$ isotherm and the surface pressure-temperature (π-T)$_A$ isochore. A drop of the surface tension, i.e. the surface film pressure $\pi = \gamma_0 - \gamma$, where γ_0 and γ are the surface tension of solvent (water) and seawater surfactant solution, respectively. Consequently, $d\gamma = -d\pi$.

The simplest equation of state to describe surface films is the 2D analog of the ideal gas law (Adamson and Gast, 1997):

$$\pi A_m = kT, \tag{6}$$

where k is the Boltzmann constant, A_m the area per film molecule related to the Gibb's adsorption Γ, $A_m = 1/\Gamma N_A$, N_A — the Avogadro number and T is the temperature in Kelvin. The description of the 2D film states depends on the dilational elasticity modulus (or Gibb's modulus) E_{isoth} expressing the static, compressional response of a film to compression or dilation corresponding to the isotherm registration in its thermodynamic equilibrium:

$$E_{isoth} = -A\left(\frac{d\pi}{dA}\right)_T. \tag{7}$$

The establishment of the thermodynamic equilibrium in the film is not trivial. The effect depends on the dimensionless parameter Deborah number (De) defined as the ratio of the film relaxation time τ to the "time of observation" (a reciprocal of the strain rate of a film: $t_{obs} = [(dA/A)/dt]^{-1}$), as argued in Kato et al. (1992). The interfacial system appears to be at the quasi-equilibrium thermodynamic state if De number is less than unity. Any relaxation process in films leads to dilational viscoelasticity, and the surface dilational viscoelastic modulus E is a complex quantity composed of real E_d (dilational elasticity) and imaginary E_i ($=\omega\eta_d$, where η_d is the dilational viscosity) parts $E = E_d + iE_i = E_0 \cos\varphi + iE_0 \sin\varphi$, where ω is the angular frequency of periodic area oscillations, $E_0 = -\Delta\pi/(\Delta A/A)$ represents the amplitude ratio between the surface stress and strain, and φ is the loss angle of the modulus (Ravera et al., 2005). For surface layers exhibiting a pure elastic behavior, the linear relation between $\Delta\pi$ and ΔA appears, as shown by Eq. (7). In the case of the viscoelastic film, the relation contains an additional term depending on the surface deformation rate:

$$\Delta\pi = E_{isoth} \cdot \Delta A/A + \eta_d d(\Delta A/A)/dt. \tag{8}$$

Diffusional relaxation time t_r is fully described by SA properties of the substance forming the monolayer (Joos and Bleys, 1983):

$$t_r = \left[a/\Gamma_\infty (1 + c/a)^2 \sqrt{D}\right]^{-2}, \tag{9}$$

where a is the Szyszkowski's surface activity coefficient, Γ_∞ the saturation adsorption, c the molar concentration of a surfactant, and D is the diffusion coefficient.

For more complex structurally surface films, the time scale of the molecular relaxation processes taking place in surface films, and the viscoelasticity modulus parts can be experimentally derived from the stress-relaxation studies (Van Hunsel and Joos, 1989).

The surface pressure-time (π-t) response of a film to a rapid step (Δt = 0.2—1.5 s) relative surface area deformation $\Delta A/A_0$ (=0.07-0.23) is registered, and presented in the following form (Nino et al., 1998):

$$\ln\frac{\pi_\infty - \pi_t}{\pi_\infty - \pi_0} = -\lambda_i t, \tag{10}$$

where π_∞, π_0, and π_t are the surface pressures at steady-state condition ($t \to \infty$), at time $t = 0$, and at any time t; λ_i is the first-order rate constant related to the relaxation time τ_i ($=1/\lambda_i$).

In the framework of a model for dilational visco-elasticity, adapted to the stepwise → surface → area; → deformation mode, the real and imaginary parts of E can be obtained from the following relations (Aksenenko et al., 2006; Jayalakshmi et al., 1995):

$$E_d = E_0\left[\frac{(1+\Omega)}{(1+2\Omega+2\Omega^2)}\right] \quad \text{and}$$
$$E_i = E_0\left[\frac{\Omega}{(1+2\Omega+2\Omega^2)}\right], \tag{11}$$

$$E_0 = \frac{(\pi_0 - \pi_\infty)}{(\Delta A/A_0)} \quad \text{is an amplitude of the modulus } E, \tag{12}$$

where

$$\Omega = \sqrt{\frac{\Delta t}{\tau_i}} \quad \text{and} \quad tg\varphi = \frac{\Omega}{1+\Omega}, \tag{13}$$

$$|E| = \sqrt{E_d^2 + E_i^2} \quad \text{is the modulus of the complex quantity } E, \tag{14}$$

and Δt is the applied step film area deformation time.

At sufficiently low film area compression rates ($De \ll 1$), the dilational viscoelasticity modulus can be approximated by E_{isoth}. Keeping in mind that dry dust loads can be trapped at the sea water interface, the mineral particles effect on E should be addressed.

Considering the total surface covered with a collection of the solid spherical particles of R radius at the surface concentration n (particles per unit area), and remaining particle-free liquid surface (having E_{free} modulus), for the modulus of the composite surface E_{com} we have (Lucassen, 1992):

$$E_{com} = \frac{E_{free}}{\left\{1 + n\pi R^2\left[(2E_{free}\ \cos^2\theta/\gamma_{LV}) - \sin^2\theta\right]\right\}}. \tag{15}$$

A position of a solid spherical particle at the air/water interface depends on the hydrophilic (particle material/water contact angle $\theta < 90^{\circ}$) and hydrophobic (CA $> 90^{\circ}$) character of the spherical particles. A solid particle which is spherical and so small (in reference to the capillary length, i.e. $R \ll (2\gamma_{LV}/\rho_L g)^{1/2}$, where γ_{LV} and ρ_L are the surface tension and density of the liquid phase, respectively) that gravity can be ignored if compared to the surface forces, will adopt a position in the air-fluid interface which is fully determined by the wetting angle (Adamson and Gast, 1997).

As can be noticed, the presence of partially wetted spherical particles can either increase or decrease the apparent dilational modulus of the whole surface depending on the sign of the term within brackets in the denominator of Eq. (15). Thus, when θ is close to 90°, or when E_{free}/γ_{LV} (values ~0.1 are found in practice) is very small, there will be increase. In contrast, when θ is close to 0° or when E_{free}/γ_{LV} is large, the surface dilational modulus will decrease due to the presence of particles.

Environmental dust characteristics (particle size distribution, wettability of dust material, and surface deposition flux) in Baltic Sea coastal waters and their effect on sea surface viscoelasticity are reported in the accompanying paper (Boniewicz-Szmyt and Pogorzelski, 2015).

3. Experimental methodology

3.1. Sampling sites

Natural marine surfactant film surface rheology and adsorption studies in shallow off-shore waters of the Baltic Sea (Gulf of Gdańsk, Poland) were carried out in the period from November 2012 to November 2013 at selected locations along the coast from Brzeźno to Gdynia. Sea surface microlayer samples were collected mostly under calm sea conditions ($V_{10} < 4$ m s^{-1}; V_{10} is the wind speed at the standard height = 10 m).

3.2. Natural film rheology — methods

The novel film sampler is a submersible rectangular double-walled vessel, integrated with the Langmuir trough, which "cuts out" an undisturbed sea area region measuring 45 cm × 35 cm and 8 cm thick. The most valuable property of this device is that the collection and Langmuir trough isotherm and isochore analyses are performed without transferring and any chemical processing of the microlayer material, as described in detail elsewhere (Pogorzelski, 1992; Pogorzelski et al., 1994). The film analyses were performed immediately after sampling. Underlying water was collected by immersing a 1 L glass bottle at a depth of 0.5—1.5 m. To perform surface isotherm studies, the initial Langmuir trough area A_0 = 1,200 cm^2 is compressed with an average deformation speed v = 0.6 cm^2 s^{-1} (corresponding to *De* value ~0.09) by moving two PTFE-coated glass sliders toward each other symmetrically around the film pressure sensor. Surface tension was measured with a Wilhelmy plate technique using a piece of filter paper (5 cm wide) attached to the arm of a electrobalance (GM2 + UL5, Scaime, France). They were accurate to within 0.1 mN m^{-1}. Dynamic film characteristics were evaluated from stress-relaxation studies (Van Hunsel and Joos, 1989). The surface pressure-time response $\pi(t)$ of a film to a rapid (Δt = 0.19—1.1 s) relative surface area deformation $\Delta A/A_0$ (=0.07—0.23) applied to the sample by barrier movement was registered for several minutes. The reported static, dynamic and thermodynamic surface parameters stand for an average value over 6—9 measuring runs performed at the given site. The sampler, leveling device, electrobalance sensor resting on the measuring table were situated near the sampling site on the shore (see Fig. 1). Surface tension was measured in the temperature range 3—14°C for seawater samples heated from the Langmuir trough bottom realized with a water thermostated system (temperature controlled with accuracy 0.1°C using a thermocouple). A detailed description of the measuring procedures and physical conditions adopted in surface pressure-area isotherm and dynamic surface pressure registrations can be found in Pogorzelski et al. (2006). For in situ seawater surfactants adsorption dynamics studies a hand-held bubble pressure tensiometer (BP 2100 PocketDyne, Krüss, Germany) with the adjustable bubble surface formation age was used.

A new type of Langmuir trough has been used for force-area and stress-relaxation studies, for A/O and O/W interfaces. Fig. 2 illustrates the essential features of the apparatus. A solid PTFE frame, or barrier, sits in a rectangular PTFE trough of dimensions 90 cm × 60 cm × 6 cm. The barrier has four, rigid solid sides 60 cm long and 5 cm high. The barrier contains the film of interest, which is omni-directionally expanded or compressed by flexing the corners, so changing the shape of the barrier. The four sides are hinged at the corners so that they provide a continuous, leak-free enclosure. The walls have PTFE pegs underneath so that liquid (generally the aqueous phase) can flow under the walls to create a well defined interfacial area inside the barrier. Two opposite corners of the barrier are connected to a geared stepper motor. The rhomboidal shape change on driving together the two opposite corners of the trough produces the area change A_r from 3,600 to 600 cm^2. The interfacial tension/pressure is measured with a Wilhelmy plate dipping into the interface, at the center of the film, suspended from a force transducer (GM2 + UL5, Scaime, France).

For measurements at an O/W interface a 6—7 mm layer of oil is gently layered over the top of the aqueous phase. A

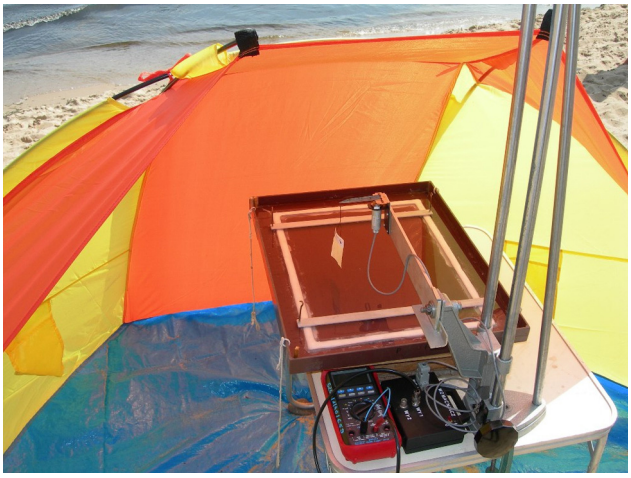

Figure 1 Experimental set-up for at-field natural sea surface film studies located near-by the southern shore line of the Baltic Sea (Jelitkowo, Gulf of Gdańsk).

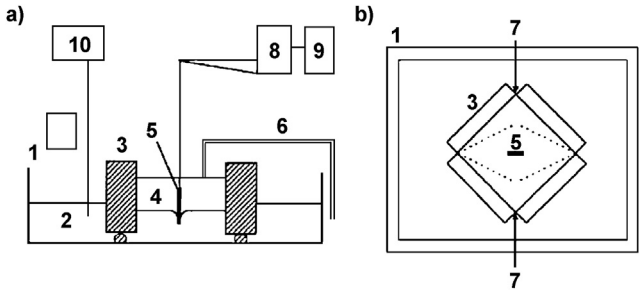

Figure 2 Schematic illustration of the frame-shaped Langmuir trough apparatus, for O/W interface studies: view from side (a) and above (b). Denotations: 1 — trough walls, 2 — lower (aqueous phase), 3 — frame-barrier, 4 — upper (oil phase), 5 — hydrophobic Wilhelmy plate, 6 — siphon (peristaltic pump system), 7 — direction of stepper motor drive for film compression, 8 — force transducer, 9 — multimeter. Area change: initial (solid line) → final (dotted line).

hydrophobic plate is completely submerged beneath the surface of the oil layer and suspended at the O/W interface by two thin stainless steel wires. On compression/expansion, the oil volume and the O/W interface are completely contained within the barrier. A change in the height of the interface causes a slight change in the buoyant force on the Wilhelmy plate. This complication is avoided by maintaining the height of the oil level constant by a siphon system. As a film is compressed the surface of the oil is continually sucked off via a peristaltic pump, to maintain a constant level (on expansion the oil can be pumped back). The film may be compressed at constant slow speed (used for π-A isotherms), or be subjected to a sudden rapid compression and the resultant π versus time t decay plot monitored.

4. Results and discussion

4.1. Surface thermodynamic parameters

An exemplary surface tension γ_{AW} versus temperature dependence registered at Brzeźno on 31 January 2013, is shown in Fig. 3, where reference data (Eq. (2) and Eq. (25)) from Sharqawy et al. (2010), for pure distilled and artificial seawater of 6 PSU salinity, respectively, are also included. In general, a linear plot is observed ($R^2 \approx 1$). The experimental dependences of practical value, provided for all the studied sites, allow one to correct the surface thermodynamic data to the desired temperature. Values of S_s for reference water surfaces are almost the same as well as the particular γ_{AW} values for the given temperature in the range of interest (2—16°C). Both S_s and γ_{AW} took higher values for Baltic Sea water sample.

Higher values of S_s point to the less complex interfacial layer structure consisting of adsorbed surface active substances and counter ions present in the sub-layer water phase. The double electric layer likely to be found here creates an interfacial system of particular thermodynamics (of higher work of cohesion = $W_{coh} = 2\gamma_{AW}$; Butt et al., 2003). For instance, the surface active substance (SAS) adsorption leads to the surface tension drop $d\gamma = -\Gamma d\mu$, where μ is the chemical potential, and the Gibbs surface excess $\Gamma = d\gamma/RT$, for a gaseous surface film (Adamson and Gast, 1997).

Surface free energy γ_{AW} and surface enthalpy versus temperature dependences are shown in Fig. 4, for Baltic Sea water sample collected at Gdynia-Orłowo on 17 April 2013. A linear plot versus T can be approximated with a relation $\gamma_{AW} = -0.149T + 77.696$. H_s was almost a constant only slightly leveling down as T increased which lead to rather low surface specific heat C_s values.

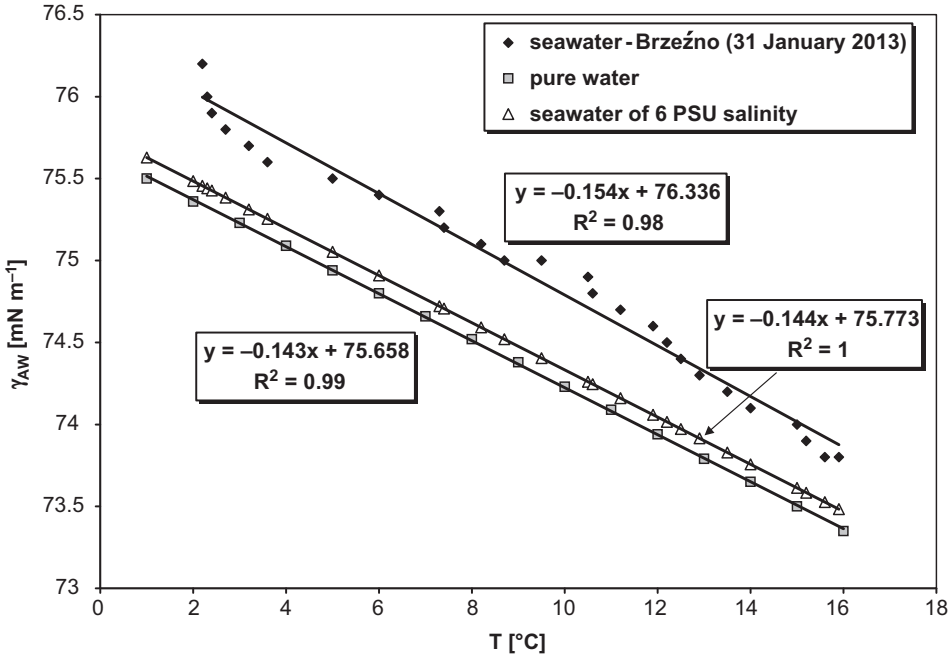

Figure 3 Seawater surface tension γ_{AW} versus temperature, for Baltic Sea sample collected at Brzeźno on 31 January 2013. The reference relations (Eq. (2) and Eq. (25)) from Sharqawy et al. (2010) are included, for pure distilled water and seawater of 6 PSU salinity, respectively.

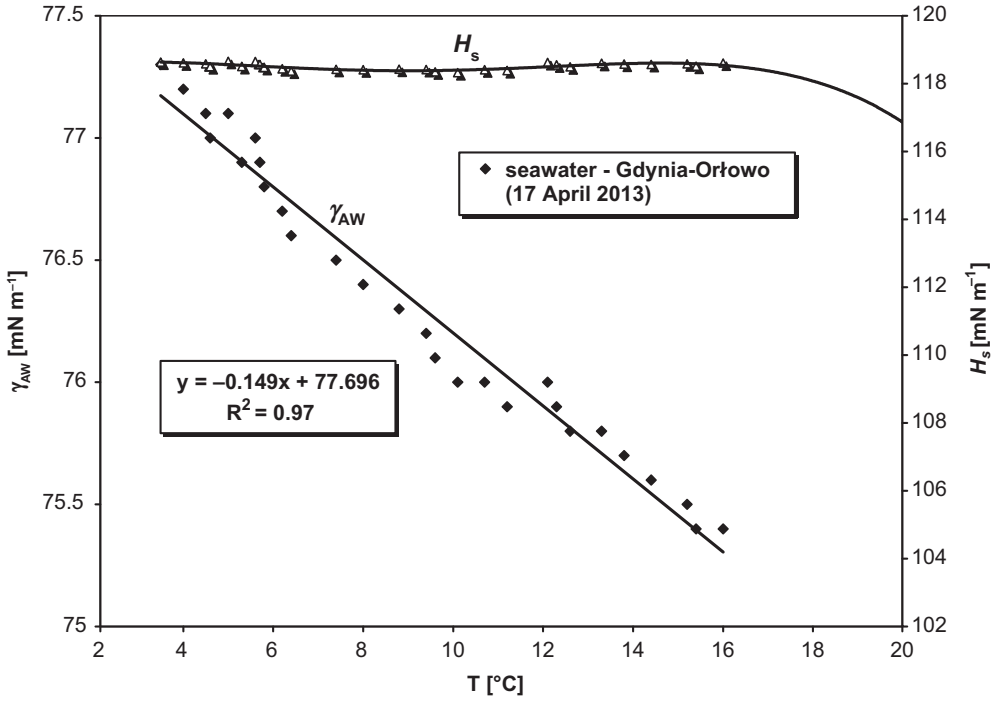

Figure 4 Surface free energy γ_{AW} and enthalpy versus T, for Baltic Sea water sample collected at Gdynia-Orłowo on 17 April 2013.

Such dependences measured at a few sampling stations allowed estimation of the surface thermodynamics functions collected in Table 1.

The parameters were corrected to the long-term surface temperature of the Baltic Sea (= 7.66°C). As a reference, surface tension seawater characteristics (derived from Eq. (25) from Sharqawy et al. (2010), for 6 PSU salinity characteristic) for the studied area were taken.

Surface tension of original Baltic Sea water samples was higher by 1.21—2.71 mN m^{-1} in reference to the salty (6 PSU) but also surfactant-free seawater. In solutions of inorganic salts the surface tension is increased because of the electric layer. Since the coastal waters are enriched in organic matter effluents and chemical process liquids, the natural surface film forms a complex molecular structure. A particular role is played by organic matter of surface-active properties. Surface entropy decreases with an increase in surface adsorption of the amphiphiles (Yamabe et al., 2000). In other words, the surface adsorption from the bulk solution brings about larger negative entropy change. S_s values were higher for all the studied samples that suggested the negative adsorption effect as a characteristic phenomenon for electrolytes applicable to only pure surface adsorption mechanism (Adamson and Gast, 1997).

However, for the natural sea surface films consisting of polymer-like structures, the thermodynamic and kinetic processes are more complex (Gelbart et al., 1994). Higher values of S_s pointed to the less-organized molecular interfacial structure in reference to the seawater data. Application of 2D polymer film scaling theory to natural sea surface films allowed expressing the structural complexity of the interfacial region with the scaling parameter y (Pogorzelski, 1996). It was

Table 1 Surface tension, surface entropy, surface enthalpy, and surface specific heat, for Baltic Sea water samples.

No.	Site (date)	γ_{AW} [mN m^{-1}]	S_s [mN m^{-1} K^{-1}]	TS_s [mN m^{-1}]	H_s [mN m^{-1}]	C_s [mN m^{-1} K^{-1}]	T [K]
1	Gdynia-boulevard 17 April 2013	75.9 (0.1)	0.146 (0.008)	41.24 (2.35)	117.14 (5.85)	−0.0080	280.6 (0.1)
2	Gdynia-Orłowo 17 April 2013	76.5 (0.1)	0.149 (0.004)	41.94 (1.39)	118.44 (5.92)	−0.0025	280.6 (0.1)
3	Sopot 17 April 2013	76.7 (0.1)	0.203 (0.007)	57.13 (2.15)	133.8 (6.69)	−0.0044	280.6 (0.1)
4	Jelitkowo 17 April 2013	77.0 (0.1)	0.179 (0.004)	50.43 (1.29)	127.43 (6.37)	−0.0141	280.6 (0.1)
5	Brzeźno 17 April 2013	77.4 (0.1)	0.199 (0.007)	55.85 (2.12)	133.25 (6.66)	−0.0153	280.6 (0.1)
6	Pure water (distilled)	74.59	0.157	44.06	118.65	−0.0175	280.66[a]
7	Seawater of 6 PSU salinity	74.69	0.144	40.42	115.11	−0.0163	280.66

Standard deviation given in brackets.
[a] The long-term average sea surface temperature in the Baltic Sea.

derived from the Langmuir trough surface pressure—area studies according to the relation $E_{isoth} = y\pi$. An increase in y from <3.5 through ~ 8 to over 10 indicating "good", θ, and "poor" solvent behavior, respectively of the interfacial system, is correlated with the structure transition in the multicomponent film beginning from a homogeneous mixed (of lowest organization state) monolayer, through a heterogeneous film with SAS substances segregated into patches or domains to at least a vertically layered structure with the most insoluble components residing on top of the microlayer. The scaling exponent y is a complex function of environmental factors affecting film structure (SAS concentration, pH, ionic strength and composition of the subphase, temperature, locations of sampling site and film collection procedure). Values of y measured at the studied locations were Gdynia (8.1), Gdynia-Orłowo (7.3), Sopot (3.7), Jelitkowo (6.2) and Brzeźno (4.2).

At the same place (Jelitkowo), y varied from 3.7 to 7.9 in the summer time (May—September) to 10—12.6 in the winter months (January, February, November, December), reflecting the film structure evolution from the less to more organized state. It can be noted that higher S_s were correlated to lower y registered in the studied stations (see Table 1). The entropic term TS_s contributions to the surface enthalpy H_s were varied from 0.35 to 0.42 and were higher if referred to the seawater reference (= 0.34) reflecting the presence of the adsorbed species. Surface specific heat C_s of the studied samples was ranging from -0.004 to -0.015 mN m^{-1} K^{-1} and was much lower than the reference value -0.016 mN m^{-1} K^{-1} suggesting the less sensitivity of the natural interfacial seawater system to temperature variations.

Seasonal changes of the surface thermodynamics parameters followed at the particular station, i.e. Gdynia-Orłowo in the period 30 November 2012 to 29 November 2013, are summarized in Table 2.

The presented parameters varied widely: γ_{AW} from 69.9 to 76.5 mN m^{-1}; S_s = 0.130—0.685 mN m^{-1} K^{-1}; H_s = 111.07—264.01 mN m^{-1}. This is an example of a particular costal area with freshwater influence (Kacza River) and municipal effluents which can screen the effect of natural waters enrichment by seasonal biological activity matter. Usually observed lower γ_{AW}, y and higher S_s, E_{isoth} noticed in the summer time as a general trend along the coastal areas of the Baltic Sea was not evidenced here (Pogorzelski and Kogut, 2003). Seasonal variability of γ and S_s, for Baltic Sea water samples is shown in Fig. 5a and b, respectively registered at the selected sites. The smallest surface tension deviations from the reference value = 74.69 mN m^{-1} were observed at the period of limited primary production in winter season months (November to February). In the summer time both the human activity and marine organisms surface active compounds adsorb at the air/water interface. The effect is less pronounced in the locations distant from industrial objects (Gdynia-boulevard, Sopot). S_s being a first derivative of γ against T is a very sensitive quantity of the water season kind. A slight deviation from the reference was noticed from November 2012 to April 2012, further from May 2012 to October 2013, S_s differed by a factor of 5.8—7.6 exhibited a drastic structural re-arrangement at the interface again less pronounced at Gdynia-boulevard and sampling stations where lowest SAS concentrations were evidenced in previous studies (Pogorzelski et al., 2006).

The establishment of the thermodynamic equilibrium in the film is not trivial. The effect depends on the dimensionless parameter Deborah number. The interfacial system appears to be at the quasi-equilibrium thermodynamic state if *De* number is less than unity. In order to evaluate the film formation rate of the equilibrium state, the adsorptive properties of film-forming by surface active substances have to be considered.

In the surface microlayer of natural waters, a great diversity of SAS organic substances has been observed. Besides proteins and glycerides, characterized by small surface activity, there are also very active esters, fatty acids, and alcohols (Jarvis et al., 1967). The latter stands for main components of the surface layer as a result of competitive adsorption (Garrett, 1967). They consist of molecules having between 11 and 22 carbon atoms in a hydrocarbon chain. The elasticity modulus of condensed monolayers of this type may reach a value of 200 mN m^{-1} ($C_{20}H_{41}OH$ — see Joly, 1972). The surface adsorption parameters characterizing several selected organic surface-active substances occurring on

Table 2 Seasonal variability of the surface thermodynamics parameters of Baltic Sea water samples collected at Gdynia-Orłowo from 30 November 2012 to 29 November 2013 corrected to the reference temperature.

No.	Date	γ_{AW} [mN m^{-1}]	S_s [mN m^{-1} K^{-1}]	TS_s [mN m^{-1}]	H_s [mN m^{-1}]
1	30 November 2012	72.6 (0.1)	0.260 (0.010)	72.95 (2.81)	145.55 (7.26)
2	28 December 2012	73.5 (0.1)	0.191 (0.004)	53.59 (1.12)	127.09 (6.35)
3	31 January 2013	75.1 (0.1)	0.184 (0.005)	51.63 (1.40)	126.73 (6.33)
4	23 February 2013	75.3 (0.1)	0.167 (0.003)	46.86 (0.84)	122.16 (6.11)
5	27 March 2013	74.6 (0.1)	0.130 (0.020)	36.47 (5.61)	111.07 (5.55)
6	17 April 2013	76.5 (0.1)	0.149 (0.004)	41.81 (1.12)	118.31 (5.92)
7	28 May 2013	74.7 (0.1)	0.245 (0.010)	68.74 (2.81)	143.44 (7.17)
8	29 June 2013	74.7 (0.1)	0.221 (0.006)	62.01 (1.68)	136.71 (6.83)
9	13 July 2013	72.0 (0.1)	0.579 (0.011)	162.46 (3.09)	234.46 (11.72)
10	10 August 2013	71.8 (0.1)	0.685 (0.029)	192.21 (8.13)	264.01 (13.20)
11	22 September 2013	71.3 (0.1)	0.531 (0.014)	148.99 (3.92)	220.29 (11.01)
12	27 October 2013	69.9 (0.1)	0.744 (0.055)	208.76 (15.43)	278.66 (13.93)
13	29 November 2013	75.2 (0.1)	0.145 (0.007)	40.69 (1.96)	115.88 (5.79)

Standard deviation given in brackets.

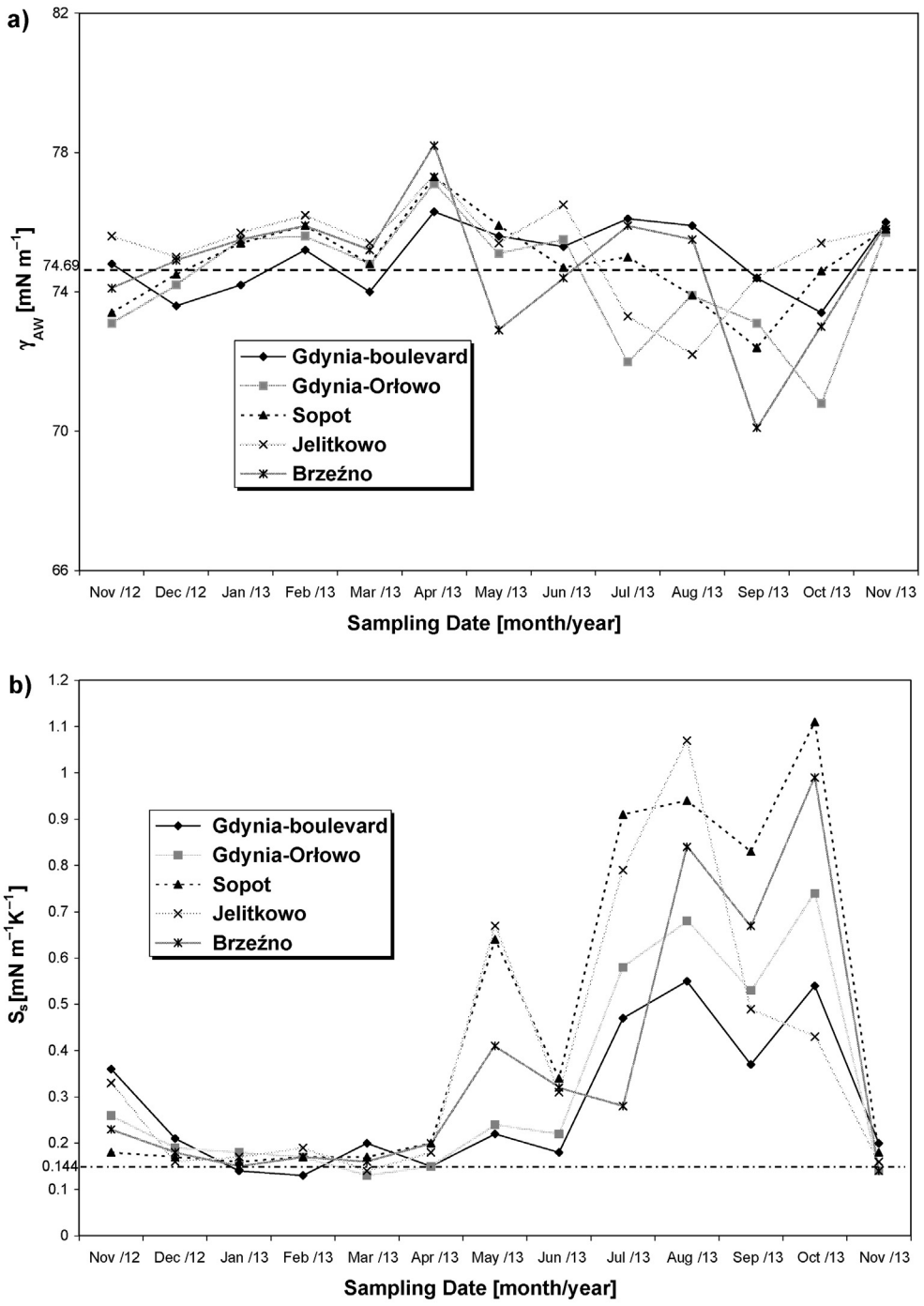

Figure 5 Seasonal variability of surface tension (a) and surface entropy (b), for Baltic Sea water samples collected at the selected locations sampled in the period from November 2012 to November 2013. Horizontal lines correspond to the reference values.

Table 3 Surface adsorption parameters of SAS composing the sea surface films.

Substance	a [kmol m^{-3}]	Γ_∞ [kmol m^{-2}]	D [m^2 s^{-1}]	t_r [s]
$C_7H_{15}COOH$	1.2×10^{-3}	2×10^{-9}	1.1×10^{-10}	0.00049
$C_{12}H_{25}SO_4Na$	4.4×10^{-4}	5.7×10^{-9}	7.3×10^{-10}	0.00284
$C_{10}H_{21}OH$	1.4×10^{-3}	6.1×10^{-9}	3.7×10^{-10}	10.3375
$C_{12}H_{25}OH$	4.3×10^{-6}	7×10^{-9}	6×10^{-10}	54.5291
$C_{11}H_{23}COOH$	1.4×10^{-6}	6×10^{-9}	7.4×10^{-10}	306.4293

the surface of natural waters, together with the characteristic relaxation times (derived from Eq. (9)) are collected in Table 3, for the state of saturated adsorption monolayer ($c = 2a$). In the case of readily soluble substances ($a = 10^{-3}$—10^{-4} kmol m^{-3}), diffusion is a very fast process with t_r of the order of 0.49—2.84 ms. Substances having the activity coefficient $a = 10^{-6}$ kmol m^{-3} and lower form effectively insoluble monolayers within the time window range of the order of several seconds to minutes demonstrating t_r ranging from 10 to 306 s.

The foreseen effect of interfacial film time formation on the sea surface thermodynamic parameters was confirmed experimentally by using a gas-bubble tensiometer with the adjustable bubble surface formation age t_b. Surface tension and S_s were equal to 75.1 mN m^{-1} and 0.189 mN m^{-1} K^{-1} for the time $t_b = 28$ ms whereas 74.7 mN m^{-1} and 0.214 mN m^{-1} K^{-1} for $t_b = 275$ ms on Baltic Sea sample measured in situ at Orłowo on 28 May 2013. The following trend of changes: $\gamma\downarrow$ and $S_s\uparrow$ with an increase of t_b was found for all the studied samples.

Under high sea states intensive water mixing takes place where subsurface water phase of different SAS content accounts in the surface film formation. That was simulated by surface tension measurements of seawater probes taken from different depths.

Surface tension of seawater as a function of time registered from the moment of creation of air/water interface, for water phases collected with a microlayer sampler and in bottles from subsurface water from depths 0.5, 1.0 and 1.5 m, is shown in Fig. 6. Measurements were performed on water samples collected at Jelitkowo on 12 May 2013 under calm sea conditions ($V_{10} < 2$ m s^{-1}).

The lowest value of γ was observed for the at-surface microlayer case ($h = 0$) in comparison to the reference value for pure (surfactant-free) water $\gamma = 74.8$ mN m^{-1} at the sample temperature $T = 6.0^{\circ}$C as a result of SAS adsorption. The corresponding film pressure attained $\pi = 8.3$ mN m^{-1}, i.e. the equilibrium value after $t = 65$ min. During this period γ evolved from 65.5 to 66.5 mN m^{-1}. The subsurface water under stable hydrodynamic conditions (no water mixing) contained lower concentrations of surface-active components that is expressed by higher values of γ taken for samples collected from deeper layers: $\gamma = 69.1$ mN m^{-1} ($h = 0.5$ m); $\gamma = 74.1$ mN m^{-1} ($h = 1.0$ m), and $\gamma = 74.4$ mN m^{-1} ($h = 1.5$ m). The subsurface water samples were capable of forming films with low π varying from 5.7 ($h = 0.5$ m) to 0.4 ($h = 1.5$ m). The surface-active components appeared to be slightly soluble compounds at low concentrations, for which the diffusion process required several minutes (or even hours) to attain the constant γ value. It can be noted that γ-t dependence did not demonstrate a horizontal part corresponding to the saturation value, for the deep-water samples ($h = 1.0$—1.5 m). Surfactants are concentrated at the air-sea interface by numerous physical processes including diffusion, turbulent mixing, bubble and particle transport, and convergent circulations driven by wind, tidal forces, and internal waves. Natural sea surface films most resemble layers composed of proteins, polysaccharides, humic-type materials and waxes (Van Vleet and Williams, 1983). The presence of relatively small amounts of certain lipids (free fatty acids, free fatty alcohols or triglycerides) in films composed primarily of proteins or carbohydrates can strongly affect the resultant film pressure of multicomponent film. The elastic behavior of sea surface films is not only controlled by diffusion and compounds concentrations, but also by pronounced conformational changes (Gelbart et al., 1994). Consequently, losses of film material could have occurred via desorption, micelle formation, or collapse to a multilayered solid phase. Conformation mechanisms could include more efficient packing due to nonpolar interactions, coiling of biopolymer chains, and looping of polymer segments into bulk solution. The

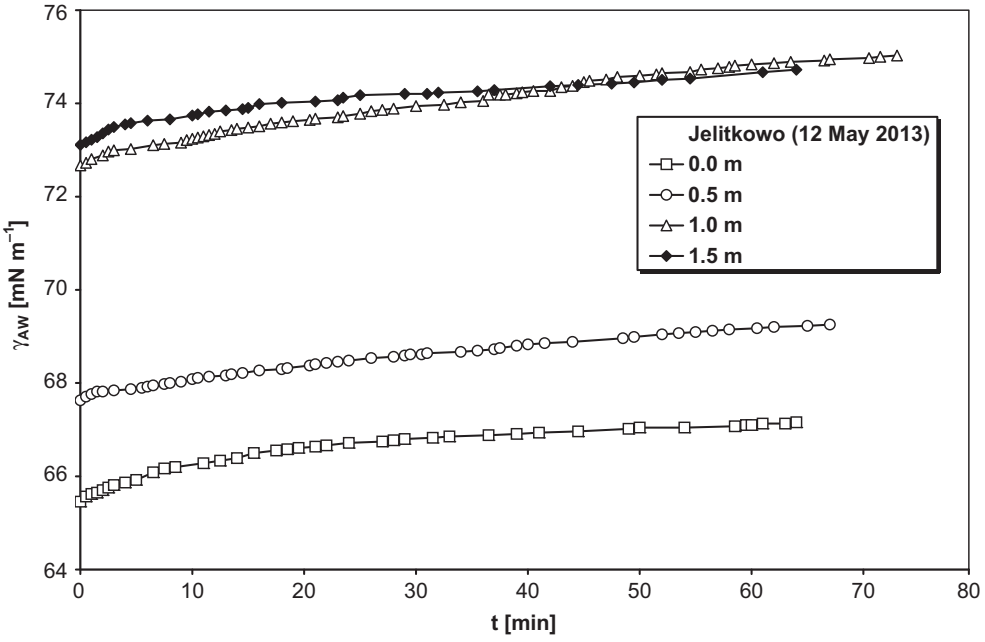

Figure 6 Dynamic surface tension $\gamma(t)$, for seawater samples collected with a surface film sampler and in bottles from different depths 0.5, 1.0 and 1 m (at Jelitkowo on 12 May 2013).

Table 4 Physicochemical properties of crude oils used in the experiments at 25°C.

No.	Crude oil	Petrobaltic	Flotta	Romashkino
1	Density [kg m^{-3}]	806.88	874.83	848.01
2	Viscosity [mPa s]	5.17	6.57	4.71
3	Surface tension [mN m^{-1}]	25.74	28.04	25.76
4	O/W Interfacial tension[a] [mN m^{-1}]	20.52	21.64	22.54
5	API	43.48	29.88	34.99
6	Pour point	−5	−2	−3
7	Asphaltenes [%w/w]	1.4	0.7	0.4
8	Resins [%w/w]	6.3	5.1	4.2
9	Classification	Light	Medium	Light
10	Origin	Baltic Sea	North Sea (UK)	Russia

[a] Crude oil in contact with Baltic Sea water sample (collected at Orłowo on 25 May 2013).

glycopeptides-lipid-oligosaccharide complex, such as that described by D'Arrigo (1984), appears to be more consistent with the observations of surface characteristics of marine films found in the Baltic Sea (Pogorzelski et al., 2006).

4.2. Interfacial thermodynamics of A/O and O/W crude oil-seawater systems

Physicochemical properties of crude oils used in the experiments (at 25°C), are collected in Table 4, and were characteristic of light to medium oils.

Interfacial thermodynamic functions for A/O and O/W systems are shown in Table 5. Surface tension of the studied crude oils and interfacial SW/oil tensions were comparable to the values reported by others (Mohammed et al., 1993; Nour et al., 2008; Yarranton et al., 2000). S_s of A/O interfaces was close to the values of long-chain paraffin oils (Birdi, 1997a, 1997b), and were higher by a factor 2.1—3.9 in reference to O/W interfaces, for the corresponding crude oil. It demonstrated that the interfacial molecular structure, for O/W systems, was more structurally ordered (of lower degrees of freedom) than exhibited by A/O interfaces for the same crude oil. It remains to better understand the surface activity of asphaltenes and resins — the main surface-active components of crude oil affecting γ_{AW} and γ_{OW} interfacial tensions (Bauget et al., 2001). Resin and asphaltene contents of the studied crude oils are of the order of 4.2—6.3 and 0.4—1.4 [wt%], respectively similarly as reported in Freer et al. (2003). The effect of concentrations of asphaltenes and resins on static and dynamic properties of air/oil and water/oil interfaces was already experimentally studied (Ese et al., 1999). The experimental data indicate that, at low concentrations, asphaltenes adsorb on the water-in-hydrocarbon interface as surfactants (Yarranton et al., 2000). Sandwich structures at oil-water interface are observed (Horvath-Szabo et al., 2002). Recent molecular dynamics simulation of the oil-water interface reveals a preferential accumulation of aromatics at the interface due to weak hydrogen bonding between hydrogen atoms of water and π-electrons of aromatics (Kunieda et al., 2010). Detailed discussion on the correlation between the chemical composition of the crude oil and interfacial tension can be found in Buckley and Fan (2007). Aromatics that are preferentially accumulated at the crude oil/water interface will promote migration of asphaltenes and polar components in the crude oil toward the interface, resulting in further reduction in the interfacial tension between crude oil and seawater to below 30 mN m^{-1} (Takamura et al., 2012). The generalized model that relates interfacial tension of crude oil/brine systems with temperature, salinity and oil viscosity is given by the equation (Isehunwa and Olanisebe, 2012): $\gamma_{OW} = A + BX_1 + CX_2 + DX_3$ where X_1 is the temperature [°C], X_2 the salinity [ppm], X_3 the oil viscosity [cP] with the empirical constants A—D collected in Table 2 of Isehunwa and Olanisebe (2012) designed for the particular crude oil system. Other important factors like pH are also considered (Olanisebe and Isehunwa, 2013).

The adsorption process at the air/oil interface is not diffusion controlled but rather involves a reorganization of asphaltene molecules in a network structure. The role of

Table 5 Surface thermodynamic parameters of A/O and O/W interfacial system crude oil—seawater at 25°C.

No.	Oil phase	γ_{AO} [mN m^{-1}] at T = 295 K	S_s [mN m^{-1} K^{-1}]	TS_s [mN m^{-1}]	H_s [mN m^{-1}]	C_s [mN m^{-1} K^{-1}]	T [K]
A/O interface							
1	Crude oil (Petrobaltic)	25.74 (0.28)	0.188 (0.006)	53.33 (1.88)	104.43 (5.22)	−0.137 (0.006)	283 (0.1)
2	Crude oil (Flotta)	28.04 (0.40)	0.141 (0.009)	41.34 (2.62)	90.24 (4.51)	−0.157 (0.007)	292 (0.1)
3	Crude oil (Romashkino)	25.76 (0.29)	0.159 (0.010)	47.53 (2.99)	76.93 (3.84)	−0.108 (0.005)	298 (0.1)
O/W interface							
4	SW/Petrobaltic	20.52 (0.18)	0.048 (0.010)	13.58 (1.32)	34.10 (0.23)	−0.241 (0.012)	283 (0.1)
5	SW/Flotta	21.64 (0.21)	0.065 (0.014)	18.98 (1.96)	40.62 (0.35)	−0.617 (0.027)	292 (0.1)
6	SW/Romashkino	22.54 (0.11)	0.057 (0.012)	16.99 (1.87)	39.53 (0.33)	−0.715 (0.032)	298 (0.1)

SW, Baltic Sea water sample (collected at Orłowo on 25 May 2013). Standard deviation given in brackets.

Table 6 Rheokinetic surface parameters derived from stress-relaxation experiments at 25°C for A/W, A/O and O/W interfaces.

No.	Sample date	$\Delta A/A_0$	Δt [s]	τ_1 [s]	τ_2 [s]	E_{isoth} [mN m^{-1}]	E_d [mN m^{-1}]	E_i [mN m^{-1}]	$\lvert E\rvert$ [mN m^{-1}]	φ [°]
1	Brzeźno 12 July 2013	0.13 (0.01)	0.4	2.0 (0.2)	21.9 (2.6)	29.12 (3.49)	12.03 (1.44)	3.72 (0.44)	12.59 (1.51)	17.1 (2.1)
2	Jelitkowo 29 June 2013	0.12 (0.01)	0.7	2.4 (0.3)	12.2 (1.5)	25.81 (3.09)	16.98 (0.83)	4.45 (0.29)	17.55 (0.88)	14.6 (2.3)
3	Orłowo 15 July 2013	0.08 (0.01)	0.3	1.6 (0.2)	10.1 (1.2)	24.48 (2.93)	17.58 (2.11)	5.31 (0.63)	18.37 (2.20)	16.8 (2.0)
4	Sopot 23 August 2013	0.08 (0.01)	0.4	2.0 (0.2)	10.2 (1.2)	23.12 (2.77)	18.55 (1.62)	4.18 (0.50)	19.01 (1.70)	12.6 (2.1)
5	Gdynia 18 June 2013	0.11 (0.01)	0.6	2.8 (0.2)	12.3 (1.1)	22.94 (1.89)	16.89 (1.22)	4.36 (0.9)	17.44 (1.41)	14.3 (1.8)
6	Petrobaltic A/O	0.12 (0.02)	0.7	1.9 (0.1)	23.2 (4.5)	3.42 (0.45)	1.06 (0.12)	0.42 (0.32)	1.55 (0.34)	21.6 (1.9)
7	Flotta A/O	0.12 (0.02)	0.7	2.0 (0.1)	27.7 (2.3)	2.78 (0.67)	0.81 (0.11)	0.34 (0.32)	0.88 (0.21)	22.7 (1.7)
8	Romashkino A/O	0.13 (0.02)	0.6	2.7 (0.1)	31.1 (2.4)	3.2 (0.82)	1.96 (0.12)	0.85 (0.37)	2.13 (0.26)	23.4 (1.7)
9	Petrobaltic SW/O	0.19 (0.02)	0.5	3.6 (0.2)	28.2 (3.4)	13.62 (2.71)	8.81 (1.62)	4.10 (0.21)	9.71 (0.13)	24.9 (2.3)
10	Flotta SW/O	0.23 (0.02)	0.4	5.2 (0.3)	35.7 (4.03)	10.24 (3.23)	7.93 (1.40)	3.87 (0.56)	8.82 (0.11)	26.1 (2.8)
11	Romashkino SW/O	0.23 (0.02)	0.6	7.3 (0.3)	42.7 (4.06)	15.43 (4.77)	10.12 (2.45)	5.32 (0.42)	11.43 (0.23)	27.7 (3.6)

resins, another crude oil surface-active component is also important: resins are through to pack around asphaltene aggregates making them more soluble in the oil and therefore less surface active. Surface tension of alkanes is a result of London dispersion interactions, which are directly proportional to density. When the surface tensions of a series of the crude oils is plotted versus their densities, they follow a close-to-linear relationship but the values fall significantly below those for alkanes of the same density due to preferential accumulation of light end alkanes at the crude oil surface. The formation of a solid skin at air/oil interfaces is well identified by an increase of the elastic modulus, as will be argued in the next section.

The entropy contribution term related to the interface creation represented 51—62% of H_s, for A/O interfaces, and less 39—46, for O/W interfaces comparable to the one noticed for A/W interfaces (see Table 5). The molecular structure of SAS at the interface between two immiscible phases depends on the phase dielectric constants. The ratio of these constants are equal to 1/80 (A/W), 4/80 (O/W) and only 1/4 (A/O). More condensed surfactant 2D monolayer phases (of lower structural entropy) are formed at A/W interfaces in reference to the O/W interface where more expanded and less structured films are obtained, for the particular SA component (Adamson and Gast, 1997). $|C_s|$ values for O/W interfaces were higher by a factor 2—7 in reference to the A/O interface that exhibited their lower heat capacity.

4.3. Interfacial viscoelasticity

Force-area isotherm and stress-relaxation studies performed on Baltic Sea water samples in contact with crude oils allowed the surface viscoelastic A/O and SW/O interfacial parameters to be determined, as collected in Table 6.

Natural seawater film studies revealed, in stress-surface pressure relaxation measurements, a two-step relaxation process with characteristic times τ_1 (1.6—2.8 s) and τ_2 (10.1—21.9 s) being in agreement with the previous data obtained in the same coastal areas (Table 2 of Pogorzelski and Kogut (2003)). They also demonstrated that we were concerned with not purely elastic films ($E_d > E_i$) with the loss angles ranging from 12.6 to 17.1°. At the applied film area compression velocities, as adopted in these stress-interface studies, *De* parameter was not lower than unity, even if the shorter τ_1 was taken. The interfacial system was not in its quasi-equilibrium thermodynamic state. As a result, the absolute value of the complex modulus E (i.e. $|E| = (E_d^2 + E_i^2)^{1/2}$) could not be approximated by the static elasticity E_{isoth}. For all the studied surfaces $E_{isoth} > |E|$, that exhibited the need for a proper selection of E values in any simulations of dynamical processes at interfaces (wind waves damping and generation, crude oil spreading, etc.). E_{isoth} values derived from the force-area isotherm studies turned out to be overestimated. The viscoelasticity of the remaining surfaces both A/O and O/W pointed to the viscoelastic behavior where E_i differed from E_d by a factor 2.3—2.5, for A/O and by 1.9—2.14, for O/W interfaces with higher φ = 21.6—27.7° in reference to A/W surfaces (=12.6—17.1°). $|E|$ values were much lower for O/W (9.71—11.43) and A/O (0.88—2.13) than measured for Baltic Sea water (12.59—19.01 mN m^{-1}).

Resin and asphaltene contents of original crude oils are of the order of 24—26 and 2.6—3.9 [wt%], respectively (Freer et al., 2003). The effect of concentrations of asphaltenes of resins on static and dynamic properties of air/oil and water/oil interfaces was already experimentally studied (Ese et al., 1999). The formation of a solid skin at air/oil interfaces is well identified by an increase of the elastic modulus. After a sufficiently long time (less than 1 week) the elasticity modulus E_{AO} can grow from its initial value (= 0.5 mN m^{-1} shortly after the air/oil interface formation) to 10—20 mN m^{-1} (Bauget et al., 2001).

The overall relaxation kinetics of a compressed air—oil interface and the resulting dynamic elasticity E was studied for two crude oil derivatives (Loglio et al., 1984). The stress-relaxation method, at the applied area strain rate, $(\Delta A/A)/\Delta t$ = 0.183 s^{-1} in a Langmuir trough, revealed a single relaxation process with long relaxation times τ_R = 623 s and 1,248 s, with low values of viscoelasticity modulus $|E|$ equal to 2.8 mN m^{-1} and 3.3 mN m^{-1}, for diesel and boiler oil, respectively. It was found for two crude oils immersed in synthetic sea water, the O/W interface behaves primarily elastically (the interfacial loss modulus $E_i < 4$ mN m^{-1} is smaller than the interfacial storage modulus $E_d < 10$ mN m^{-1}) and that more asphaltenic the oil the stronger is the interfacial elasticity (Freer et al., 2003). Moreover, interfacial O/W elasticity grows slowly in time over days and is clearly manifest even when "rigid skins" are not visible to the eye. Formation of such "skins" at the oil/water interface with significant mechanical strength demands interconnection of a growth into large-scale network structures. These structures are expected to evolve slowly that could lead to another oil spreading rate-limiting mechanism, for instance (Boniewicz-Szmyt and Pogorzelski, 2008).

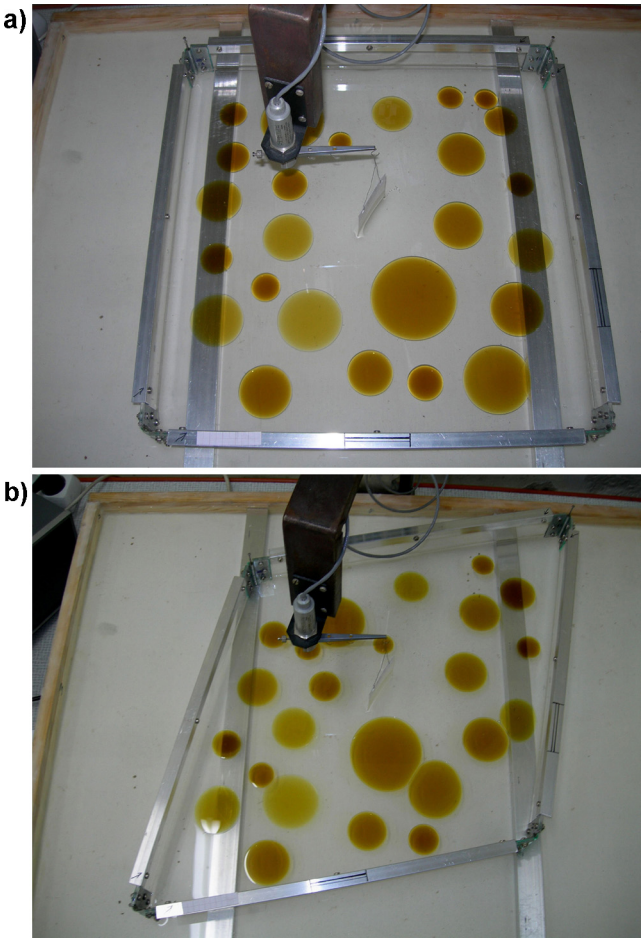

Figure 7 Composite crude oil (Petrobaltic) lenses-seawater (Baltic Sea water from Orłowo station) surface studied in a frame-type Langmuir trough (a) before and (b) after short pulse (Δt = 0.5 s); area compression $\Delta A/A_0$ = 0.08 and F_0 = 0.33.

4.4. Elasticity of composite seawater—oil interface

The apparent modulus E_{com} of the composite surface consisting of different homogeneous parts (i.e. oil-covered and oil-free water surfaces) can be derived from the relation (Ravera et al., 2005):

$$\frac{1}{E_{com}} = \frac{F_1}{E_1} + \frac{F_2}{E_2} + \cdots + \frac{F_n}{E_n} = \sum_{i=1}^{n} \frac{F_i}{E_i}. \tag{16}$$

Here $F_i = A_i/A_{tot}$ and E_i represent the area fraction of the total surface A_{tot} ($\Sigma F_i = 1$), and dilational elasticity modulus of ith component occupying A_i area, respectively.

For our case considered here, crude oil lenses covering a certain area of seawater as shown in Fig. 7, we need to know the fraction of the total area occupied by oil (F_0) and dilational modulus $E_{O/W}$ attributed to such a part, in general $E_O = E_{O/W} + E_{AO}$ (modulus E_{AO}, for the air/oil interface is rather small (see Table 6) and often assumed as 0). The remaining oil-free surface has the modulus E_{AW} with the area fraction $F_{AW} = 1 - F_0$. As a result, we have:

$$\frac{1}{E_{com}} = \frac{F_0}{E_{OW}} + \frac{(1 - F_0)}{E_{AW}}. \tag{17}$$

The theoretical E_{com} value was calculated from Eq. (17) with the following input values: E_{AW} = 28.8 mN m^{-1}, E_{OW} = 13.6 mN m^{-1}, E_{AO} = 3.4 mN m^{-1} (E_O = 17.0 mN m^{-1}) and F_0 = 0.33 was equal to 23.4 mN m^{-1}. The experiment demonstrated similar E_{com} = 26.6 mN m^{-1} being in agreement within 12%. The presence of an oil lens at natural surfactant-covered sea surface leads to a significant drop of E (from E_{AW} to E_{com}) even for low oil coverage ($F_0 < 0.1$).

5. Conclusions

Thermodynamic properties of seawater studied in Baltic Sea coastal waters differ significantly from the reference literature data and exhibited location-specific, seasonal and temporal variability likely related to the surface-active organic matter fraction of natural and man-made origin.

The measured surface tension and interfacial tension temperature dependences allowed correcting surface thermodynamic data to the desired temperature range.

For the first time temperature dependences of AO and OW interfaces for seawater in contact with model crude oils were measured as well as the elasticity modules. All the studied interfaces turned out to be viscoelastic with the characteristic relaxation times of the order of several seconds, and the absolute modules were found to follow the order: $E_{AW} > E_{OW} \gg E_{AO}$.

For the composite crude oil/seawater contaminated surface, the elasticity modulus was significantly lowered even for a low covering fraction F_0 of lens-shaped areas.

The obtained data are essential to test the corrected model of crude oil kinetics spreading at sea proposed by the authors where the dynamic spreading coefficient instead of the static one was postulated (Boniewicz-Szmyt and Pogorzelski, 2008).

References

Adamson, A.W., Gast, A.P., 1997. Physical Chemistry of Surfaces, 6th ed. Wiley and Sons, NY.

Aksenenko, E.V., Kovalchuk, V.I., Fainerman, V.B., Miller, R., 2006. Surface dilational rheology of mixed adsorption layers at liquid interfaces. Adv. Colloid Interface Sci. 122, 57–66.

Bauget, F., Langevin, D., Lenormand, R., 2001. Dynamic surface properties of asphaltenes and resins at the oil–water interface. J. Colloid Interface Sci. 239, 501–508.

Birdi, K.S., 1997a. Surface crystallization of hexadecane at hexadecane/air and hexadecane/water interfaces and effect of proteins. Colloids Surf. Physicochem. Eng. Aspects 123–124, 543–548.

Birdi, K.S., 1997b. Prediction of critical temperature of n-alkanes and n-alkenes from surface tension vs. temperature data. Colloid Polym. Sci. 275, 561–566.

Boniewicz-Szmyt, K., Pogorzelski, S.J., 2008. Crude oil derivatives on sea water: signatures of spreading dynamics. J. Mar. Syst. 74, S41–S51.

Boniewicz-Szmyt, K., Pogorzelski, S.J., 2015. Mineral dust particles effect on viscoelasticity of seawater: Baltic Sea case studies. Mar. Environ. Res. (submitted).

Buckley, J.S., Fan, T., 2007. Crude oil/brine interfacial tensions. Petrophysics 48, 175–185.

Butt, H.-J., Graf, K., Kappl, M., 2003. Physics and Chemistry of Interfaces. Wiley-VCH Verlag & Co., New York.

Cini, R., Loglio, G., Ficalbi, A., 1972. Temperature dependence of the surface tension of water by the equilibrium ring method. J. Colloid Interface Sci. 41, 287–297.

D'Arrigo, J.S., 1984. Surface properties of microbubble-surfactant monolayers at the air/water interface. J. Colloid Interface Sci. 100, 106–111.

Druffel, E.R.M., Bauer, J.E., 2000. Radiocarbon distributions in Southern Ocean dissolved and particulate organic matter. Geophys. Res. Lett. 27, 1495–1498.

Ese, M-H., Galet, L., Clausse, D., Sjoblom, J., 1999. Properties of Langmuir surface and interfacial films built up by asphaltenes and resins: influence of chemical demulsifiers. J. Colloid Interface Sci. 220, 293–301.

Freer, E.M., Svitova, T., Radke, C.J., 2003. The role of interfacial rheology in reservoir mixed wettability. J. Petrol. Sci. Eng. 39, 137–158.

Garrett, W.D., 1967. The organic chemical composition of the ocean surface. Deep Sea Res. Oceanogr. Abstr. 14, 221–227.

Gelbart, W.M., Ben-Shaul, A., Roux, D. (Eds.), 1994. Micelles, Membranes, Microemulsions and Monolayers. Springer-Verlag, New York, p. 608.

Harkins, W.D., 1952. The Physical Chemistry of Surface Films. Reinhold, New York.

Horvath-Szabo, G., Czarnecki, J., Masliyah, J.H., 2002. Sandwich structures at oil–water interfaces under alkaline conditions. J. Colloid Interface Sci. 253, 427–434.

Hunter, K.A., Liss, P.S., 1981. Organic sea surface films. In: Duursma, E.K., Dawson, R. (Eds.), Marine Organic Chemistry. Elsevier Oceanography Series 31, New York, 259–298.

Isehunwa, S.O., Olanisebe, E.B., 2012. Interfacial tension of crude oil-brine systems in the Niger delta. Int. J. Recent Res. Aspects 10, 460–465.

Jarvis, N.L., Garrett, W.D., Scheiman, M.A., 1967. Surface chemical characterization of surface active material in sea surface. Limnol. Oceanogr. 12, 88–96.

Jayalakshmi, Y., Ozanne, L., Langevin, D., 1995. Viscoelasticity of surfactant monolayers. J. Colloid Interface Sci. 170, 358–366.

Joly, M., 1972. Rheological properties of monomolecular films. Part II. Experimental results, theoretical interpretation, applications. In: Matijevic, E. (Ed.), Surface and Colloid Science, vol. 5. Wiley, New York, 79–194.

Joos, P., Bleys, G., 1983. Desorption from slightly soluble monolayer. Colloid Polym. Sci. 261, 1038–1042.

Kato, T., Iriyama, K., Araki, T., 1992. The time of observation of π–A isotherms. III. Studies on the morphology of arachidic acid monolayers, observed by transmission electron microscopy of replica samples of one-layer Langmuir–Blodgett films using plasma-polymerization. Thin Solid Films 210/211, 79–81.

Kunieda, M., Nakaoka, K., Liang, Y., Miranda, C.R., Ueda, A., Takahashi, S., Okabe, H., Matsuoka, T., 2010. Self-accumulation of aromatics at the oil–water interface through weak hydrogen bonding. J. Am. Chem. Soc. 132, 18281–18286.

Loglio, G., Tesei, U., Cini, R., 1984. Dilational properties of monolayers at the oil–water interface. J. Colloid Interface Sci. 100, 393–396.

Lucassen, J., 1992. Dynamic dilational properties of composite surfaces. Colloids Surf. A: Physicochem. Eng. Aspects 65, 139–149.

Mazurek, A.Z., Pogorzelski, S.J., Boniewicz-Szmyt, K., 2008. Evolution of natural sea surface film structure as a tool for organic matter dynamics tracing. J. Mar. Syst. 74, 52–64.

Mohammed, R.A., Baily, A.I., Luckham, P.F., Taylor, S.E., 1993. Dewatering of crude oil emulsions. 2. Interfacial properties of the asphaltene constituents of crude oil. Colloids Surf. 80, 237–245.

Nino, M.R.R., Wilde, P.J., Clark, D.C., Patino, J.M.R., 1998. Surface dilational properties of protein and lipid films at the air–water interface. Langmuir 14, 2160–2166.

Nour, A.H., Suliman, A., Hadow, M.M., 2008. Stabilization mechanism of water-in-crude oil emulsions. J. Appl. Sci. 8, 1571–1575.

Olanisebe, E.B., Isehunwa, S.O., 2013. Effect of pH on interfacial tension and crude oil–water emulsion resolution in the Niger delta. J. Petrol. Gas Eng. 4, 198–202.

Pogorzelski, S.J., 1992. Isotherms of natural sea surface films: a novel device for sampling and properties studies. Rev. Sci. Instrum. 63, 3773–3776.

Pogorzelski, S.J., 1996. Application of 2D polymer film scaling theory to natural sea surface films. Colloids Surf. Physicochem. Eng. Aspects 114, 297–309.

Pogorzelski, S.J., Kogut, A.D., 2003. Structural and thermodynamic signatures of marine microlayer surfactant films. J. Sea Res. 49, 347–356.

Pogorzelski, S.J., Kogut, A.D., Mazurek, A.Z., 2006. Surface rheology parameters of source-specific surfactant films as indicators of organic matter dynamics. Hydrobiologia 554, 67–81.

Pogorzelski, S.J., Stortini, A.M., Loglio, G., 1994. Natural surface film studies in shallow coastal waters of the Baltic and Mediterranean Seas. Cont. Shelf Res. 14, 1621–1643.

Ravera, F., Ferrari, M., Santini, E., Liggieri, L., 2005. Influence of surface processes on the dilational visco-elasticity of surfactant solutions. Adv. Colloid Interface Sci. 117, 75–100.

Sharqawy, M.H., Lienhard, J.H., Zubair, S.M., 2010. Thermophysical properties of seawater: a review of existing correlations and data. Desalin. Water Treat. 16, 354–380.

Takamura, K., Loahardjo, N., Winoto, W., Buckley, J., Morrow, N.R., Kunieda, M., Liang, Y., Matsuoka, T., 2012. Spreading and retrac-

tion of spilled crude oil on sea water. In: Younes, M. (Ed.), Crude Oil Exploration in the World. In Tech, China, 107—124.

Van Hunsel, J., Joos, P., 1989. Study of the dynamic interfacial tension at the oil/water interface. Colloid Polym. Sci. 267, 1026—1035.

Van Vleet, E.S., Williams, P.M., 1983. Surface potential and film pressure measurements in seawater systems. Limnol. Oceanogr. 28, 401—414.

Vargaftik, N.B., Volkov, B.N., Voljak, L.D., 1983. International tables of the surface tension of water. J. Phys. Chem. Ref. Data 12, 817—820.

Yamabe, T., Moroi, Y., Abe, Y., Takahasi, T., 2000. Micelle formation and surface adsorption of N-(1,1-dihydroperfluoroalkyl)-N,N,N-trimethylammonium chloride. Langmuir 16, 9754—9758.

Yarranton, H.W., Hussein, H., Masliyah, J.H., 2000. Water-in-hydrocarbon emulsions stabilized by asphaltenes at low concentrations. J. Colloid Interface Sci. 228, 52—63.

Oceanologia (2016) 58, 39—45

Available online at www.sciencedirect.com

ScienceDirect

journal homepage: www.elsevier.com/locate/oceano

ORIGINAL RESEARCH ARTICLE

Influence of dissolved organic nitrogen on surface waters☆

Krzysztof Czerwionka *

Faculty of Civil and Environmental Engineering, Gdańsk University of Technology, Gdańsk, Poland

Received 7 June 2015; accepted 11 August 2015
Available online 29 August 2015

KEYWORDS
Dissolved organic nitrogen;
Biodegradability;
Bioavailability;
Nitrogen load;
Baltic Sea

Summary The aim of this study was to determine the susceptibility of dissolved organic nitrogen (DON) contained in biologically treated wastewater disposed from municipal wastewater treatment plants (WWTPs) to biodegradability and bioavailability in a water environment. Additionally an evaluation was performed of the participation of this organic nitrogen fraction, including bioavailable DON (bDON), in the nitrogen balance for the Baltic Sea.

Based on the samples of secondary effluent taken from two large municipal WWTPs located in Northern Poland DON bioavailability and biodegradability tests were carried out. It was concluded that DON concentration in the tested samples was on average from 1.5 to 2.0 g N m^{-3}. This fraction constituted as much as 50% of organic nitrogen and 15—18% of total nitrogen contained in treated wastewater.

The participation of biodegradable DON (brDON) in activated sludge tests was on average 24—35%. In the bioavailability tests *Selenastrum capricornutum* were able to use from 19 to 26% of DON, however taking into account the results of the control test, these values are reduced to 3—4%. On the other hand, taking into account the combined effect of bacteria and algae it was possible to reduce the DON concentration by nearly 40%.

The estimated annual bDON load introduced to Baltic Sea waters from Poland through disposal of treated biological wastewater in 2010 reached up to 1.7 thousand tons of N $year^{-1}$.
© 2015 Institute of Oceanology of the Polish Academy of Sciences. Production and hosting by Elsevier Sp. z o.o. This is an open access article under the CC BY-NC-ND license (http://creativecommons.org/licenses/by-nc-nd/4.0/).

☆ This research has been financially supported by the Norwegian Financial Mechanism under the grant no. PL0085-PIP-00151-E-V1.
* Correspondence to: Faculty of Civil and Environmental Engineering, Gdańsk University of Technology, ul. Narutowicza 11/12, 80-233 Gdańsk, Poland. Tel.: +48 58 347 16 82.
E-mail address: kczer@pg.gda.pl.
Peer review under the responsibility of Institute of Oceanology of the Polish Academy of Sciences.

Production and hosting by Elsevier

http://dx.doi.org/10.1016/j.oceano.2015.08.002
0078-3234/© 2015 Institute of Oceanology of the Polish Academy of Sciences. Production and hosting by Elsevier Sp. z o.o. This is an open access article under the CC BY-NC-ND license (http://creativecommons.org/licenses/by-nc-nd/4.0/).

1. Introduction

European Union legal regulations in terms of disposal of treated municipal wastewater are specified particularly in the Council of European Communities directive 91/271/EEC dated May 21st, 1991. It imposes the obligation on member states to ensure at least a good condition of surface waters by the year 2015. In Poland the priority task in protecting surface waters, flowing waters and the Baltic Sea waters against pollution caused by municipal wastewater is to ensure complete biological treatment of wastewater and increased removal of biogenic compounds in urban centers above 15,000 PE. This should at minimum provide 75% reduction of the total nitrogen (TN) and phosphorus load in municipal wastewater from all over the country. The achievement of the intended nitrogen load reduction effect is associated with reducing the concentration of inorganic forms of nitrogen contained in secondary effluents and primarily involves improving the effectiveness of the nitrification and denitrification processes carried out in bioreactors of municipal wastewater treatment plants (WWTPs). However, in biologically treated wastewater, organic nitrogen (ON) may constitute a significant participation of the TN. This directly influences the functioning of large municipal WWTPs in Poland (above 100,000 PE), for which the admissible TN concentration in sewage disposed to the receiving bodies is 10 g N m^{-3}. The results of studies conducted so far domestically and abroad show that the participation of dissolved organic nitrogen (DON) in treated wastewater is less than 2% up to as much as 85% of the total nitrogen (e.g. Pagilla et al., 2008). In such a case, the origin, fate and degree of bioavailability of the dissolved fraction of ON in treated wastewater constitutes a significant issue in the perspective of protecting waters against eutrophication. If the degree of this fractions availability in wastewater receiving bodies is high, the goal should be to develop wastewater treatment technologies taking into account removal of DON. If, however, the fraction is not bioavailable also outside of wastewater treatment plants, this fact should be reflected in regulations on the quality of treated wastewater. In the treated wastewater receiving bodies as a result of ammonification the increase of the ammonia concentration may occur. The limiting factor of this increase is the ammonification process rate. Ryzhakov et al. (2010) have identified this value at 0.004–0.035 mg N dm^{-3} d^{-1} based on the studies of the four lakes. In a typical municipal wastewater treatment plants ammonification rate was higher, and amounted above 50 mg N dm^{-3} d^{-1} (Katipoglu-Yazan et al., 2012). However, the studies concerning the impact of wastewater discharge (containing DON) on the Chesapeake Bay Lake did not show a significant increase of ammonia concentration, which was completely consumed within 2 days (Filippino et al., 2011).

Organic nitrogen is disposed into ground waters from natural sources (atmospheric precipitation, swamp areas, infiltration) and as a result of the human activity (agriculture, intensive animal farming and treated wastewater). It accesses the water as a result of a single point disposal (e.g. from treatment plants), surface flows and atmospheric precipitation (Seitzinger and Sanders, 1997, 1999). DON may have a significant participation in the total amount of nitrogen available in most water systems, also including oligotrophic waters (lacking in biogenic compounds), in which original production is limited by the availability of nitrogen (Bronk et al., 2006). In such cases ON may constitute a significant source of this element for the growth of microorganisms. It should be, however, taken into account that DON is created by compounds of varying molecular weight, lability and bioavailability. Literature features publications regarding the possibility of using DON by the water ecosystem, including bacterioplankton, cyanobacteria and phytoplankton (Berman, 1997; Berman and Chava, 1999; Bronk et al., 2006). Results of experimental studies show that in river and lake waters DON constitutes an average of 40–50% of TN, however its participation may exceed 85% (Kroeger et al., 2006). An inverse relation between DON concentration and the concentration of dissolved inorganic nitrogen was observed, which indicates that DON may be an alternative source of nitrogen for microorganisms. According to Seitzinger and Sanders (1997) the participation of DON varies between 20 and 90% of the TN load in estuaries.

The participation of DON biologically utilizable for microorganisms primarily depends on its characteristics. It has been concluded that compounds of a low molecular weight (LMW) are more easily available in sea waters, as well as fresh-waters compared to the high molecular weight (HMW) compounds, whereas a significant part of DON consists of compounds not susceptible to biodegradation (Stepanauskas and Leonardson, 1999). The sources of DON origin and environmental conditions may also be of particular significance. Based on the results of tests incorporating bacteria and algae it was concluded that the degree of DON use also depends on the season. During spring floods Seitzinger et al. (2002) have observed an increase in DON bioavailability despite its concentration being maintained at a stable level. The authors point out that DON released from the soil is less utilizable for microorganisms than DON originating from other sources, e.g. discharged from a treatment plant. This may be due to the fact that DON from agriculture and forest areas contains aromatic compounds, while municipal wastewater DON contains primarily aliphatic compounds. Aliphatic compounds are more easily utilizable for microorganisms compared to aromatic compounds, which may indicate the existence of a correlation with the availability of nitrogen. The degree of DON usage was between 0 and 73%, whereby the higher values were observed for ON originating from municipal, rather than natural sources (like forest area runoff). Also, in the opinion of Wiegner and Seitzinger (2004) DON from municipal sources influences higher bacteria growth. The degree of DON usage by microorganisms in a water environment (rivers, streams, swamp areas and seas) is variable and fluctuates depending on the author from 0 to 80% (Bronk et al., 2006; Stepanauskas and Leonardson, 1999; Wiegner and Seitzinger, 2004).

Berman (1997) presents data indicating that LMW compounds included in DON may be directly or indirectly digested by microorganisms. In the Kinneret lake (Israel) studied by him the concentration of DON decreased from 0.371 to 0.125 g N m^{-3}, and the concentration of dissolved inorganic nitrogen decreased from 0.065 to 0.013 g N m^{-3}, as a result of the development of *Aphanizomenon ovalisporum* Cyanobacteria. These results indicate, that compounds which comprise DON are an important direct and indirect source of nitrogen for microplankton. This conclusion has been

confirmed by laboratory studies, in which pure cultures of bacteria developed well in a medium supplemented with ON compounds (such as urea, hypoxanthine, lysine, guanine and glucosamine). Later studies conducted by Berman and Chava (1999) have not only confirmed that DON constitutes an important direct and indirect source of nitrogen for phytoplankton, but have also shown that different types of algae may use this source to a different degree. This means that DON may selectively impact the type of algae types dominant in a given environment.

The bioavailability of DON in natural waters depends primarily on the differences in composition and molecular weight of compounds which form this fraction of ON. Compounds such as free amino-acids, urea and nucleic acids are easily taken in by heterotrophic bacteria, as well as sea and fresh-water algae. Veuger et al. (2004) have shown that apart from urea and free amino-acids also dissolved linked amino-acids may serve as an important source of nitrogen for heterotrophic bacteria and phytoplankton. Further, HMW compounds may constitute an alternative source of nitrogen needed for the development of microorganisms. Pehlivanoglu-Mantas and Sedlak (2008) have stated, that dissolved free amino-acids may be used directly by algae as a source of nitrogen, while dissolved linked amino-acids must be initially subjected to the process of hydrolysis to the form of monomers before they become available to algae. Also inorganic compounds created as a result of DON hydrolysis and ammonification are easily utilizable for algae.

Hasegawa et al. (2001) have conducted studies on the intake and release of DON by microorganisms based on the measurement of ^{15}N isotope concentration. The authors have concluded that nitrogen released by microorganisms feeding on phytoplankton was easily utilizable by bacteria. This indicates the occurrence of a significant nitrogen flow from phytoplankton to bacteria through micro-consumers of the former.

The evaluation of bioavailability of dissolved organic matter routinely uses biological studies based on the growth of bacteria. In this approach a very important, yet often omitted notion is the achievement of environment samples with limited access to nitrogen during incubation. This stems from the fact that microorganisms are more likely to use inorganic nitrogen than DON. This DON bioavailability evaluation method is based on three types of measurements: the usage of dissolved oxygen and the associated mineralization of DON (Moran et al., 1999), decrease of DON concentration overtime (Wikner et al., 1999) and increase of biomass concentration (Stepanauskas and Leonardson, 1999).

The aim of this study was to determine the susceptibility of DON fraction contained in biologically treated wastewater on biodegradability and bioavailability, as well as evaluate the participation of this ON fraction in the TN load discharged into the Baltic Sea.

2. Material and methods

2.1. Study sample

The biologically treated wastewater originated from the Gdańsk and Gdynia WWTPs. They are the largest municipal WWTPs located in Northern Poland carrying out disposal of wastewater to the Gdańsk Bay which forms a part of the Baltic Sea. They enable biological removal of biogenic compounds and their detailed description has been presented in prior publications (Czerwionka et al., 2012). The test samples were taken as daily average, in proportion to time. The characteristic of biologically treated wastewater is presented in Table 1.

In order to limit the availability of inorganic forms of nitrogen, their concentration was reduced below 1 g m^{-3}. Due to the fact that in all biologically treated wastewater samples studied the concentrations of ammonia nitrogen and nitrite nitrogen were very low, in practice the concentration of nitrate nitrogen was reduced. For that purpose denitrification with an external source of organic carbon in the form of sodium acetate was used (at a dose of 6 $gCOD/gNO_3$-N).

The activated sludge used in the studies was taken as an immediate sample directly from the nitrification chamber of the studied WWTP. After transportation to the laboratory the sludge was intensely aerated (oxygen concentration approx. 6 g O_2 m^{-3}) for 1 day in order to mineralize the organic contaminants contained in the sludge's biomass. Afterwards the sludge was separated from the supernatant water through spinning, the sludge was flushed two times with distilled water and again condensed by spinning. After the last spinning session, the sludge was dissolved in distilled water in order to receive a solution with the desired concentration (1 cm^3 of solution contained a sludge mass discharged to 80 cm^3 of wastewater).

The bioavailability tests incorporated a pure cultivation of *Selenastrum capricornutum* algae on a standard microbiological medium.

2.2. Experimental procedure

Four variants of performed tests were planned:

- secondary effluent without additions (control test);
- secondary effluent + algae (bioavailability test);
- secondary effluent + activated sludge (biodegradability test);
- secondary effluent + activated sludge + algae (evaluation of interaction with bioavailability and biodegradability).

The analyzed samples were mixed using a mechanical mixer (250 rpm). The algae tests were irradiated with a fluorescent

Table 1 The average concentration of nitrogen forms (±standard deviation) in secondary effluent in the studied municipal WWTPs.

WWTP	NH_4-N [g N m^{-3}]	NO_3-N [g N m^{-3}]	NO_2-N [g N m^{-3}]	TN [g N m^{-3}]	ON [g N m^{-3}]
Gdańsk	0.73 (±0.31)	6.43 (±0.90)	0.17 (±0.08)	11.24 (±0.82)	3.91 (±0.82)
Gdynia	0.37 (±0.32)	6.28 (±0.92)	0.23 (±0.22)	9.61 (±0.91)	2.73 (±0.43)

lamp with a 12 h light/dark cycle, while the samples without algae were isolated from light. Tests were carried out at a temperature of 20°C. The initial concentration of activated sludge biomass in the biodegradability tests amounted 20 g m^{-3}, and the initial content of algae suspended matter in the bioavailability tests was 5 g m^{-3}. The samples for analysis were taken in the first day of measurements and after 1, 2, 4, 7, 10, 14 and 21 days, respectively.

2.3. Analytical methods

The samples were filtered through membrane Millipore nitrocellulose filters (Billerica, MA) with different pore sizes (1.2 and 0.1 μm, respectively). The filtrates were analyzed for TN using a TOC analyzer (TOC-VCSH) coupled with a TN module (TNM-1) (SHIMADZU Corporation, Kyoto, Japan), and inorganic forms of nitrogen (NH_4-N, NO_3-N and NO_2-N) using Xion 500 spectrophotometer (Dr Lange GmbH, Berlin, Germany). The analytical procedures, which were adapted by Dr Lange GmbH (Germany) and SHIMADZU (Japan), followed the Standard Methods for Examination of Water and Wastewater (APHA, 2005). The DON concentrations were estimated from the difference between TN after filtration and the sum of inorganic N concentrations (Eq. (1)):

$$DON = TN_{0.1\,\mu m} - (NH_4\text{-}N + NO_3\text{-}N + NO_2\text{-}N). \quad (1)$$

Total suspended solids (TSS) were measured by the gravimetric methods in accordance with standard methods (APHA, 2005).

3. Results and discussion

Studies on the bioavailability and biodegradability of dissolved fractions of organic nitrogen contained in biologically treated wastewater were carried out during the period from March 2009 to June 2010. Five series of tests were carried out on each of the two selected municipal treatment plants.

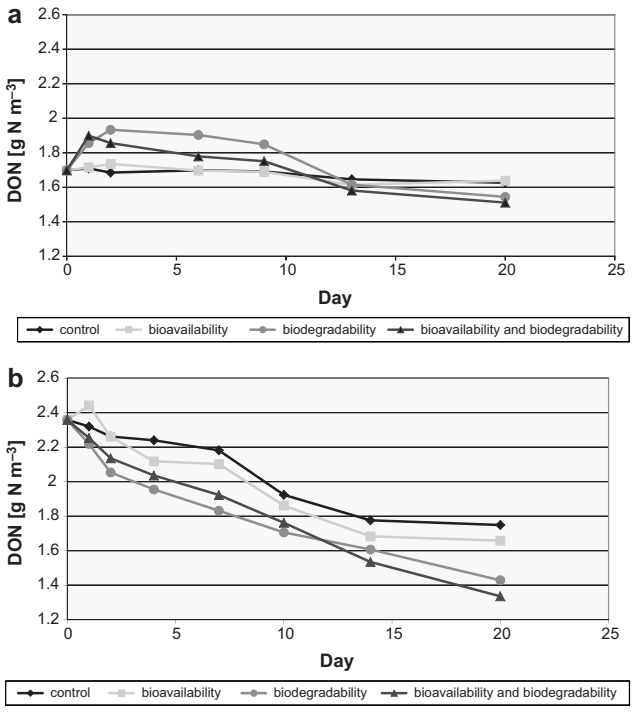

Figure 1 DON concentration changes during test 1 for secondary effluent from the Gdynia WWTP (a) and test 4 for secondary effluent from the Gdańsk WWTP (b).

Table 2 presents the DON removal efficiency values achieved during individual tests.

During the tests it was possible to observe two primary trends in the progress of DON changes. The first (most often occurring) was characterized by an initial period in which the DON content would increase (especially in samples with added activated sludge). In subsequent days of the tests a decrease in the content of this organic nitrogen fraction was observed. An example of such a process is presented in Fig. 1a

Table 2 Efficiency of DON removal from secondary effluents originating from the analyzed municipal WWTPs.

WWTP	Value	DON [g N m^{-3}]	Efficiency of DON removal [%]			
			Control	Bioavailability	Biodegradability	Bioavailability and biodegradability
Gdańsk	Test 1	1.45	20.87	22.56	35.78	38.89
	Test 2	1.78	17.67	23.23	28.67	32.78
	Test 3	2.56	19.45	24.87	31.09	37.59
	Test 4	2.36	25.83	29.69	39.40	43.34
	Test 5	2.08	23.89	28.97	38.75	42.54
	Average	**2.05**	**21.54**	**25.86**	**34.74**	**39.03**
	SD	0.40	2.96	2.94	4.22	3.80
Gdynia	Test 1	1.70	4.24	3.53	9.07	11.01
	Test 2	1.14	14.56	16.32	21.92	24.08
	Test 3	1.56	18.88	20.56	25.71	29.17
	Test 4	2.02	21.23	26.08	30.11	37.67
	Test 5	1.13	11.15	14.02	19.76	23.58
	Average[a]	**1.46**	**16.46**	**19.25**	**24.38**	**28.63**
	SD[a]	0.37	4.59	3.94	5.66	3.89

[a] The values of test 1 were not taken into account when calculating the mean and standard deviation.

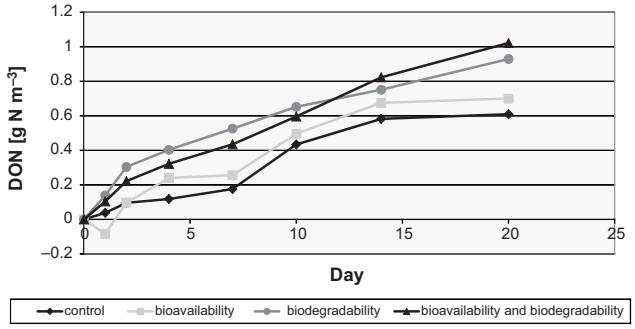

Figure 2 Changes to the content of biodegradable/bioavailable DON during test 4 of secondary effluent from the Gdańsk WWTP.

(test 1 for wastewater from the Gdynia WWTP). In certain tests a trend of continued decrease of DON value during the entire incubation period was observed. An example of such a process is presented in Fig. 1b (test 4 for wastewater from the Gdańsk WWTP).

The amount of DON susceptible to biodegradation/utilizable by Chlorophyta can also be presented in the form of a chart similar to the BOD test. Fig. 2 presents an example of such a chart (test 4 for wastewater from the Gdańsk WWTP).

The amount of DON susceptible to biodegradation with the participation of activated sludge microorganisms (brDON) varied between 20 and 40%. Simultaneously in the control sample (containing filtered biologically treated wastewater containing bacterial biomass, which went through a filter with a pore size of 1.2 μm) a reduction of DON was observed within 10—25%. The achieved results show that a significant increase in biomass concentration (from trace values to approx. 20 g m^{-3}) resulted in an approx. double increase in the amount of DON which was removed through biodegradation. Simultaneously these are values close to the ones presented by Pagilla et al. (2006), who in his studies achieved a value of brDON at a level of approx. 26%. At the same time, the initial increase of DON concentration in samples with activated sludge occurring in most tests may be associated with the release of soluble microbial products (SMP) by microorganisms. It was also observable during earlier studies of DON conversions in bioreactors with activated sludge, at a laboratory scale as well as at a full scale. Each time an increase of DON was observed in the nitrification zone, where the processes of final wastewater purification in aerobic conditions occurred (Czerwionka et al., 2012).

The amount of DON digested by *S. capricornutum* varied between 12 to nearly 30%. Pagilla et al. (2006) have shown that a participation of bioavailable DON (bDON) was approx. 21%. Also the results of the 30-day test with the participation of those Chlorophyta have shown that 26% of DON was bioavailable (Litman et al., 2008). However, the results of studies by Porro et al. (2008) were less conclusive and have shown a participation of bDON at a level of 25—50%. All the while, the participation of bDON in studies conducted by Sedlak and Jeong (2011) was significantly higher and reached approx. 50%. At the same time, based on the results of the DON composition analysis, they have shown that only 10—29% of DON is biologically not utilizable to algae (inert). Therefore, the results received in the presented studies are within the lower ranges of bDON participation contained in secondary effluent.

Such an interpretation, however, raises doubts due to the usage method of nitrogen contained in DON by Chlorophyta which are unable to break down organic compounds. An explanation of this situation can be found by comparing the value of removed DON in the control sample and the bioavailability test. Based on the values presented in Table 2 it can be concluded that a significant portion of DON undergoes decomposition with the participation of bacteria contained in wastewater, and is only available to algae in that form. A confirmation of this situation is the very quick decrease in concentration of inorganic forms during the bioavailability tests. It should be noted however, that in all of those tests the achieved values of bDON were higher than the amount of removed DON in the control sample. A clarification of such a situation comes in the form of study results presented by Litman et al. (2008), in which the incorporation of an algae inoculum varied in composition contributed to the increase in the bDON amount to 68% compared to 26% achieved for the pure *S. capricornutum* culture. In the analyzed studies the biologically treated wastewater samples were not disinfected and could have contained other types of algae, whereby some of them could have the ability to decompose organic compounds in order to gain nitrogen (e.g. blue algae). A significant influence on the availability of inorganic forms of nitrogen on the development of algae is shown by the results of a test in which activated sludge and Chlorophyta cultures are simultaneously added to the biologically treated wastewater. In these types of tests the decrease in DON concentration was the highest, ranging from 21 to 43% of the initial value. Even larger decreases, up to nearly 58%, were recorded in studies by Pagilla et al. (2006).

The fertilizing degree of the Baltic Sea with biogenic compounds (including nitrogen) is very important for living conditions of organisms in these waters. An excess of biogenic compounds contributes to the intense eutrophication. Due to its specificity (the time period of total water exchange is very long, approx. 25—30 years) the Baltic Sea is particularly sensitive to the increased flow of nutrients. Based on the analysis of data from the year 2000 regarding the origin of biogenic compounds disposed to the Baltic Sea basin it was concluded, that up to 58% of nitrogen compounds originated from area sources, 32% constituted natural ambience, and 10% originated from point sources (treated municipal and industrial wastewater discharge) (HELCOM, 2005). In the year 2000 the total nitrogen load disposed to the Baltic Sea was 822 thousand tons of N $year^{-1}$, including Polish participation accounted for approx. 28%. The load disposed by rivers and point sources from the area of Poland was approx. 186.2 thousand tons of N $year^{-1}$, including 36.8 thousand tons of N $year^{-1}$ as a discharge of treated municipal wastewater. As a result of constructing new and modernizing existing main and local treatment plants as a activated sludge, trickling filter or wetland systems (Obarska-Pempkowiak and Gajewska, 2003), in 2010 the load from municipal wastewaters was reduced by nearly 40% (to 22.4 thousand tons of N $year^{-1}$).

Reported effluent ON contributions vary widely in municipal WWTPs from less than 2% to 85% of the effluent TN (Gajewska, 2011; Pagilla et al., 2006; Pehlivanoglu-Mantas and Sedlak, 2008). Czerwionka et al. (2012) based on similar

studies carried out in eight large municipal treatment plants with biological nutrients removal located in Northern Poland have concluded that the average DON concentration in treated wastewater varied from 0.5 to 1.3 g N m^{-3}. At the same time DON constituted 12—45% of ON contained in such wastewater. Within the scope of this study it was concluded that in the 2 analyzed WWTPs, the DON constituted 15—18% of TN contained in secondary effluents up to 50% of ON, which is within the variable range specified in prior studies. Assuming similar proportions for treated wastewater discharged from other municipal WWTPs in Poland it can be estimated, that the annual DON load discharged into the Baltic Sea waters in 2010 ranged from 3.4 to 4.0 thousand tons of N $year^{-1}$, whereby the annual load of bDON may reach up to 1.7 thousand tons of N $year^{-1}$.

This was approx. 7.5% of the total nitrogen load entering with secondary effluent from municipal wastewater treatment plants. It is also only 4 times lower load in relation to estimated submarine groundwater discharge for the entire Baltic Sea (7.1 thousand tons of N $year^{-1}$) (Szymczycha et al., 2012). This indicates the great importance of bDON on nitrogen balance for this basin.

4. Conclusions

An analysis of literary data and results achieved during conducted research shows that the use of the method involving determination of brDON based on a test similar to measurement of dissolved biodegradable organic carbon is a reliable method of determining its contribution. The only value which requires clarification in further studies is the recommended duration of the test which, depending on the authors, varies within a range between 7 and 30 days (Khan et al., 2009; Simsek et al., 2013).

The situation is drastically different in terms of determining the bDON fraction. The application of a standard test with Chlorophyta does not guarantee reliable and repeatable results of bDON content. Literature presents results of studies involving various methods, whereby currently it cannot be concluded which of them should be considered appropriate.

The results achieved during the performed studies indicate, that it is possible to significantly decrease the DON concentration at a biological level, ranging from 20 to 40% for the studied wastewater samples. Simultaneously, up to 43% of the DON load discharged into the water environment with biologically treated wastewater may be used by algae. Therefore, the DON should be considered as a form of nitrogen, which may have a significant and direct impact on the conditions obtaining at the treated wastewater receiving bodies.

The estimated annual bDON load deposited into Baltic Sea waters from Poland through discharge of biologically treated wastewater in the year 2010 reached 1.7 thousand tons of N $year^{-1}$.

References

APHA, 2005. Standard Methods for Examination of Water and Wastewater, 21st ed. American Public Health Association, Washington, DC.

Berman, T., 1997. Dissolved organic nitrogen utilization by an *Aphanizomenon bloom* in Lake Kinneret. J. Plankt. Res. 19, 577—586.

Berman, T., Chava, S., 1999. Algal growth on organic compounds as nitrogen sources. J. Plankt. Res. 21, 1423—1437.

Bronk, D.A., See, J.H., Bradley, P., Killberg, L., 2006. DON as a source of bioavailability nitrogen for phytoplankton. Biogeosci. Discuss. 3, 1247—1277.

Czerwionka, K., Makinia, J., Pagilla, K.R., Stensel, H.D., 2012. Characteristics and fate of organic nitrogen in municipal biological nutrient removal wastewater treatment plants. Water Res. 46, 2057—2066.

Filippino, K.C., Mulholland, M.R., Bernhardt, P.W., Boneillo, G.E., Morse, R.E., Semcheski, M., Marshall, H., Love, N.G., Roberts, Q., Bronk, D.A., 2011. The bioavailability of effluent-derived organic nitrogen along an estuarine salinity gradient. Estuar. Coast. 34, 269—280.

Gajewska, M., 2011. Fluctuation of nitrogen fraction during wastewater treatment in a multistage treatment wetland. Environ. Protect. Eng. 37, 119—128.

Hasegawa, T., Koike, I., Mukai, H., 2001. Release of dissolved organic nitrogen by a planktonic community in Akkeshi Bay. Aquat. Microb. Ecol. 24, 99—107.

HELCOM, 2005. Nutrient pollution to the Baltic Sea in 2000. In: Baltic Sea Environment Proceedings no. 100, Helsinki Commission.

Katipoglu-Yazan, T., Ubay Cokgor, E., Insel, G., Orhon, D., 2012. Is ammonification the rate limiting step for nitrification kinetics? Bioresour. Technol. 114, 117—125.

Khan, E., Awobamise, M., Jones, K., Murthy, S., 2009. Method development for measuring biodegradable dissolved organic nitrogen in treated wastewater. Water Environ. Res. 81 (8), 779—787.

Kroeger, K.D., Cole, M.L., Valiela, I., 2006. Groundwater-transported dissolved organic nitrogen exported from coastal watersheds. Limnol. Oceanogr. 51, 2248—2261.

Litman, M.R., Majed, N., Gu, A.Z., 2008. Specific availability of wastewater-derived refractory dissolved organic nitrogen (rDON) to eutrophying algae *Selenastrum capricornutum* and *Anabaena variabilis* ATCC 29413. In: Proc. of the 81st Annual WEF Technical Exhibition and Conference, WEFTEC'08, 18—22 October 2008, Chicago (USA), 2186—2201.

Moran, M.A., Sheldon, W.M., Sheldon, J.E., 1999. Biodegradation of riverine dissolved organic carbon in five estuaries of the southern United States. Estauries 22, 55—64.

Obarska-Pempkowiak, H., Gajewska, M., 2003. The removal of nitrogen compounds in constructed wetlands in Poland. Pol. J. Environ. Stud. 12 (6), 739—746.

Pagilla, K.R., Czerwionka, K., Urgun-Demirtas, M., Mąkinia, J., 2008. Nitrogen speciation in wastewater treatment plant influents and effluents — the US and Polish case studies. Water Sci. Technol. 57 (10), 1511—1517.

Pagilla, K.R., Urgun-Demirtas, M., Ramani, R., 2006. Low effluent nutrient treatment technologies for wastewater treatment. Water Sci. Technol. 53 (3), 165—172.

Pehlivanoglu-Mantas, E., Sedlak, D.L., 2008. Measurement of dissolved organic nitrogen forms in wastewater effluents: concentrations, size distribution and NDMA formation potential. Water Res. 42, 3890—3898.

Porro, J.C., Brown, J.A., Sharp, R.R., Dubanowitz, N.J., 2008. Method development for determining the biodegradability of dissolved organic nitrogen in the Stamford WPCA effluent. In: Proc. of the 81st Annual WEF Technical Exhibition and Conference, WEFTEC'08, 18—22 October 2008, Chicago (USA), 3240—3245.

Ryzhakov, A.V., Kukkonen, N.A., Lozovik, P.A., 2010. Determination of the rate of ammonification and nitrification in natural water by kinetic method. Water Resour. 37 (1), 70—74.

Sedlak, D.L., Jeong, J., 2011. Bioavailability of dissolved organic nitrogen in wastewater effluent as determined by resin separation. In: Proc. WEF Specialty Conference "Nutrient Recovery and Management 2011", 9—12 January 2011, Miami (USA), 109—115.

Seitzinger, S.P., Sanders, R.W., 1997. Contribution of dissolved organic nitrogen from rivers to estuarine eutrophication. Mar. Ecol. Prog. Ser. 159, 1—12.

Seitzinger, S.P., Sanders, R.W., 1999. Atmospheric inputs of dissolved organic nitrogen stimulate estuarine bacteria and phytoplankton. Limnol. Oceanogr. 44, 721—730.

Seitzinger, S.P., Sanders, R.W., Styles, R., 2002. Bioavailability of DON from natural and anthropogenic sources to estuarine plankton. Limnol. Oceanogr. 47, 353—366.

Simsek, H., Kasi, M., Ohm, J.B., Blonigen, M., Khan, E., 2013. Bioavailable and biodegradable dissolved organic nitrogen in activated sludge and trickling filter wastewater treatment plants. Water Res. 47, 3201—3210.

Stepanauskas, R., Leonardson, L., 1999. Bioavailability of wetland-derived DON to freshwater and marine bacterioplankton. Limnol. Oceanogr. 44, 1477—1485.

Szymczycha, B., Vogler, S., Pempkowiak, J., 2012. Nutrient fluxes via submarine groundwater discharge to the Bay of Puck, southern Baltic Sea. Sci. Total Environ. 438, 86—93.

Veuger, B., Middelburg, J.J., Boschker, H.T.S., Nieuwenhuize, J., Rijswijk, P.V., Rochelle-Newall, E.J., Navarro, N., 2004. Microbial uptake of dissolved organic and inorganic nitrogen in Randers Fjord. Estuar. Coast. Shelf Sci. 61, 507—515.

Wiegner, T.N., Seitzinger, S.P., 2004. Seasonal bioavailability of dissolved organic carbon and nitrogen from pristine and polluted freshwater wetlands. Limnol. Oceanogr. 49, 1703—1712.

Wikner, J., Cuadros, R., Jansson, M., 1999. Differences in consumption of allochthonous DOC under limnic and estuarine conditions in a watershed. Aquat. Microb. Ecol. 17, 289—299.

Oceanologia (2016) 58, 46—53

Available online at www.sciencedirect.com

ScienceDirect

journal homepage: www.elsevier.com/locate/oceano

ORIGINAL RESEARCH ARTICLE

Baltic herring prey selectively on older copepodites of *Eurytemora affinis* and *Limnocalanus macrurus* in the Gulf of Riga☆

Līna Livdāne [a,*], Ivars Putnis [b], Gunta Rubene [b], Didzis Elferts [b], Anda Ikauniece [a]

[a] *Latvian Institute of Aquatic Ecology, Riga, Latvia*
[b] *Institute of Food Safety, Animal Health and Environment "BIOR" Fish Resources Research Department, Riga, Latvia*

Received 23 October 2014; accepted 29 September 2015
Available online 6 November 2015

KEYWORDS
Clupea harengus membras;
Zooplankton;
Selective feeding;
Condition factor;
The Gulf of Riga

Summary Zooplankton availability is a major factor affecting herring body condition that in turn describes its well-being. As herring feeding is known to be selective, it is relevant to access its preferences upon zooplankton species and particular copepod developmental stages to forecast possible intraspecific competition for resources in the species scarce environment of the Gulf of Riga where herring stock size due to successful recruitment has almost doubled since 1989. This study tries to answer whether the small-sized plankters dominated zooplankton community permits herring to be a selective eater. Also how herring body condition has changed in connection to environment driven zooplankton community changes. The time series of zooplankton abundance and herring condition from 1995—2012 were studied; and a detailed study of herring diet was performed monthly by stomach content analysis during the main feeding season in 2011 and 2012. We found that herring selectively prey on *Limnocalanus macrurus* and older copepodite stages of *Eurytemora affinis*, and moreover these were species of whose selected copepodite stages explained most of variation in herring condition factor. The found

☆ The study was supported by ERDF project "Development of a mechanistic model of the Gulf of Riga ecosystem in support of efficient national policy to ensure the protection of the Baltic Sea and to promote the sustainable use of its ecosystem" (Ref. No. 010/0287/2DP/2.1.1.1.0/10/APIA/VIAA/040). No involvement in study design by the financial supporters was provided.

* Corresponding author. Present address: Leibniz Institute for Baltic Sea Research Warnemünde, Seestrasse 15, D 18119 Rostock, Germany. Tel.: +49 152 57161933.
E-mail address: lina.livdane@lhei.lv (L. Livdāne).

Peer review under the responsibility of Institute of Oceanology of the Polish Academy of Sciences.

Production and hosting by Elsevier

http://dx.doi.org/10.1016/j.oceano.2015.09.001

0078-3234/© 2015 Institute of Oceanology of the Polish Academy of Sciences. Production and hosting by Elsevier Sp. z o.o. This is an open access article under the CC BY-NC-ND license (http://creativecommons.org/licenses/by-nc-nd/4.0/).

relationship between herring feeding selectivity and long-term variation of herring condition allows applying spring zooplankton abundance of *E. affinis* and *L. macrurus* to estimate favourable feeding conditions for herring, and could also require the revision of currently used model for herring recruitment estimations, where only biomass of *E. affinis* is taken into account. In recent years, the high condition of herring can be associated with a considerable increase of lipid-rich copepod species *L. macrurus*.

© 2015 Institute of Oceanology of the Polish Academy of Sciences. Production and hosting by Elsevier Sp. z o.o. This is an open access article under the CC BY-NC-ND license (http://creativecommons.org/licenses/by-nc-nd/4.0/).

1. Introduction

Herring *Clupea harengus membras* L. is one of the most important zooplanktivorous pelagic fish species in the Baltic Sea fishery, where a considerable decrease of its weight-at-age and condition has been detected since 1980/90s (Cardinale and Arrhenius, 2000). The Gulf of Riga herring, a separate population of the Baltic Sea herring, is characterized by the lowest growth rates compared with herring stocks of the remaining Baltic Sea (Arrhenius and Hansson, 1993). Two paired explanations can be connected to this issue (Casini et al., 2006). Both are determined by prey availability: density dependent factors of increased herring stock size, a pattern of stock shift inverse to that of the Central Baltic since the late 80s (ICES, 2009); and hydro-climatic condition driven changes in the zooplankton community (Cardinale and Arrhenius, 2000; Kornilovs et al., 1992).

A considerable amount of literature has been published on zooplankton predation by clupeid fish in the Baltic Sea. Sandström (1980) was first to demonstrate selective feeding by herring. Then, in a zooplankton species and copepod development stage-resolved study Flinkman et al. (1992) identified that herring feeding is limited by the availability of suitably sized plankters, not the total amount of zooplankton, thus, herring mainly controls older copepodite stages and adult specimens. Long-term studies have outlined that the climate change induced salinity decrease has affected food availability, emphasizing decline in *Pseudocalanus* sp., main prey item of herring and sprat (*Sprattus sprattus* L. 1758) of the Central Baltic (Kornilovs et al., 2001; Möllmann et al., 2000, 2004b, 2005). Therefore, food availability has been also coupled with inter- and intraspecific competition as a result of the sprat stock increase after predation release by collapsed cod (*Gadus morhua* L. 1758) stock (Alheit et al., 2005; Casini et al., 2010; Margonski et al., 2010; Möllmann et al., 2004a; Möllmann and Köster, 2002; Rudstam et al., 1994).

Unlike in the Central Baltic, sprat stock is assessed to be at a low level in the Gulf of Riga where it does not control zooplankton biomass but instead, herring strongly dominates in commercial catches at about 90% of total values (Kotta et al., 2008). Therefore, the gulf is a pleasingly simple, few-species ecosystem for pelagic trophic studies. Due to large freshwater runoff and restricted water exchange to the Baltic Proper, low salinity (5—7 psu) (Berzinsh, 1995) determines the zooplankton community in the gulf. That consists of a limited number of occurring species, dominated by small-sized plankters, such as cladocerans (in summer) and few taxa of copepods (Ikauniece, 2001; Ojaveer et al., 1998). Lankov et al. (2010) showed *Eurytemora affinis* prevailing herring diet by annual summer investigations on pooled data basis. Whereas, detailed studies on zooplankton stage-selective and season-specific feeding in the Gulf of Riga are unknown so far. Recognizing herring as a selective feeder (Flinkman et al., 1992) in this few-species environment, it is important to assess its preferences upon both zooplankton species and particular copepod developmental stages. This is to forecast possible intraspecific competition for resources in the light of almost doubled stock size since the late 1980s (ICES, 2009). In this study we analyse: (1) juvenile and adult herring selective predation on cladocerans and development stage-resolved copepods, (2) and the zooplankton community relation to the changes in herring condition in the Gulf of Riga, using a time series of 18 years (1995—2012).

2. Material and methods

2.1. Study area and sampling in 2011 and 2012

Herring was collected in monthly cruises along the main feeding season from May to October in 2011 and 2012 in the coastal area of the Gulf of Riga. One trawl haul per month was performed, using OTM pelagic mid-water trawl (duration: 15—30 min; depth range: 23—30 m), close to the thermocline (20—30 m) (Stipa et al., 1999). On the basis of diurnal feeding cycle, the hauls were conducted only during second half of the day. The total fish length was measured to the nearest 0.5 cm and mean wet body weight per length class determined to a precision of 0.1 g. Stomachs of 5 randomly chosen fish per sampling time and length class were removed and preserved in 4% formaldehyde solution immediately on board ($n < 5$, where number of fish per 0.5 cm length class was not reached). Otoliths were removed for age determination later in laboratory using a stereomicroscope.

To evaluate prey availability, zooplankton sampling was performed on each hauling station, as well as on additional stations representing the central part of the Gulf of Riga from the bottom to the surface with a 160 μm Juday net (diameter of the upper aperture: 37 cm; diameter of the middle section: 50 cm) (UNESCO, 1968).

2.2. Sample analysis

Every herring stomach was cut open, and the complete content weighed to a precision of 0.001 g and analysed using

a light microscope (magnification 50–100×). If a stomach contained a large number of prey, a subsample of at least 100 individuals was analysed. Each of the prey was determined to the lowest possible taxonomic level. The following stages were distinguished for copepods: early copepodites C1–3, older copepodites C4–5, adult females C6 and adult males C6, and cladocerans measured to 0.2 mm. Nauplii and rotifers were excluded from analyses as herring consumed an inconsiderable number of them. A total of 797 stomachs were analysed.

Zooplankton samples were preserved and analyses were performed according to the standard protocol of the Manual for Marine Monitoring in the COMBINE Programme of HELCOM (2013). Biomasses were estimated from values on individual wet weight (Hernroth, 1985; Simm and Ojaveer, unpubl. data).

2.3. Data series for 1995 to 2012

To assess historical zooplankton abundance and biomass trends, and variability of herring condition factor, monitoring data collected in the Gulf of Riga by the Institute of Food Safety, Animal Health and Environment "BIOR" from 1995–2012 were used.

Zooplankton was sampled from the bottom to the surface with a 160 μm Juday net (UNESCO, 1968) and analysed according to internal procedures (Kornilovs et al., 2001) and the standard protocol of the Manual for Marine Monitoring in the COMBINE Programme of HELCOM (2013). Mean abundance and biomass (Hernroth, 1985; Simm and Ojaveer, unpubl. data) values of stations sampled in May were used.

Fish condition was estimated by Fulton's (1904) condition factor, an index assuming heavier fish of a given length are in better condition (Froese, 2006). To determine herring condition, on average about 1000 individuals were analysed based on fish individual biological data in commercial trawl fishery each year, and mean condition in June and July was used.

Zooplankton species dynamics are related to water and air temperature. Freimane (1967, 1968) found a tight correlation between Copepoda abundance and a sum of daily negative values of air temperature, and that a particular species, *L. macrurus*, abundance depended on water temperature, salinity and amount of solar radiation. Severe winters are associated with sharp environmental changes that could be major drivers of zooplankton dynamics. To describe winter severity, the data used were a sum of daily negative values of air temperature [°C] in Riga, measured by the Latvian Environment, Geology and Meteorology Centre from 1995–2012. These data were further used in a correlation with main forage zooplankton species.

2.4. Data analysis

All statistical analyses were done using the software package R 3.0.2 (R Core Team, 2013). Feeding selectivity on size-ranged zooplankton species- and season-specific individual wet weights (Hernroth, 1985; Simm and Ojaveer, unpubl. data) (Table 1) was described using a Yates' corrected chi-square (χ^2_y) test based (abundance of individuals was expressed as percentage of total wet weight of stomach content or zooplankton sample; see the supplementary material) *C*-index (Pearre, 1982) (Eq. (1)):

$$C = \pm\left(\frac{\chi^2_y}{n}\right)^{1/2}, \quad (1)$$

where *n* was total percentage (200) of zooplankton in the sea and in the stomachs. The index is zero-valued for no selection and ranges between −1 and +1, wherein negative values was associated with rejection and positive values with selection. *C*-index is not sensitive to rare prey species and is statistically testable. The prey data used was an average number of a zooplankton identification category per herring length class and sampling time. Zooplankton abundance was expressed per m^3 according to the same identification categories.

The potential influence of the factors: (i) season, (ii) herring age group, (iii) prey category, and (iv) combination of herring age group and prey category, as well as (v) combination of season and prey category on the differences in selectivity index was evaluated using Linear mixed-effects (lme) model fit with the REML method as implemented in the package nlme of the program R (Pinheiro et al., 2013). A combination of multiple samples from each month and year (same sampling occasion) was used as a random effect. Due to variable haul locations throughout the study area and therefore a limitation of simultaneous spatial data, analyses that were performed assumed no differences between trawl sites. As herring is known to actively search for its food items, we expected it to school in locations where the desired food was most available. Therefore, the trawl sites varied along the coastal area of the Gulf of Riga making it possible to sample respective to occurrence of herring.

Table 1 Identification categories and mean individual wet weight [WW, μg ind.$^{-1}$] (Hernroth, 1985; Simm and Ojaveer, unpubl. data) of mesozooplankton studied in the Gulf of Riga in 2011 and 2012. For calculations of *C*-index (Pearre, 1982) herring prey data were used as an average number of an identification category per length class and sampling time, and zooplankton abundance expressed as ind. m^{-3} according to the same identification categories. C, copepodite stages.

Species	Mean WW [μg ind.$^{-1}$]	Prey category
Evadne nordmanni	6	
Podon/Pleopis spp.	6	Cladoc
Bosmina coregoni	7	
Cyclopoida C1–5	4	
Acartia spp. C1–3	4	
Eurytemora affinis C1–3	5	Cop_C1–6
Cyclopoida C6	9	
Acartia spp. C4–5	10	
Eurytemora affinis C4–5	14	Eury_C4–5
Acartia spp. C6	22	Acar_C6
Eurytemora affinis C6	30	Eury_C6
Limnocalanus macrurus C1–5	50	Limn_C1–5
Cercopagis pengoi	120	Cercop
Limnocalanus macrurus C6	652	Limn_C6

If the model showed a statistically significant effect of factor or factor combination, simultaneous tests with adjusted p values for general linear hypothesis (post-hoc test) of the package multcomp in the program R were used to assess which levels showed statistically significant difference (Hothorn et al., 2008). A selectivity value for each prey category level was compared to 0. In the "prey category and age" combination and the "prey category and season" combination, comparisons were performed at each prey level between age classes and between seasons.

As zooplankton species dynamics are related to water and air temperature, the Pearson correlation was applied to relate *L. macrurus* and *E. affinis* long-term abundance in May with winter air temperatures from 1995–2012. Correlation was used to relate long-term changes in the body condition of herring with May abundance of these dominant prey species.

3. Results

3.1. Juvenile and adult herring selective predation on zooplankton

The overall model resulted in a "prey category", a combination of "herring age group and prey category", and a combination of "season and prey category" influencing differences in herring selectivity index (lme model, $p < 0.0001$) (Table 2). Further tests for these significant interactions (Table 3) revealed that both juvenile and adult herring rejected small-sized early copepodites (Cop_C1–6 × age, $p < 0.0001$). All herring selectively preyed on large cold-water calanoid *L. macrurus* C1–5 (Limn_C1–5, $p = 0.01$) and C6 stages (Limn_C6, $p < 0.001$).

3.2. Seasonal variation of herring feeding selectivity

In absolute numbers, the herring diet was dominated by copepods *L. macrurus* during all the main feeding periods and *E. affinis* in spring and summer; and along with an invasive opportunistic cladoceran *Cercopagis pengoi* in summer and autumn, when it is available in the zooplankton community. Proportion of mysids increased with a reduced zooplankton biomass in autumn period.

Table 2 The overall linear mixed-effects model results (ANOVA table) of variables (i) season, (ii) herring age, (iii) prey categories, (iv) combination of herring age group and prey category, and (v) combination of season and prey category ($p < 0.0001$).

Interactions between variables	*F*-value	d.f.	*p*-value
Season	0.32	2	0.7308
Age	1.97	1	0.1609
Prey category	51.53	7	<0.0001
Age × Prey category	17.61	7	<0.0001
Season × Prey category	24.62	14	<0.0001

Seasonal variation of prey abundance largely did not correspond to herring consumption though. Highly abundant small copepodites of *E. affinis* up to C3, *Acartia* spp. up to C5 and Cyclopoida up to C6 were truly rejected along the main feeding season. *Acartia* spp. C6 despite its relatively large mean individual mass of 22 μg ind.$^{-1}$ did not seem to be desirable prey for herring. An inconsiderable amount of fish eggs and extremely abundant rotifers and copepod nauplii were consumed.

In spring, herring selectively fed on both *E. affinis* C4–6 and *L. macrurus* C1–6 and in summer on *E. affinis* C4–5 and *L. macrurus* C1–6. Invasive cladoceran *C. pengoi* was positively selected in the autumn, along with *L. macrurus* copepodites and adults (Fig. 1). Unfortunately, nectobenthos was not sampled during this study; therefore, selectivity on mysids could not be calculated.

3.3. Long-term relation of herring condition, *Limnocalanus macrurus* and *Eurytemora affinis*

We became particularly interested in long-term variation of *E. affinis* and *L. macrurus*, as herring consumed a considerable biomass of these copepods along the feeding study in 2011 and 2012 (43% of herring had *L. macrurus* and 66% had *E. affinis* in their stomachs that made up 45 and 12% of total consumed biomass respectively). Moreover, *L. macrurus* C1–5 (Limn_C1–5, $p = 0.01$) and adults (Limn_C6, $p < 0.001$) were zooplankton groups herring indicated selective predation on throughout the period of May to October, while *E. affinis* C4–5 was positively selected by adult herring both in spring and summer, without a significant difference between these two seasons (Eury_C4–5 × age, $p < 0.0001$) (Fig. 1).

Since the last peak of *L. macrurus* in the 1980s, afterwards it had almost disappeared from the zooplankton community in the gulf (Yurkovskis et al., 1999). Fig. 2 provides an anomaly of May data 1995–2012 that indicates a shift has occurred. Since 2005 mostly positive abundance anomalies of *L. macrurus* have dominated and in recent years it has reached the long-term mean abundance of 20 800–79 730 μg m^{-3}, while *E. affinis* spring abundance has oscillated mostly inversely to *L. macrurus*.

In order to describe winter severity (conditions influencing spring productivity), a sum of daily negative values of air temperature in winter was used, and that correlated with *L. macrurus* abundance in May ($r = 0.58$, $p < 0.012$), while negative correlation with *E. affinis* was found ($r = -0.61$, $p < 0.008$).

Selectivity estimates indicate that herring preys on older copepodites of *E. affinis* and *L. macrurus* (Fig. 1). An abundance sum of *E. affinis* C4–5 and *L. macrurus* C1–6 stages in May had the tightest correlation with the herring condition factor in June and July, as a response to feeding conditions in spring ($r = 0.70$, $p = 0.007$) (Table 4).

4. Discussion

We found that herring selectively targets older copepodites of *E. affinis* and large-sized *L. macrurus*. These findings further support the idea that herring feeding is strictly zooplankton species- and copepod stage-selective (Flinkman et al., 1992).

Table 3 Mean and standard deviation of selectivity values (*C*-index) (Pearre, 1982) for each prey category and each prey category by age groups. The index ranges between −1 and +1, wherein negative values are associated with rejection and positive values with selection; *p*-values given for the comparison of mean selectivity values with 0 for prey categories and between age groups. Juveniles are 1 year and adults 2−12 year old fish. For prey categories refer to Table 1.

Prey category	Prey category		Prey category × Age		
	Mean ± S.D.	*p*-value	Mean ± S.D.		*p*-value
			Juveniles	Adults	
Cladoc	−0.04 ± 0.23	0.22	0.07 ± 0.23	−0.10 ± 0.21	<0.0001
Cop_C1−6	−0.28 ± 0.29	<0.001	−0.26 ± 0.31	−0.29 ± 0.28	<0.0001
Eury_C4−5	−0.03 ± 0.24	1	−0.12 ± 0.24	0.01 ± 0.23	<0.0001
Acar_C6	−0.04 ± 0.06	1	−0.05 ± 0.06	−0.04 ± 0.06	0.97
Eury_C6	−0.01 ± 0.14	0.9	−0.06 ± 0.11	0.01 ± 0.14	0.59
Limn_C1−5	0.05 ± 0.22	0.01	−0.07 ± 0.26	0.09 ± 0.17	0.88
Cercop	0.08 ± 0.47	<0.001	0.22 ± 0.52	−0.00 ± 0.41	<0.0001
Limn_C6	0.13 ± 0.34	<0.001	−0.06 ± 0.38	0.20 ± 0.29	0.73

Herring avoids small early copepodites, nauplii and rotifers even in the species scarce environment of the Gulf of Riga, prevailed by small sized plankters. The particulate-feeding we have identified, consequently assists in our understanding of the role of changes in the well-being of the herring, as these were zooplankton species whose abundance sum of selected copepodite stages explained most of the variation in a historical time series of herring condition factor.

As small-sized plankters prevailed in the Gulf of Riga, we expected diet overlap between adult and juvenile herring towards larger but restricted food fractions, what was indeed true. The main difference was in juveniles consuming cladocerans, both small- (*Bosmina coregoni*, *Evadne nordmanni*, *Podon*/*Pleopis* spp.) and large-sized (*C. pengoi*), while adults preferred older copepodites of *E. affinis*. Therefore, body size of the prey was not the only determining cause of selection. For length classes studied here (>8 cm), the feeding of herring might not be limited by gape-size (Arrhenius, 1996) but rather by prey motility. Because of their low escape response, cladocerans were more likely to be captured (Drenner, 1978; Viitasalo et al., 2001) so that an opportunistic shift to cladocerans in summer could be energetically advantageous. Most likely adult herring had a greater capture success on far more motile copepods, as *E. affinis*, attained through learning to forage, as shown for other fish species (Brown and Laland, 2003). As there were no differences in diet between herring juveniles and adults towards mature *E. affinis* and all stages of large-sized *L. macrurus* suggesting

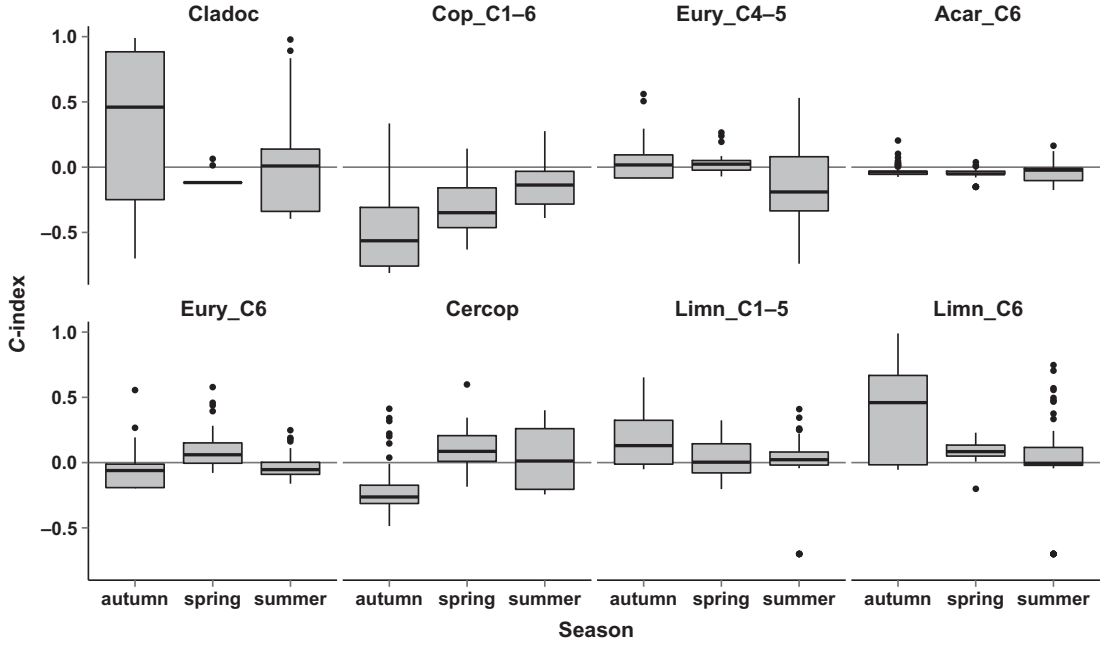

Figure 1 Seasonal variation of herring feeding selectivity (*C*-index) (Pearre, 1982) in each prey category. The index ranges between −1 and +1, wherein negative values are associated with rejection and positive values with selection. For prey categories refer to Table 1.

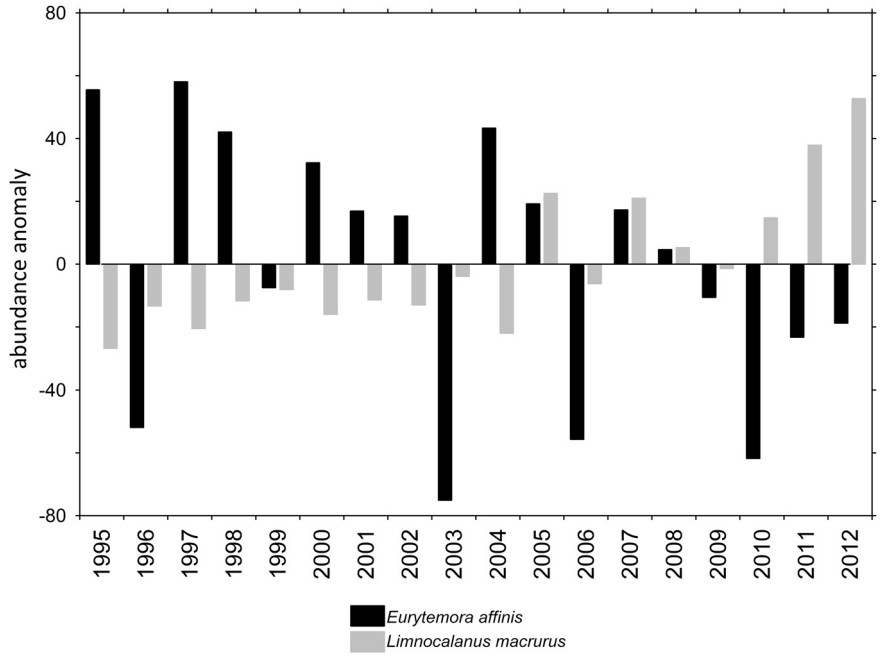

Figure 2 Abundance [ind. m^{-3}] anomaly of *Eurytemora affinis* and *Limnocalanus macrurus* in the Gulf of Riga in May 1995—2012.

dietary overlap at some level, we address the point that mature herring do not feed in spring while spawning (Link, 2001; Slotte, 1999). In the meantime, juveniles feed actively and could be considerable consumers of the shared food resources of copepods in the season when cladocerans are not widely available in the zooplankton community yet.

A striking finding to emerge from our study was that both the juvenile and adult herring strongly preferred *L. macrurus* species only lately recovered in the Gulf of Riga. Increased herring condition in recent years could be associated with a considerable increase of *L. macrurus*. A distinct characteristic of *L. macrurus* is its lipid content of 67% of dry weight, one of the highest among zooplankton species (Vanderploeg et al., 1998) combined with individual size and weight largest among holoplankton species in the Baltic Sea (Hernroth, 1985).

As already mentioned, since late 1980s *L. macrurus* was almost extinct in the gulf. No significant relationship with herring predation was found at previous studies (Kornilovs et al., 2004). Our study was in contrast to earlier findings by Lankov et al. (2010) who conducted annual summer investigations from 1999—2006, and detected no evidence of *L. macrurus* in herring stomachs. Therefore, extremely low numbers of *L. macrurus* or even an absence in the gulf could not be explained by herring predation for the named period but rather abiotic factors.

Table 4 Pearson correlations between abundance of major development stage-resolved prey copepods *Eurytemora affinis* and *Limnocalanus macrurus* in spring and herring condition factor (CF) in successive summer studied in the Gulf of Riga in 1995—2012. C, copepodite stages. For prey categories refer to Table 1.

Prey category	*r*	*p*-value
Eury_C1—3	0.39	0.182
Eury_C4—5	0.68	0.011
Eury_C6	0.33	0.266
Limn_C1—3	0.05	0.869
Limn_C4—5	0.37	0.208
Limn_C6	0.20	0.514
Eury_C4—5 + Limn_C1—6	0.70	0.007

In spring, zooplankton abundance increases mostly as a response to abiotic factors (e.g. water temperature) and a subsequently increased food availability (Jurgensone et al., 2011). As predation rates are still relatively low, due to herring spawning, zooplankton community is comparatively unaffected by fish (Rudstam et al., 1994). Although the species development could be affected by food availability in spring, we explained the recent increase of *L. macrurus* by the positive correlation between its abundance in spring and sum of daily negative values of air temperature in previous winter. Evidently, more frequent cold winters in the last decade have contributed recovery of *L. macrurus*, a glacial relict species. It should be noted that in 1990s there was only one cold winter with the gulf frozen, as ice occurrence due to a sharp environmental change is the factor affecting species development in spring. *L. macrurus* is known to be restricted between narrow environmental limits of upper temperature limit of 14°C, and a lower limit of dissolved oxygen of 5.6 mg L^{-1} (Kane et al., 2004; Strøm, 1946). Accordingly, the possible interference of oxygen levels (even though dependent on temperature) cannot be ruled out, as the critical combination could be the case in August, when water temperature is often high, water stratified, and oxygen levels lower than optimal under the thermocline (most regular habitat of *L. macrurus*) (LHEI unpubl. monitoring data, 2012). Yet, the situation in summer and later in autumn can hardly be described by direct link between copepods and hydrological conditions, as it disappears due to predation pressure by fish (Casini et al., 2009).

Cold winters have benefited *L. macrurus* development, but those winters also have resulted with lower water temperature in successive springs, delaying development of more thermophilic species like *E. affinis*. As *E. affinis* abundance explained most of variation in the herring condition, without a doubt these findings will be much scrutinized, but dependable conclusions for significant *L. macrurus* impact on high condition in last years can be made. One caveat in interpreting our results is that the herring condition failed to be explained by biomass of these zooplankton species. The biomass of *L. macrurus* increased towards the end of the time series, therefore the period of its higher biomass is rather short. The biomass appears to be of a great importance, as these two copepod species have considerably different individual weights: *L. macrurus* is about tenfold heavier than *E. affinis* (Hernroth, 1985).

However, more research on this topic needs to be undertaken before the association between herring condition and variation of its preferred food items is more clearly understood. Investigating the effects of density-dependent mechanisms on herring growth and condition with the association of biotic factors, as young and adult herring should compete for the available zooplankton specimens (Casini et al., 2006). It will be curious to survey future trends of *L. macrurus* abundance in the light of changing climate, as it (while being restricted between narrow environmental limits) plays an important role in pelagic food web. Although, a common viewpoint is that higher temperature ensures higher zooplankton biomass and better feeding conditions in the Baltic Sea (Cardinale et al., 2009), we suggest that a pronounced seasonality (cold winters with ice cover) could benefit herring feeding conditions and ensure higher body condition, as in the Norwegian Sea, where a cold water copepod *Calanus finmarchicus* is the most important prey species for herring (Engelhard and Heino, 2006). Body condition of a fish is the "fast line" to explain its well-being (Froese, 2006) that in turn, is provided by availability of desired food items. High condition is linked to better recruitment thereafter, due to higher fecundity (Arula et al., 2012), lower mortality rates (Engelhard and Heino, 2006) and indirectly indicates a magnitude of possible intraspecific competition.

So far herring recruitment in the Gulf of Riga has been forecasted using Ricker model approach by using two complementary factors: *E. affinis* biomass in May and average water temperature in August that has encountered issue of poor predictions of rich year classes during the last years (ICES, 2013). We speculate that the combination of our findings provides some support for the conceptual premise that the found relationship between the herring feeding selectivity and long-term variation in the herring condition factor has implications to use spring abundance trends of selected copepodite stages of *E. affinis* and *L. macrurus* to estimate feeding situation and, therefore, body condition of herring in the successive year.

Acknowledgments

We thank the anonymous reviewers as well as Juris Aigars and Georgs Korņilovs for constructive comments on earlier drafts of the manuscript, and Tyson Duffy for revising the English.

Appendix A. Supplementary data

Supplementary material related to this article can be found, in the online version, at http://dx.doi.org/doi:10.1016/j.oceano.2015.09.001.

References

Alheit, J., Möllmann, C., Dutz, J., Kornilovs, G., Loewe, P., Mohrholz, V., Wasmund, N., 2005. Synchronous ecological regime shifts in the central Baltic and the North Sea in the late 1980s. ICES J. Mar. Sci. 62, 1205—1215.

Arrhenius, F., 1996. Diet composition and food selectivity of 0-group herring (*Clupea harengus* L.) and sprat (*Sprattus sprattus* (L.)) in the northern Baltic Sea. ICES J. Mar. Sci. 53, 701—712.

Arrhenius, F., Hansson, S., 1993. Food consumption of larval, young and adult herring and sprat in the Baltic Sea. Mar. Ecol. Prog. Ser. 96, 125—137.

Arula, T., Ojaveer, H., Shpilev, H., 2012. Individual fecundity of the autumn spawning Baltic herring *Clupea harengus membras* L. Estonian J. Ecol. 61, 119—134.

Berzinsh, V., 1995. Dynamics of hydrological parameters of the Gulf of Riga. In: Ojaveer, E. (Ed.), Ecosystem of the Gulf of Riga Between 1920 and 1990. Estonian Acad. Publ., Tallinn, 8—31.

Brown, C., Laland, K., 2003. Social learning in fishes: a review. Fish Fish. 4, 280—288.

Cardinale, M., Arrhenius, F., 2000. Decreasing weight-at-age of Atlantic herring (*Clupea harengus*) from the Baltic Sea between 1986 and 1996: a statistical analysis. ICES J. Mar. Sci. 57, 882—893.

Cardinale, M., Möllmann, C., Bartolino, V., Casini, M., Kornilovs, G., Raid, T., Margonski, P., Grzyb, A., Raitaniemi, J., Gröhsler, T., Flinkman, J., 2009. Effect of environmental variability and spawner characteristics on the recruitment of Baltic herring *Clupea harengus* populations. Mar. Ecol. Prog. Ser. 388, 221—234.

Casini, M., Bartolino, V., Molinero, J., Kornilovs, G., 2010. Linking fisheries, trophic interactions and climate: threshold dynamics drive herring *Clupea harengus* growth in the central Baltic Sea. Mar. Ecol. Prog. Ser. 413, 241—252.

Casini, M., Cardinale, M., Hjelm, J., 2006. Interannual variation in herring, *Clupea harengus*, and sprat, *Sprattus sprattus*, condition in the central Baltic Sea: what gives the tune? Oikos 112, 638—650.

Casini, M., Hjelm, J., Molinero, J.-C., Lovgren, J., Cardinale, M., Bartolino, V., Belgrano, A., Kornilovs, G., 2009. Trophic cascades promote threshold-like shifts in pelagic marine ecosystems. Proc. Natl. Acad. Sci. 106, 197—202.

Drenner, R., 1978. Capture probability: the role of zooplankter escape in the selective feeding of planktivorous fish. J. Fish. Board Can. 35, 1370—1373.

Engelhard, G.H., Heino, M., 2006. Climate change and condition of herring (*Clupea harengus*) explain long-term trends in extent of skipped reproduction. Oecologia 149, 593—603.

Flinkman, J., Vuorinen, I., Aro, E., 1992. Planktivorous Baltic herring (*Clupea harengus*) prey selectively on reproducing copepods and cladocerans. Can. J. Fish. Aquat. Sci. 49, 73—77.

Freimane, S.O., 1967. The study of zooplankton population dynamics in the Baltic Sea and the Gulf of Riga using the correlation method. Fish. Res. Baltic Sea 3, 77—96, (in Russian).

Freimane, S.O., 1968. The application of Newton's second law and numerical characteristics for studies of zooplankton biology and abundance. Fish. Res. Baltic Sea 4, 46—60, (in Russian).

Froese, R., 2006. Cube law, condition factor and weight—length relationships: history, meta-analysis and recommendations. J. Appl. Ichthyol. 22, 241—253.

Fulton, T.W., 1904. The Rate of Growth of Fishes. Twenty-Second Annual Report, Part III. Fisheries Board of Scotland, Edinburgh, 141—241.

HELCOM, 2013. Manual for marine monitoring in the COMBINE Programme of HELCOM. http://helcom.fi/action-areas/monitoring-and-assessment/manuals-and-guidelines/combine-manual/.

Hernroth, L., 1985. Recommendations on methods for marine biological studies in the Baltic Sea. Mesozooplankton biomass assessment. Baltic Mar. Biol. Publ. 10, 1—32.

Hothorn, T., Bretz, F., Westfall, P., 2008. Simultaneous inference in general parametric models. Biom. J. 50, 346—363.

ICES, 2009. Report of the Baltic Fisheries Assessment Working Group. ICES Document CM 2009\ACOM, 07. 626 pp.

ICES, 2013. Report of the ICES/HELCOM Working Group on Integrated Assessments of the Baltic Sea (WGIAB), 8—12 April 2013, Chioggia, Italy. ICES CM 2013/SSGRSP:05. 40 pp.

Ikauniece, A., 2001. Long-term abundance dynamics of coastal zooplankton in the Gulf of Riga. Environ. Int. 26, 175—181.

Jurgensone, I., Carstensen, J., Ikauniece, A., Kalveka, B., 2011. Long-term changes and controlling factors of phytoplankton community in the Gulf of Riga (Baltic Sea). Estuar. Coast. 34, 1205—1219.

Kane, D.D., Gannon, J.E., Culver, D.A., 2004. The status of *Limnocalanus macrurus* (Copepoda: Calanoida: Centropagidae) in Lake Erie. J. Great Lakes Res. 30, 22—30.

Kornilovs, G., Berzinsh, V., Sidrevics, L., 1992. The analysis of mean weight-at-age changes of Baltic herring in the Gulf of Riga. ICES CM 1992/J:24. 1—9.

Kornilovs, G., Möllmann, C., Sidrevics, L., Berzins, V., 2004. Fish predation modified climate induced long-term trends of mesozooplankton in a semi-enclosed coastal gulf. ICES CM 2004/L:13. 1—26.

Kornilovs, G., Sidrevics, L., Dippner, J.W., 2001. Fish and zooplankton interaction in the Central Baltic Sea. ICES J. Mar. Sci. 58, 579—588.

Kotta, J., Lauringson, V., Martin, G., Simm, M., Kotta, I., Herkül, K., Ojaveer, H., 2008. Gulf of Riga and Pärnu Bay. Ecol. Baltic Coast. Water. 217—243.

Lankov, A., Ojaveer, H., Simm, M., Põllupüü, M., Möllmann, C., 2010. Feeding ecology of pelagic fish species in the Gulf of Riga (Baltic Sea): the importance of changes in the zooplankton community. J. Fish Biol. 77, 2268—2284.

Link, J., 2001. The relationship between stomach contents and maturity state for major northwest Atlantic fishes: new paradigms? J. Fish Biol. 59, 783—794.

Margonski, P., Hansson, S., Tomczak, M.T., Grzebielec, R., 2010. Climate influence on Baltic cod, sprat, and herring stock—recruitment relationships. Prog. Oceanogr. 87, 277—288.

Möllmann, C., Kornilovs, G., Fetter, M., Köster, F., 2004a. Herring and sprat growth changes in the Central Baltic Sea. ICES CM 2004/L:27. 1—25.

Möllmann, C., Kornilovs, G., Fetter, M., Köster, W.F., 2004b. Feeding ecology of central Baltic Sea herring and sprat. J. Fish Biol. 65, 1563—1581.

Möllmann, C., Kornilovs, G., Fetter, M., Köster, W.F., 2005. Climate, zooplankton, and pelagic fish growth in the central Baltic Sea. ICES J. Mar. Sci. 62, 1270—1280.

Möllmann, C., Kornilovs, G., Sidrevics, L., 2000. Long-term dynamics of main mesozooplankton species in the central Baltic Sea. J. Plankton Res. 22, 2015—2038.

Möllmann, C., Köster, F., 2002. Population dynamics of calanoid copepods and the implications of their predation by clupeid fish in the Central Baltic Sea. J. Plankton Res. 24, 959—977.

Ojaveer, E., Lumberg, A., Ojaveer, H., 1998. Highlights of zooplankton dynamics in Estonian waters (Baltic Sea). ICES J. Mar. Sci. 55, 748—755.

Pearre, S., 1982. Estimating prey preference by predators: uses of various indices, and a proposal of another based on χ^2. Can. J. Fish. Aquat. Sci. 39, 914—923.

Pinheiro, J., Bates, D., DebRoy, S., Sarkar, D., the R Development Core Team, 2013. 'nlme: Linear and Nonlinear Mixed Effects Models'. R package version 3.1-111.

R Core Team, 2013. R: A Language and Environment for Statistical Computing. R Foundation for Statistical Computing, Vienna. http://www.R-project.org/.

Rudstam, L., Aneer, G., Hildén, M., 1994. Top-down control in the pelagic Baltic ecosystem. Dana 10, 105—129.

Sandström, O., 1980. Selective feeding by Baltic herring. Hydrobiologia 69, 199—207.

Slotte, A., 1999. Differential utilization of energy during wintering and spawning migration in Norwegian spring-spawning herring. J. Fish Biol. 54, 338—355.

Stipa, T., Tamminen, T., Seppälä, J., 1999. On the creation and maintenance of stratification in the Gulf of Riga. J. Mar. Syst. 23, 27—49.

Strøm, K.M., 1946. The ecological niche. Nature 157, 375.

UNESCO, 1968. Zooplankton sampling. Monographs on Oceanographic Methodology, vol. 2. UNESCO Press, New York, 174 pp.

Vanderploeg, H.A., Cavaletto, J.F., Liebig, J.R., Gardner, W.S., 1998. *Limnocalanus macrurus* (Copepoda: Calanoida) retains a marine arctic lipid and life cycle strategy in Lake Michigan. J. Plankton Res. 20, 1581—1597.

Viitasalo, M., Flinkman, J., Viherluoto, M., 2001. Zooplanktivory in the Baltic Sea: a comparison of prey selectivity by *Clupea harengus* and *Mysis mixta*, with reference to prey escape reactions. Mar. Ecol. Prog. Ser. 216, 191—200.

Yurkovskis, A., Kostrichkina, E., Ikauniece, A., 1999. Seasonal succession and growth in the plankton communities of the Gulf of Riga in relation to long-term nutrient dynamics. Hydrobiologia 393, 83—94.

Oceanologia (2016) 58, 54—58

Available online at www.sciencedirect.com

ScienceDirect

journal homepage: www.elsevier.com/locate/oceano

SHORT COMMUNICATION

The first report on the establishment and spread of the alien clam *Rangia cuneata* (Mactridae) in the Polish part of the Vistula Lagoon (southern Baltic)☆

Jan Warzocha *, Lena Szymanek, Bartosz Witalis, Tycjan Wodzinowski

Department of Fisheries Oceanography and Marine Ecology, National Marine Fisheries Research Institute, Gdynia, Poland

Received 17 September 2015; accepted 5 October 2015
Available online 28 October 2015

KEYWORDS
Rangia cuneata;
Alien species;
Vistula Lagoon;
Southern Baltic

Summary Information on distribution of the bivalve *Rangia cuneata* in the Polish part of the Vistula Lagoon is presented. The species, first recorded in the Lagoon in 2010, has since rapidly colonized almost the entire basin. The distribution and population structure of the species have been studied in the Polish part of the Lagoon since 2012. Preliminary results on distribution and size structure of the population highlight extensive fluctuations in 2012—2014. A drastic reduction in the abundance following the relatively long winter of 2012/2013 suggests that the winter oxygen deficiency associated with the ice cover could be critical for the population development. Potential effects of the new invasive bivalve on the structure of benthic habitats and macrozoobenthos communities are discussed.
© 2015 Institute of Oceanology of the Polish Academy of Sciences. Production and hosting by Elsevier Sp. z o.o. This is an open access article under the CC BY-NC-ND license (http://creativecommons.org/licenses/by-nc-nd/4.0/).

☆ The study was financed by the Ministry of Science and Higher Education, Republic of Poland (grant NMFRI-P1-3/2012-2014).
* Corresponding author at: Department of Fisheries Oceanography and Marine Ecology, National Marine Fisheries Research Institute, Kołłątaja 1, PL-81-332 Gdynia, Poland. Tel.: +48 587356232; fax: +48 587356110.
E-mail address: janw@mir.gdynia.pl (J. Warzocha).
Peer review under the responsibility of Institute of Oceanology of the Polish Academy of Sciences.

Production and hosting by Elsevier

1. Introduction

The Vistula Lagoon is situated in the south-eastern Baltic and extends for about 91 km along the Polish and Russian coast of the Gulf of Gdańsk (Fig. 1). After the Curonian Lagoon, the Vistula Lagoon is the second largest coastal lagoon in the southern Baltic. At present, the Lagoon is connected with the Baltic via the Pilawska Strait in the eastern, Russian, part of the Lagoon. The Lagoon's total surface area, maximum and mean depths are 833 km^2, 5.1 m, and 2.6 m, respectively. The state border between Poland and Russian Federation divides the Lagoon into the eastern part (64% of the area)

http://dx.doi.org/10.1016/j.oceano.2015.10.001
0078-3234/© 2015 Institute of Oceanology of the Polish Academy of Sciences. Production and hosting by Elsevier Sp. z o.o. This is an open access article under the CC BY-NC-ND license (http://creativecommons.org/licenses/by-nc-nd/4.0/).

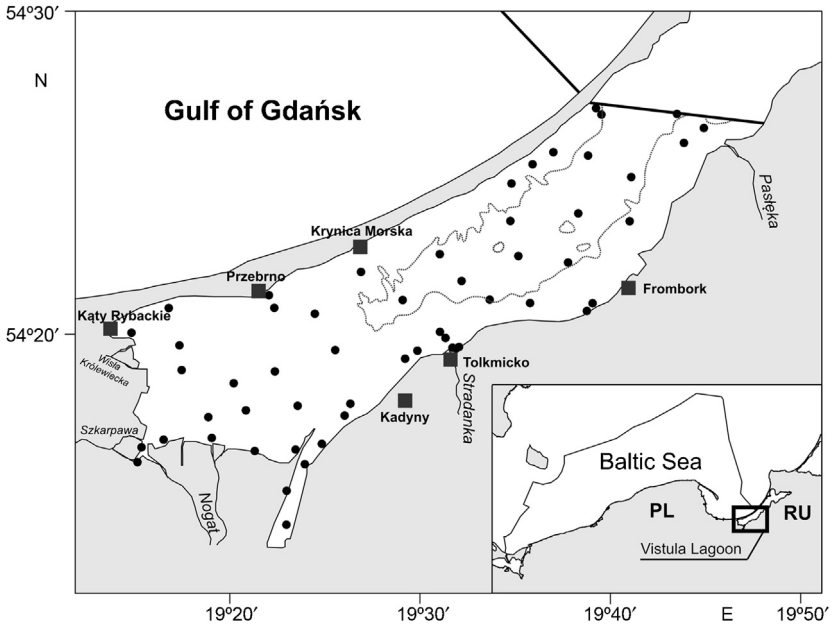

Figure 1 Map of the study area and the grid of stations sampled in 2012—2014.

belonging to Russia and called the Kaliningrad Lagoon, and the western part (36% of the area) belonging to Poland. The Lagoon's bottom is primarily muddy; sands are found only in a narrow belt close to the shore and on shallows, down to the depth of about 1.0—2.0 m. The Lagoon's water typically warms up rapidly in spring. In winter, the Lagoon may become ice-bound. The Lagoon's salinity is variable and ranges, within the Polish part, from about 0.5 to about 4.8 psu (Czubarenko and Margoński, 2008). At present, the Lagoon is classified as a eutrophic (and even hypereutrophic in the Polish part) water body (Aleksandrov, 2010; Nawrocka and Kobos, 2011). The western (Polish) part of the Lagoon is a protected area within the NATURA 2000 network (PLB 280010).

It is a species native to the Gulf of Mexico. In the 1960s, the species colonized coastal Atlantic waters (the Chesapeake Bay) to spread north up to the mouth of the Hudson River, New York (e.g. Pfitzenmeyer and Drobeck, 1964). According to some authors, it could have occurred along the Atlantic coast of North America earlier, and became extinct in the Pleistocene to reappear in the 1960s (Hopkins and Andrews, 1970). Other authors are of the opinion that the species has continued to be present there since the Pleistocene, but was rare and therefore not spotted (Pfitzenmeyer and Drobeck, 1964). In the European waters, it was first recorded in 2005 in the Belgian harbour of Antwerp (Verween et al., 2006). In the Vistula Lagoon, *R. cuneata* was first reported from the eastern, Russian, part in 2010 (Ezhova, 2012; Rudinskaya and Gusev, 2012), the first record from the western, Polish, part dating to 2011 (Warzocha and Drgas, 2013). In both cases, the presence of individuals up to 30—40 mm long suggests the introductions to have occurred 2—3 years earlier. *Rangia cuneata* is the first mactrid species in the fauna of Poland. The species is regarded (e.g. Tarver, 1972) as preferring low-salinity heavily turbid water and a soft bottom (mud or sand).

This report is aimed at presenting preliminary results of research, carried out since 2012, on the establishment, spread, and spatial distribution of *R. cuneata* in the Polish part of the Vistula Lagoon. The survey covered the bottom area beyond the inshore belt of reeds and bulrush, known as the Mid-lagoon (Klimowicz, 1958; Żmudziński, 1957). The sampling station grid is shown in Fig. 1. In total 55 stations were visited in summer seasons (July—September) from 2012 to 2014. The sediment was sampled with a 225 cm^2 Ekman grab weighing 7 kg and sieved with a 1 mm mesh sieves. A minimum of five replicate samples was taken at each station.

2. Results and discussion

The occurrence of *R. cuneata* in the Polish part of the Vistula Lagoon in 2012—2014 is shown in Fig. 2. In terms of the species' distribution in summer 2012, the area surveyed was divided into two distinct parts: one was the western part, including also areas off river mouths, supported no *R. cuneata*, the other being the remaining part of the Polish section of the Lagoon, where the bivalve was present at most stations (Fig. 2A). The area colonized by the species supported both juveniles and adults (from 2 to 48 mm). The absence of *R. cuneata* off river mouths could be explained by the prevalent low salinity (usually not more than 0.5 psu) which is too low for the survival of veliger larvae. *R. cuneata* can adapt to salinities varying from nearly 0 to 33 psu, but the young of the species have a much lower salinity tolerance than adults (Cooper, 1981; LaSalle and de la Cruz, 1985). Moreover, the interactions between temperature and salinity may increase the mortality of young stages (Cain, 1973). In 2013, following winter, there were almost no *R. cuneata* present (Fig. 2B) except for numerous live individuals found on the sandy bottom in the southern part of the Lagoon, close to the mouth of River Stradanka (Fig. 2B). Stations in the remaining part of the area yielded very few live individuals. As shown by the data collected by the Institute of

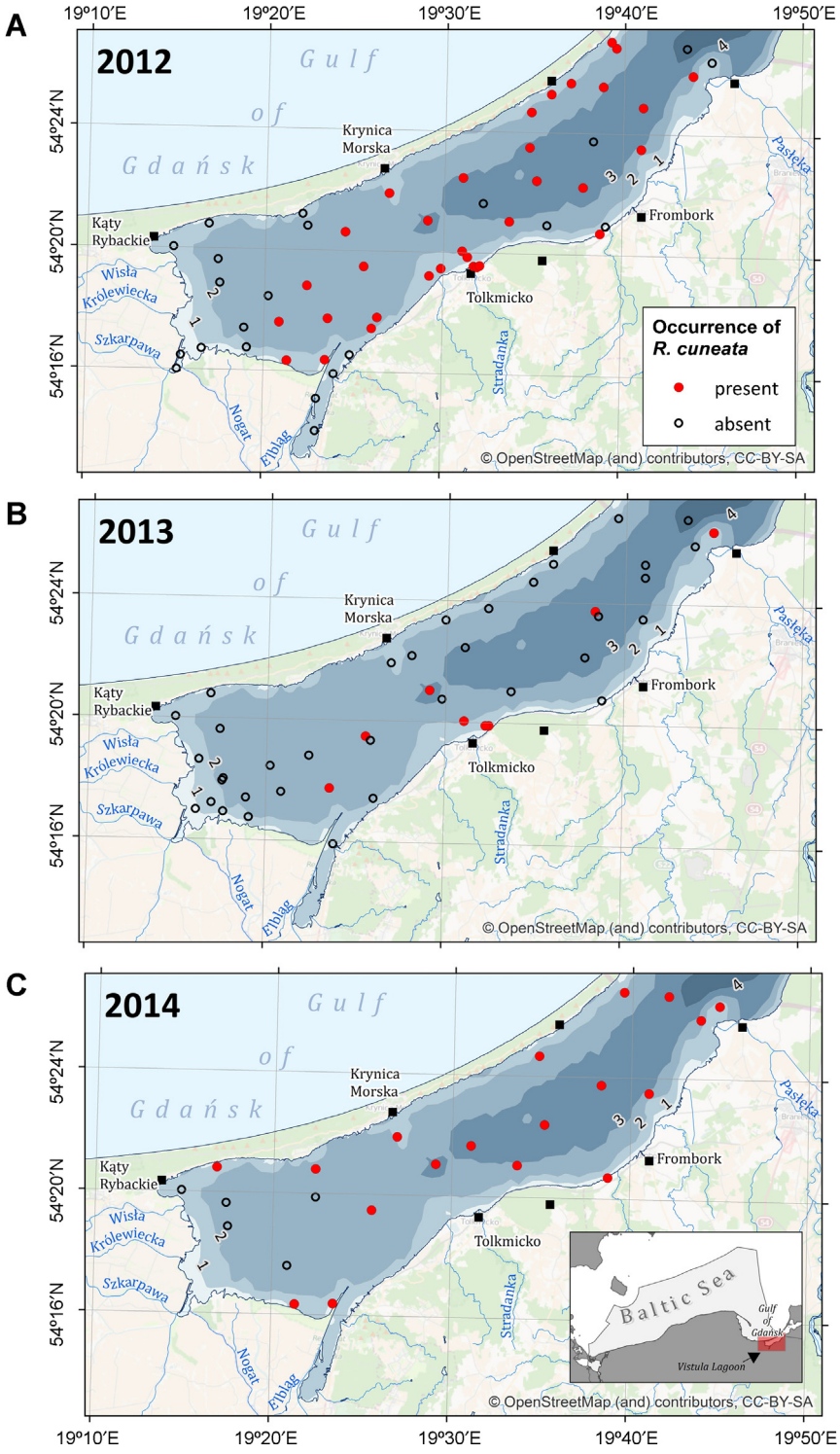

Figure 2 The occurrence of *Rangia cuneata* in the Polish part of the Vistula Lagoon in 2012—2014.

Meteorology and Water Management (IMWM), the winter of 2012/2013 in the Lagoon was characterized by the ice cover persisting longer than in the winter of 2011/2012 and 2013/2014. This may indicate an effect of winter severity on the survival of *R. cuneata*, oxygen deficiency resulting from the absence of seawater inflows via the Pilawska Strait (e.g. Lazarienko and Majewski, 1975; Łomniewski, 1958) being a potential stress factor acting during the ice cover persistence. Klimowicz (1958) suggested winter oxygen deficiency to be a potential factor affecting mollusc survival, while Rychter et al. (2011) found the abundance of the crab *Rhithropanopeus harrisii* to be substantially reduced after long, severe winters in the Vistula Lagoon. Gallagher and Wells (1969) observed high mortality of *R. cuneata* after the strong winter in Chesapeake Bay suggesting low winter temperature as a limiting factor. As the duration of ice cover

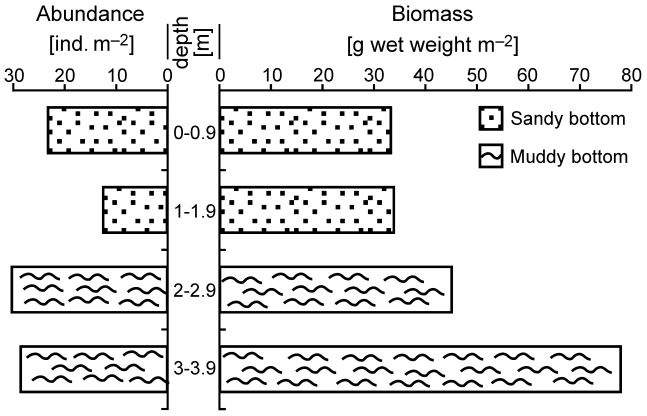

Figure 3 The mean abundance and biomass (formalin wet weight, including shells) of *Rangia cuneata* in 2012, in different depth strata.

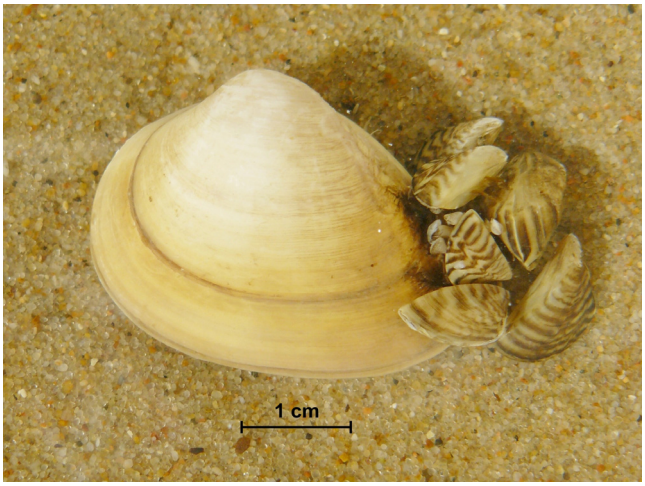

Figure 4 Settlement of *Dreissena polymorpha* on *Rangia cuneata* shells in the Vistula Lagoon.
Photographed by Katarzyna Horbowa.

persistence in the Lagoon has been observed to decrease in the recent years (IMWM data) compared to earlier years (e.g. Łomniewski, 1958), the *R. cuneata* population dynamics in the Lagoon may be greatly affected by climate changes. Preliminary data collected in 2014 point to the presence of *R. cuneata* (mainly young specimens; 0+ and 1+) throughout almost the entire Polish part of the Lagoon (Fig. 2C). Fig. 3 shows the mean abundance and biomass, as calculated from the 2012 data, in the function of depth and sediment type. Although the plot disregards horizontal variability, these preliminary data suggest the absence of any significant effect of depth and sediment type on the presence of *R. cuneata*. However, some studies (e.g. Wong et al., 2010) have revealed that sediment may be the important determinant of the distribution of this species. As deeper (>3 m) areas with the highest biomass found so far occur only in the eastern part of the Lagoon, higher biomasses recorded in the 3—4 m depth range (Fig. 3) may reflect also an effect of a closer distance to the Pilawska Strait, and hence better oxygen conditions, e.g. during winter time.

The *R. cuneata* invasion in the Vistula Lagoon gives rise to questions as to potential effects of the bivalve on benthic habitats and macrozoobenthos structure in the Lagoon. There is no doubt that the total macrozoobenthos biomass will change, particularly on the muddy bottom. The maximum biomass of *R. cuneata*, found in the study area reaches about 160 g m^{-2}. So far, there has been no bivalve that could have occurred throughout the Mid-lagoon and would have produced such a high biomass (Klimowicz, 1958). The bivalve has a relatively large, thick shell and lives on the sediment surface. It is then capable of modifying benthic habitats by acting as a substratum for other species. Settlement of *Dreissena polymorpha* on *R. cuneata* shells has already been observed (Fig. 4). To sum up, regardless of the preliminary nature of the results obtained so far, they indicate that *R. cuneata* may become a permanent component of the macrozoobenthos community in the Polish part of the Vistula Lagoon. Even though the size structure, abundance, and biomass of *R. cuneata* may vary widely, the habitat conditions fit the species' preference very well allowing a very high colonization rate and a rapid population recovery after drastic disturbances.

Acknowledgements

We are grateful to Ms Hanna Wróblewska for sorting samples and to the crew of the cutter r/v MIR-2; Mr Janusz Kościanowski and Mr Andrzej Walotka, for their help with sampling and their fruitful collaboration.

References

Aleksandrov, S.V., 2010. Biological production and eutrophication of Baltic estuarine ecosystems: the Curonian and Vistula Lagoons. Mar. Pollut. Bull. 61 (4—6), 205—210.

Cain, T.D., 1973. The combined effects of temperature and salinity on embryons and larvae of the *Rangia cuneata*. Mar. Biol. 21 (1), 1—6.

Cooper, R.B., 1981. Salinity tolerance of *Rangia cuneata* (Pelecypoda: Mactridae) in relation to its estuarine environment: a review. Walkerana 1, 19—31.

Czubarenko, B., Margoński, P., 2008. The Vistula Lagoon. In: Schiever, U. (Ed.), Ecology of Baltic Coastal Waters. Springer, 167—174.

Ezhova, E.E., 2012. New alien species in the Baltic Sea — the clam *Rangia cuneata* (Bivalvia: Mactridae). Mar. Ecol. J. 11 (1), 29—32, (in Russian).

Gallagher, J.L., Wells, H.W., 1969. Northern Range Extension and winter mortality of *Rangia cuneata*. Nautilus 83 (1), 22—25.

Hopkins, S.H., Andrews, J.D., 1970. *Rangia cuneata* on the east coast: thousand mile range extension or resurgence? Science 167, 868—869.

Klimowicz, H., 1958. Distribution of the molluscs of the Vistula Lagoon in relation to salinity. Pol. Arch. Hydrobiol. 18 (1), 93—123, (in Polish).

LaSalle, M.W., de la Cruz, A.A., 1985. Species profiles: life histories and environmental requirements of coastal fishes and invertebrates (Gulf of Mexico): common rangia. US Fish. Wild. Serv. Biol. Rep., 82 (11.31). US Army Corps of Engineers, TR EL-82-4, 16 pp.

Lazarienko, N.N., Majewski, A. (Eds.), 1975. Hydrometeorological System of the Vistula Lagoon. WKiŁ, Warszawa, 491 pp., (in Polish).

Łomniewski, K., 1958. The Firth of Vistula. Polska Akademia Nauk. Instytut Geografii, Prace Geograf., 15, 106 pp., (in Polish).

Nawrocka, L., Kobos, J., 2011. The trophic state of the Vistula Lagoon: an assessment based on selected biotic and abiotic

parameters according to the Water Framework Directive. Oceanologia 53 (3), 881—894, http://dx.doi.org/10.5697/oc.53-3.881.

Pfitzenmeyer, H.T., Drobeck, K.G., 1964. The occurrence of brackish water clam *Rangia cuneata*, in the Potomac River, Maryland. Chesapeake Sci. 5 (4), 209—215.

Rudinskaya, L.V., Gusev, A.A., 2012. Invasion of the North American wedge clam *Rangia cuneata* (G.B. Sowerby I, 1831) (Bivalvia: Mactridae) in the Vistula Lagoon of the Baltic Sea. Russ. J. Biol. Invasions 3 (3), 220—229.

Rychter, A., Paturej, E., Jabłońska-Barna, I., 2011. Animals of the Vistula Lagoon. In: Kruk, M., Rychter, A., Mróz, M. (Eds.), Vistula Lagoon, 67—90, (in Polish).

Tarver, J.W., 1972. Occurrence, distribution and density of *Rangia cuneata*, in Lakes Pontchartrain and Maurepas, Louisiana. Tech. Bull. Louisiana Wildlife Fish. Comm. 1, 8 pp.

Verween, A., Kerckhof, F., Vincx, M., Degraer, S., 2006. First European record of the invasive brackish water clam *Rangia cuneata* (G.B. Sowerby I, 1831) (Mollusca: Bivalvia). Aquat. Invasions 1 (4), 198—203.

Warzocha, A., Drgas, A., 2013. The alien gulf clam (*Rangia cuneata* G. B. Sowerby I, 1831) (Mollusca: Bivalvia: Mactridae) in the Polish part of the Vistula Lagoon (SE. Baltic). Folia Malacol. 21 (4), 291—292.

Wong, H.W., Rabalais, N.N., Turner, R.E., 2010. Abundance and ecological significance of the clam *Rangia cuneata* (Sowerby, 1831) in the upper Barataria Estuary (Louisiana, USA). Hydrobiologia 651, 305—315.

Żmudziński, L., 1957. Zoobenthos of the Vistula Lagoon. Pr. Mor. Inst. Ryb. Gdynia, 9, 453—491, (in Polish).

Oceanologia (2016) 58, I—IV

Available online at www.sciencedirect.com

ScienceDirect

journal homepage: www.elsevier.com/locate/oceano

CHRONICLE

The Polish National Scientific Conference "Baltic 2015" and the inauguration of the "SatBałtyk" satellite monitoring system

The Polish National Conference on *The state, trends and contemporary changes in monitoring the Baltic Sea environment "Baltic 2015"* took place at the Institute of Oceanology, Polish Academy of Sciences, on 14—16 October 2015. The event was held under the patronage of the Polish Space Agency and the Marshals of the Provinces of Pomerania and Western Pomerania. Among the personages appointed to the Honorary Conference Committee were the Minister for Science and Higher Education Lena Kolarska-Bobińska and the Minister for the Environment Maciej Grabowski.

The Conference was co-organised by the following institutions:

- The Polish Scientific Committee on Oceanic Research (Polish Academy of Sciences);
- The Polish Space Agency;
- The Marine Fisheries Institute;
- The Institute of Meteorology and Water Management — Maritime Branch;
- The Maritime Institute, Gdańsk;
- The Polish Geological Institute (Department of Marine Geology);
- The SatBałtyk Consortium, whose members are:
  - The Institute of Oceanology, Polish Academy of Sciences (coordinator);
  - The Marine Science Institute, University of Szczecin;
  - The Institute of Oceanography, University of Gdańsk;
  - The Institute of Physics, Pomeranian Academy, Słupsk.

The Conference covered five themes: **Session 1. The history and future of monitoring the Baltic environment** (chaired by Prof. Tomasz Linkowski); **Session 2. The climate and circulation of Baltic waters** (chaired by Prof. Witold Cieślikiewicz), **Session 3. Monitoring chemical threats to the Baltic** (chaired by Prof. Lucyna Falkowska), **Session 4. Satellite monitoring — the SatBałtyk System** (part 1: chaired by Prof. Vladimir Tomin, part 2: chaired by Prof. Marek Moszyński), **Session 5. Processes on the bottom and shores of the Baltic** (chaired by Prof. Ryszard Kotliński), **Session 6. Threats to and transformations of the Baltic biosphere** (part 1: chaired by Prof. Maciej Wołowicz, part 2: chaired by Prof. Marcin Pliński).

During the conference the experts in various oceanological disciplines, invited by the Honorary Conference Committee, delivered 23 lectures. In addition, there were 32 posters, selected from those submitted. The conference was broadcast live on TASK television.

More information on the aims of the Conference and its programme, as well as abstracts of the lectures and posters, can be found at http://www.iopan.gda.pl/baltyk2015/. The lectures, recorded by TASK TV, are accessible at http://tv.task.gda.pl.

More than 250 people participated in the Conference, including invited representatives of local and national administrations — decision-makers regarding the utilisation and conservation of the resources and environment of the Baltic Sea.

One of the key aspects of the programme was the ceremonial inauguration of the Satellite System for the Comprehensive Monitoring of the Baltic Sea Environment, which continually monitors some 70 different structural and functional properties of this ecosystem, presenting them in the form of maps, numerical data and graphs on the website http://satbaltyk.iopan.gda.pl/.

The SatBałtyk system utilises measurement data from a number of satellites systematically monitoring the Baltic as well as two complex systems of mathematical models: the

Peer review under the responsibility of Institute of Oceanology of the Polish Academy of Sciences.

ELSEVIER Production and hosting by Elsevier

http://dx.doi.org/10.1016/j.oceano.2015.11.001
0078-3234/© 2015 Institute of Oceanology of the Polish Academy of Sciences. Production and hosting by Elsevier Sp. z o.o. This is an open access article under the CC BY-NC-ND license (http://creativecommons.org/licenses/by-nc-nd/4.0/).

Table 1 Selected parameters of the Baltic Sea environment determined by the SatBałtyk System (translation from Ostrowska et al., 2015).

Parameter	Additional information
1. Parameter group: Atmosphere, meteorology	
Air temperature	1.5 or 2 m above the surface
Cloudiness	Total, low-, medium- and high-level
Wind	Speed and direction 10 m above the surface
Air humidity	Relative and specific 1.5 or 2 m above the surface
Water equivalent of clouds	Integrated water vapour content in the atmospheric column
Energy flux	Fluxes of radiation (solar, photosynthetically active and long-wave) and sensible and latent heat
Rainfall	Convectional and stratiform
Snowfall	Convectional and stratiform
2. Parameter group: Hydrology	
Sea level	Inclination of the sea surface with respect to its mean level
Sea surface temperature	In the surface layer of sea water
Water temperature	At different depths
Water salinity	At different depths
Sea currents	Speed and direction
Ice	Range, concentration, thickness, drifting speed
Secchi depth	Range of visibility of a Secchi disc (a white disc in daylight)
3. Parameter group: Marine optics	
Coefficient of light attenuation	In the surface water layer, for different wavelengths
Coefficient of light absorption	At different depths, for different wavelengths
Coefficient of light scattering	In the surface water layer, for different wavelengths
Coefficient of irradiance attenuation with increasing depth in the sea	At different depths in the visible light spectral interval (photosynthetically active, 400—700 nm)
Range of visibility in the water	In the horizontal direction in the surface water layer
Extent of the euphotic zone	The depth reached by 1% of the visible (photosynthetically active) light flux penetrating the sea surface
4. Parameter group: Energy balance	
Solar radiation	Downward and upward flux of short-wave radiation (0.3—4 μm) above the sea surface; instantaneous, mean daily, doses
Thermal radiation	Downward and upward flux of long-wave radiation (4—100 μm) above the sea surface; daily mean values
Radiation balance	Resultant daily mean values above the sea surface
Remote reflectance	For different wavelengths
Energy in photosynthesis	Photosynthetically active entering the sea (400—700 nm); absorbed by phytoplankton cells; converted into the chemical energy of organic matter
Latent heat	Mean 24 h flux
Sensible heat	Mean 24 h flux
5. Parameter group: Sea water components	
Dissolved oxygen concentration	In the surface water layer
Nutrient concentrations	Nitrates NO_3, phosphates PO_4, silicates SiO_4 in the surface water layer
Chlorophyll concentrations	Chlorophyll *a*, chlorophyll *b* and chlorophyll *c* at different depths
Carotenoid concentrations	Photosynthetic, photo-protecting, at different depths
Phycobilin concentration	At different depths
SPM concentration	In the surface water layer
6. Parameter group: Phytoplankton, photosynthesis	
Photosynthetic yield	Maximum, and in the surface water layer
Rate of photosynthesis	24 h mean in the water column under 1 m^2 of sea surface
Primary production	The mass of organic matter produced during photosynthesis in the water column under 1 m^2 of sea surface in 24 h
Phytoplankton biomass	The mass of carbon in phytoplankton cells in the surface water layer
Energy absorbed by phytoplankton	In 24 h in the water column under 1 m^2 of sea surface
Molecular oxygen flux	Released during 24 h as a result of photosynthesis in the water column under 1 m^2 of sea surface

Table 1 (*Continued*)

Parameter	Additional information
7. Parameter group: Coastal zone	
Extent of swash zone	Reached by storm waves along the Polish coast
Width of dry beach	Not inundated — to the base of the dune
Danger from rip currents	Potential occurrence, pilot-programme sections
Dune erosion	The volume of material carried away as a result of erosion by storm waves, pilot-programme sections
8. Parameter group: Threats	
Storm threats	Areas of strong winds
Oil spills	Areas where petroleum derivatives may occur on the water surface
Icing	Extent of ice cover
Threats to the shoreline	Erosion and inundation by storm waves, rip currents

diagnostic ones go by the general name of DESAMBEM[1] (Darecki et al., 2008; Woźniak et al., 2008), while the prognostic ones are referred to as BALTFOS[2] (Nowicki et al., 2015; Ołdakowski et al., 2005 and others cited in Ostrowska et al., 2015). The environmental parameters determined with the aid of these two systems complement one another: BALTFOS assimilates empirical data obtained from satellite information using the DESAMBEM algorithm, while at the same time filling in gaps in the DESAMBEM data when the measurements could not be made because the relevant areas were covered by clouds, i.e. when the satellite did not "see" the sea.

The SatBałtyk System is continually being calibrated and corrected on the basis of in situ measurements acquired during cruises on the Baltic of the research vessels r/v *Oceania*, k/h *Oceanograf 2* and the motor launch *Sonda 2*, as well as from autonomous measurement buoys, the *Baltic Beta* drilling platform and the shore stations situated along the southern coast of the Baltic.

This system was established as a result of earlier optical, bio-optical and other studies, which enabled the scientific foundations for the remote-sensing of the complex Baltic Sea environment to be laid. Those studies were performed over many years by cooperating teams of scientists from the Institute of Oceanology (Polish Academy of Sciences, Sopot), the Institute of Oceanography (University of Gdańsk), the Institute of Physics (Pomeranian Academy, Słupsk), the Institute of Marine Sciences (University of Szczecin) and the Sea Fisheries Institute (Gdynia). In 2010 the first four of these institutes formed the SatBałtyk Consortium, and as a consequence of winning a competition, were able to jointly carry out a large research project in 2010—2015: Project No. POIG.01.01.02-22-011/09-00 *The Satellite Monitoring of the Baltic Sea Environment* (*SatBałtyk*).[3] As a result, the operational **SatBałtyk System** came into being. The Institute of Oceanology PAN is coordinator of this research, and the initiator and manager of the project was the late Prof. Bogdan Woźniak until the end of 2014.[4] His work was taken up by Assoc. Prof. Mirosława Ostrowska, who has been the Project Manager since 1st January 2015 (earlier she was the Deputy Project Manager).

Most of the parameters currently being monitored by the **SatBałtyk System** are set out in Table 1, which is a translation of Annex 1 from the brochure (Ostrowska et al., 2015 — in Polish), published in print and in electronic form, accessible at http://www.iopan.gda.pl/baltyk2015/.

With ongoing scientific research continuing to expand knowledge of the Baltic environment, it will become possible to derive ever more accurate mathematical descriptions of the interrelationships among the various processes taking place in the sea and the atmosphere. In consequence, the set of parameters available in the SatBałtyk System describing the Baltic ecosystem will be extended and matched to the needs of its users.

The parameters currently available in the System have been divided into eight groups under the following working headings: 1. Atmosphere, meteorology, 2. Hydrology, 3. Marine optics, 4. Energy balance, 5. Sea water components, 6. Phytoplankton, photosynthesis, 7. Coastal zone, 8. Threats. The spatial distributions of these parameters are systematically monitored and made accessible to users on the System's website (see above) in the form of distribution maps of their values in the Baltic area. From these maps one can read off (and export) the numerical values of these

[1] The DESAMBEM algorithm (DEvelopment of a SAtellite Method for Baltic Ecosystem Monitoring) came into being in 2001—2005 as a result of the implementation of the project. The study and development of a satellite system for monitoring the Baltic Sea ecosystem (project No. PBZ-KBN 056/P04/2001) by the Institute of Oceanology (Polish Academy of Sciences, Sopot) in cooperation with the Institute of Oceanography (University of Gdańsk), the Institute of Physics (Pomeranian Academy, Słupsk), and the Sea Fisheries Institute (Gdynia).

[2] BALTFOS (BALTic FOrecasting System) is a complex system of prognostic models described in many of the papers cited in the brochure (Ostrowska et al., 2015).

[3] Project No. POIG.01.01.02-22-011/09, The Satellite Monitoring of the Baltic Sea Environment SatBałtyk, co-financed by the European Union from the European Regional Development Fund within the framework of the Operational Programme — Innovative Economy; Priority axis 1: Research and development of modern technologies; Action 1.1: Support for scientific research for the building of a knowledge-based economy.

[4] Sadly, Professor Bogdan Woźniak, died on 30 December 2014, having succumbed to an incurable disease (see *In Memoriam* Oceanologia 57/1, 2015).

parameters anywhere on the Baltic and for any length of time during the monitoring period; their changes with time are also available. The System provides descriptions of the relevant parameters and a range of subsidiary information.

References

Darecki, M., Ficek, D., Krężel, A., Ostrowska, M., Majchrowski, R., Woźniak, S.B., Bradtke, K., Dera, J., Woźniak, B., 2008. Algorithm for the remote sensing of the Baltic ecosystem (DESAMBEM). Part 2: Empirical validation. Oceanologia 50 (4), 509—538.

Nowicki, A., Dzierzbicka-Głowacka, L., Janecki, M., Kałas, M., 2015. Assimilation of satellite SST data in the 3D CEMBS model. Oceanologia 57 (1), 17—24, http://dx.doi.org/10.1016/j.oceano.2014.07.001.

Ołdakowski, B., Kowalewski, M., Jędrasik, J., Szymelfenig, M., 2005. Ecohydrodynamic model of the Baltic Sea. Part I: Description of the ProDeMo model. Oceanologia 47 (4), 477—516.

Ostrowska, M., Darecki, M., Kowalewski, M., Krężel, A., Dera, J., 2015. System SatBałtyk: satelitarny monitoring środowiska Bałtyku, struktura, funkcjonowanie, możliwości operacyjne. In: SatBałtyk Consortium and IO PAN. Sopot 54 pp., available online (in Polish): http://www.iopan.gda.pl/baltyk2015/

Woźniak, B., Krężel, A., Darecki, M., Woźniak, S.B., Majchrowski, R., Ostrowska, M., Kozłowski, Ł., Ficek, D., Olszewski, J., Dera, J., 2008. Algorithm for the remote sensing of the Baltic ecosystem (DESAMBEM). Part 1: Mathematical apparatus. Oceanologia 50 (4), 451—508.

Jerzy Dera*
Mirosława Ostrowska
Institute of Oceanology of the Polish Academy of Sciences, Sopot, Poland

*Corresponding author at: Institute of Oceanology, Polish Academy of Sciences, Powstańców Warszawy 55, Sopot 81-712, Poland
*E-mail address:*dera@iopan.gda.pl (J. Dera)

Received 15 October 2015
Available online 18 November 2015